



DIFFERENTIAL PATHWAY CONTROL IN NUCLEOTIDE EXCISION REPAIR

Differential Pathway Control in Nucleotide Excision Repair

Gijsbert J.C. van Belle | 2015

Gijsbert Jacob Christiaan van Belle

Colofon

ISBN: 978-94-6295-342-0

Cover design: H.M. de Gruiter & G.J.C. van Belle

Chapter icons: Matthew C. Nielsen

Lay-out: G.J.C. van Belle

Printed by: Proefschriftmaken.nl | | Uitgeverij BOXPress

Published by: Uitgeverij BOXPress, 's-Hertogenbosch

The work described in this thesis was performed at the Department of Pathology and the Department of Genetics of the Erasmus University Medical Center, Rotterdam, The Netherlands.

© Copyright 2015 by G.J.C. van Belle. All rights reserved

No part of this thesis may be reproduced, stored in a retrieval system, or transmitted in any form or by any means, without prior written permission of the author, or when appropriate, of the publisher of the presented published articles.

Differential Pathway Control in Nucleotide Excision Repair

Differentiële controle over nucleotide excisie herstel routes

Proefschrift

ter verkrijging van de graad van doctor aan de
Erasmus Universiteit Rotterdam
op gezag van de rector magnificus

Prof.dr. H.A.P. Pols

en volgens besluit van het College voor Promoties.

De openbare verdediging zal plaatsvinden op
vrijdag 11 september 2015 om 9:30 uur.

door

Gijsbert Jacob Christiaan van Belle

geboren te Zoetermeer

Promotiecommissie

Promotor: Prof.dr. A.B. Houtsmuller

Overige leden: Prof.dr. L.H.F. Mullenders
Prof.dr. J.H.J. Hoeijmakers
Dr. P.J. Verschure

Tabel of contents

	Scope of this thesis	
Chapter I	General introduction	11
Chapter II	RNF111/Arkadia is a SUMO-targeted ubiquitin ligase that facilitates the DNA damage response	43
Chapter III	SUMO and ubiquitin-dependent XPC exchange drives nucleotide excision repair	65
Chapter IV	A bimodal switch regulates priority for repair of active genes under mild genotoxic stress	87
Chapter V	A minimal model for regulation of DNA damage recognition by XPC	111
Appendix	Summary	137
	Samenvatting	139
	Curriculum Vitae	142
	List of publications	143
	PhD portfolio	144
	Dankwoord	146

Scope of the thesis

The stability and integrity of the genome is crucial for all cellular life on earth. This integrity is continuously challenged by internal and external genotoxic agents. These agents cause DNA damages which interfere with important cellular processes like replication of the genome and transcription of the genetic code. To protect the DNA against these agents, a complex network of dedicated DNA repair- and associated signalling pathways is in place. Collectively, these pathways are known as the DNA Damage Response (DDR).

NER is the main pathway for mammalian cells to remove UV-induced DNA lesions. The recognition of lesions in NER is either achieved by stalling of active RNA polymerase II during transcription or the stable binding of the protein XPC to the lesion. Although the majority of the factors involved in NER damage recognition have been identified, little is known about the molecular mechanisms and the regulation of this crucial step. The aim of the research described in this thesis focusses on the damage recognition, its regulation, and downstream effects in the NER pathway.

Chapter I provides the needed background by introducing the current knowledge of the DDR pathways and their functioning. We discuss how proteins are modified and how this influences cellular signalling. Additionally we introduce different microscopy techniques and associated Monte Carlo modelling approaches used in this thesis.

The Ubiquitin and SUMO protein modifications introduced in Chapter I, play key roles in cellular signalling pathways.

In **Chapter II** we identify a new SUMO-targeted ubiquitin ligase (STUbL), RNF111/Arkadia. Utilizing its special SIM domains it specifically recognizes poly-SUMO chains on target proteins. Subsequently, it promotes non-proteolytic K63-linked ubiquitylation of the target protein using UBC13-MMS2 as the cognate E2 enzyme. RNF111 promotes ubiquitylation of the SUMOylated form of XPC, the damage sensor in NER. This ubiquitylation regulates the binding of XPC to the damaged DNA.

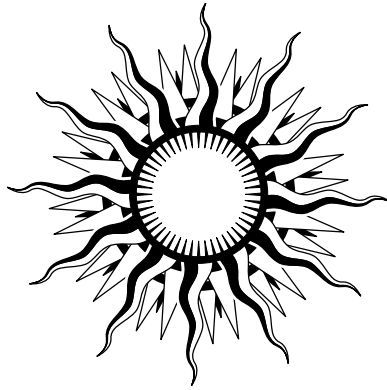
In **Chapter III** we go in further detail of what role the ubiquitylation of XPC by RNF111 plays in the NER pathway. We show that RNF111 is required for efficient repair of UV-induced DNA lesions. Furthermore, the RNF111-mediated ubiquitylation promotes the release of XPC from the lesion after NER initiation. This release of XPC is needed to ensure stable incorporation of the NER endonucleases XPG and ERCC1/XPF. This sequential modification of XPC upon UV irradiation represents an extra layer of control of the NER reaction. Under natural conditions, NER mostly operates at low damage levels, occasionally interrupted by higher levels, for instance by exposure to intense sunlight. Although highly relevant, knowledge on how cells respond to such fluctuations is sparse if not absent.


In **Chapter IV** we show that cells switch between transcription-coupled repair (TCR) and global genome repair (GGR) dependent on damage load and therefore not only depend on the genomic location of the DNA lesion. At DNA damage concentrations below a threshold level, recruitment of the NER machinery by the global damage-sensor XPC is suppressed using regulatory ubiquitylation by E3 ligase Cul4a. Above threshold, damage-bound XPC switches to active recruitment of core NER factors. This bimodal switch allows cells under mild genotoxic stress to prioritize repair of the highly cytotoxic lesions that block transcription and are detected by RNA polymerase II in transcribed strands of active genes.

The bimodal switch described in chapter IV is very well suited to be described by Monte Carlo simulation. In **Chapter V** we use *in silico* experiments using in house modeling software to build on the experimental data. We hypothesized models with and without feedback loop systems governing this bimodality and see if damage marking can play a role. Furthermore we simulate what the effects are of competition for XPA by RNA polymerase II (TCR) and XPC (GGR). This data combined is used to further elucidate the regulatory mechanism described and propose new *in vivo* experiments.

Chapter I

General introduction





All cellular life we know depends on an intact and stable genome. It serves as a blueprint for the mechanisms of life and insures proper behaviour of all cellular functions. In eukaryote species the genome is stored by the nucleus. This compartmentalisation not only allows regulation of the different processes acting on the genome, but also protects it. The genome is comprised of two intertwined, anti-parallel polynucleotide chains of Deoxyribonucleic Acid (DNA). These chains are shaped as a double helix which are highly condensed into structures called chromosomes. This condensation is established by tightly wrapping the DNA double helix around the nucleosome, an eight subunit complex of specialized proteins called histones.

The polynucleotide chains contain the genetic code. This code is established by the order in which four different nucleotides are present in the chains. These nucleotides are adenine (A), guanine (G), thymine (T), and cytosine (C). Each of these four nucleosides can be covalently bound to the phosphate group of the next via the sugar group, forming a helical sugar-phosphate backbone. DNA molecules consist of two of these biopolymer strands coiled around each other to form a double helix. The helical double strand nature of the DNA is established by the pairing rules of the nucleotides. Via either two or three hydrogen bonds, respectively, adenine pairs with thymine and guanine pairs with cytosine. Three nucleotides together form a so-called codon, which codes for a specific amino acid which is part of a protein.

Complete proteins are coded in the DNA as a gene. When a protein is needed these genes are transcribed in a process known as transcription. During transcription the DNA-sequence is copied to a temporary messenger from which a protein can be synthesised. This temporary messenger is Ribonucleic acid (RNA). Similar to DNA, RNA is composed of a chain of nucleotides. In contrast to DNA it is more often found as a single-strand folded unto itself. Another difference with DNA is the use of uracil (U) instead of thymine (T). Messenger RNAs (mRNAs) carry the genetic information the ribosomes, which are responsible in translating the mRNA to protein.

When a cell divides a complete copy of the genetic code has to be transferred to each daughter cell. This tightly regulated process, called replication, ensures the propagation of the genetic code and forms the basis for biological inheritance over many cellular generations.

DNA Damage and DNA repair

DNA integrity is constantly challenged by internal and external DNA-damaging agents that induce DNA lesions. When not properly repaired DNA lesions may result in malignant transformation or accelerated ageing. Errors which arise in the genetic code can have an impact on all levels of the cell and its survival. Insults can stem from different sources, either externally or internally (Figure 1). For instance, the ultraviolet (UV) wavelengths in sunlight induce lesions in one of the strands of the double helix and ionizing radiation induce Double Strand Breaks (DSBs) (van Gent et al., 2001; Ravanat et al., 2001; Sancar, 1996). DNA damage can also be induced by internal insults like the formation of reactive oxygen species (ROS) which are created during normal cellular metabolism which have important functions in cellular signalling (Finkel, 2011). However, they can also oxidize DNA resulting in base modifications, abasic sites, non-conventional single-strand breaks and intra/interstrand DNA crosslinks (Waris and Ahsan, 2006). If left unrepaired, these lesions can have a myriad of negative effects on a cell's functioning. Damaged DNA can result in problems during transcription and replication, cause mutations and other chromosomal aberrations. In turn, these effects can increase the risk of developing cancer or contribute to premature aging (Niedernhofer et al., 2006, 2011; de Boer et al., 2002). Therefore, it is easily understood that the genome is well maintained and protected against the dangerous effects of DNA damage by what is called the DNA Damage Response (DDR). This response combines several specialized DNA repair systems working and communicating alongside DNA damage signalling pathways (Jackson and Bartek, 2009).

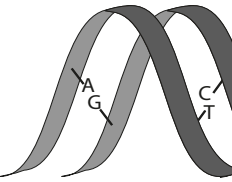
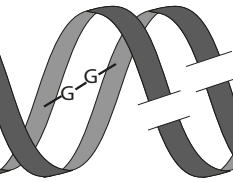
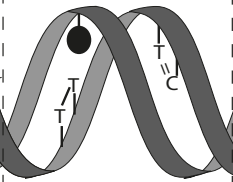
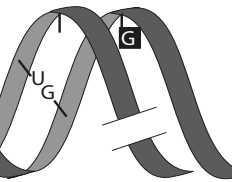
Replication errors	X-rays Anti-tumour agents (cis- Pt, MMC)	UV light Polycyclic aromatic hydrocarbons	X-rays Oxygen radicals Alkylating agents Spontaneous reactions
			
A-G Mismatch T-C Mismatch Insertion Deletion	Interstrand cross-link Double-strand break	(6-4)PP Bulky adduct CPD	Uracil Abasic site 8-Oxoguanine Single-strand break
Mismatch repair (MMR)	Double strand break repair (HR, NHEJ)	Nucleotide excision repair (NER)	Base excision repair (BER)

Figure 1. Different DNA damages, their sources, and the linked repair pathways. Many different endogenous and exogenous sources continuously damage the DNA (upper row). The cell has developed specific pathways to deal with these different types of lesions: mismatch repair (MMR), double strand break repair (HR, NHEJ), nucleotide excision repair (NER), and base excision repair (BER) (lower row). Adapted from Hoeijmakers et al, Nature 2001.

Non-homologues end joining (NHEJ) and homologous recombination (HR)

DSBs are breaks in both strands of the DNA double helix. DSBs can stem from external sources like ionizing irradiation, but also occur during normal cellular processes like mitosis (Fulford et al., 2001; Inagaki et al., 2010). These breaks are repaired via either one of two pathways: non-homologues end joining (NHEJ) or homologous recombination (HR). In NHEJ the two broken ends of the DNA helix are simply ligated using special ligating enzymes. Because of this lack of quality control, the NHEJ pathway is the most error prone of the two: nucleotides can be lost or added to the DNA during the ligation step, changing the genetic code and possibly introducing mutations (Weterings and van Gent, 2004). In repair of DSBs through the HR-pathway, the intact copy of the sister chromatid serves as a template to repair the damage, which reduces the possibility that errors occur. This template however, is only available in cells which are in either G2 phase, or partly during S-Phase, of the cell cycle. This explains why cells frequently use NHEJ to deal with DSBs: The vast majority of the cells in our bodies do not cycle. This cell phase is known as G0 and in this phase the DNA is not replicated. Therefore these cells only use the more error-prone NHEJ pathway to deal with their DSBs (Kanaar et al., 1998).

Detection of DSBs by NHEJ is performed by the Ku70/80 heterodimer (Figure 2, left pathway). This complex binds at the ends of the broken dsDNA and serves as a scaffold at which subsequent repair factors can dock. (Walker et al., 2001). Among the factors are members of the DNA-PKcs (for DNA protein kinase catalytic subunit) family (Gottlieb and Jackson, 1993). After binding of these factors an auto-phosphorylation step takes place and the DNA ends are aligned (Chan and Lees-Miller, 1996). The DNA ends are then resected by the nuclease Artemis and the MRN complex. The MRN complex consists of Meiotic Recombination 11 homolog A (MRE11A), RAD50, and Nibrin (NBS1) (Ma et al., 2002; Mahaney et al., 2009). This resection step is where nucleotides can be lost and the main reason why NHEJ is not error-free. The resected ends are then ligated together by the Ligase IV/XRCC4 complex (Grawunder et al., 1997; Mari et al., 2006).

HR is initiated when the MRN complex binds to the ends of the broken DNA (Figure 2, right pathway). The MRN complex is likely to stabilize the broken DNA and is implicated in activation of the checkpoint kinase ataxia telangiectasia-mutated (ATM) (de Jager et al., 2001; Lavin, 2008). Following the recognition of the DSB, two nucleases, CtBP-interacting protein (CtIP) and Exonuclease 1 (EXO1), resect the 5' DNA ends at the break. This exposes a 3' ssDNA overhang to which Replication protein A (RPA) binds to protect this ssDNA. (Lee et al., 1998; Tauchi et al., 2002). Under influence of the protein breast cancer 2, early onset (BRCA2) RPA is replaced by monomers of RAD51 which form into a nucleoprotein filament on the ssDNA ends. The RAD51 filament mediates homology search and strand invasion in the homologous dsDNA template. The subsequently formed joint molecule is called a displacement loop (D-loop). The newly formed 3'-end then serves as a primer for the novel DNA synthesis, which is promoted by the dsDNA-dependant ATPase RAD54. Two different options for resolving the damage are now available. The first option entails the invasion of the homologous template by the second end of DNA in a RAD51-mediated fashion (second strand invasion). The resulting joint structures are called Holliday Junctions (HJs) which can be resolved by specific endonucleases. To complete the repair reaction the resulted pieces of DNA are ligated together. The second option is when the first invading DNA strand is displaced from the joint molecule, but re-anneals with the second end of the break in a process termed synthesis-dependent strand annealing (SDSA) (Sung and Klein, 2006; Lisby and Rothstein, 2009).

As already stated before, the persistence of damaged DNA can have grave consequences. An example where these consequences become apparent is when mutations in the gene coding for BRCA2 cause abnormal behaviour of the protein. This can lead to damages not being processed (correctly) and mutations in other genes will accumulate. This in turn can lead to uncontrolled cell growth and cancer. Mutations in BRCA2 are mostly linked to breast cancer, but can also cause ovarian cancer, prostate cancer, and pancreatic cancer (Antoniou et al., 2003; Struewing et al., 1997; Ryan et al., 2014).

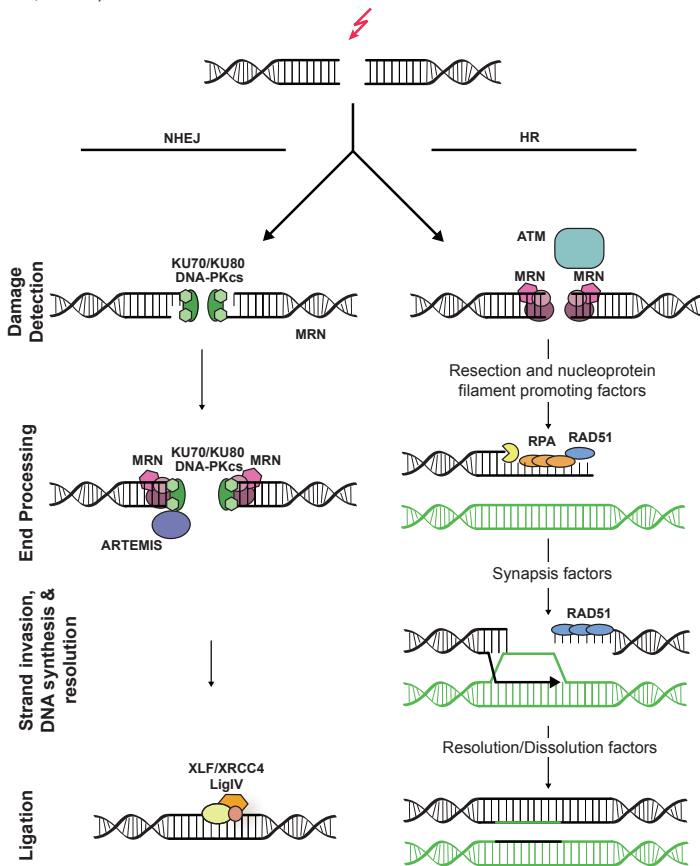


Figure 2. Schematic overview of double-strand break repair via non-homologous end-joining (NHEJ) or homologous recombination (HR). In the NHEJ pathway the recognition of the DSB is initiated by the KU70/KU80 heterodimer which coordinates the activity of the downstream repair factors and serves as a scaffold. Subsequently, the heterodimer recruits DNA-PKcs which phosphorylates and thereby activates the nuclease ARTEMIS. Together with the MRN complex, ARTEMIS then processes the DNA ends to make them suitable to be ligated. This ligation step is then performed by a ligase complex consisting of XRCC4, XLF, and LigIV.

In the HR pathway the DSB is recognized by the MRN complex. This complex then recruits the phosphatidylinositol 3-kinase ATM, which in turn phosphorylates histone H2AX and others to invoke repair and checkpoint signalling. The DNA is resected and the resulting ssDNA is bound by RPA, which is subsequently replaced by RAD51. This protein then promotes the invasion of the ssDNA to the homologous DNA template. The resulting synapsis is then used for new DNA synthesis, dissolution, and repair. HR is less error-prone than the NHEJ pathway since it uses nucleotide sequence in the homologous sister chromatid to restore genetic information in the broken strand. Figure adapted from Lans et al, Epigenetics & chromatin 2012

Base excision repair (BER)

Apart from damages affecting the structural integrity of whole chromosomes, also the bases of the DNA helix can become damaged and non-bulky small nuclelease lesions can be formed. Such lesions are most often caused by reactive oxygen species (ROS) which are produced during normal cellular metabolism. Other sources include the oxidation, deamination, and alkylation of nucleotides which in turn result in the formation of damaged nucleotide derivatives such as 8-dihydroguanine (8-oxoG), 8-oxo-7, 3-methyladenine, and hypoxanthine (Hegde et al., 2008). 8-oxoG lesions are the most harmful of this set and can lead to GC to TA transversion during replication. To deal with these types of lesions the Base Excision Repair (BER) pathway is in place. This pathway excises the damaged or incorrect nucleotide and replaces it with the correct one (Kim and Wilson, 2012). The downstream steps of BER are also used in dealing with single-strand breaks (SSBs). Recognition of lesions in this pathway is achieved by specific glycosylases, each recognizing a specific type or subgroup of damaged bases (Figure 3). The known DNA glycosylases which have been described in literature have a broad overlap in their specificity, leading to high levels of redundancy (Hang et al., 1997; Engelward et al., 1997; Klungland et al., 1999). In general, DNA-glycosylases recognize and remove damaged nucleotides by a process called 'base flipping'. The glycosylase continuously tries to bind to the DNA by bending the DNA double helix. When this is performed at the site of a lesion the bending of the double helix causes the damaged base to flip out and enter the binding pocket of the enzyme. (Huang et al., 2003). Subsequently the N-glycosidic bond between the substrate base and the 2'-deoxyribose is cleaved by endonucleases specific for the resulting apurinic/apyrimidinic (AP) site. The major AP endonuclease in mammals is AP-endonuclease 1 (APE1) and is thought to perform more than 95% of the total AP site incision activity (Dempfle and Sung, 2005). The incision leaves a SSB which, depending on the recognizing glycosylase, can be processed by either short-patch BER (SP-BER) or long-patch BER (LP-BER). When processed by SP-BER, the single nucleotide gap is filled by DNA polymerase β (Pol β) and the DNA ends are ligated together by the XRCC1-DNA ligase III α (Dianov and Hübscher, 2013). If the gap is processed by LP-BER, the APE1 induced nick on the 5' end of the AP site leads to recruitment of Proliferating Cell Nuclear Antigen (PCNA) and DNA polymerase δ (Pol δ). The recruitment of these enzymes displaces the strand while Pol δ incorporates 2 to 8 nucleotides of new DNA. This strand displacement produces a DNA flap that is refractory to ligation and needs to be resolved. Flap structure-specific endonuclease 1 (FEN1) is recruited and degrades the displaced DNA fragment, after which DNA ligase 1 can ligate the remaining ends of the newly incorporated nucleotides (Robertson et al., 2009).

The clinical consequences of defective BER are not as common as with the earlier discussed DSBs pathways. This might be because most of severe defects in core BER factors seem to be incompatible with life. Mouse knock outs with Pol β , APE1, and DNA ligase 1 are embryonic lethal (Maynard et al., 2009). This however does not mean there are no links to disease at all. It has been found that about 30% of all human tumours have mutations in Pol β . In 50% of these cases only one amino acid has changed (Starcevic et al., 2004). Another example is the decreased expression of APE1 in patients with sporadic amyotrophic lateral sclerosis (ALS) (Kisby et al., 1997). These and other examples show that it is more mutations and problems with regulation of the BER pathway that have pathological impact.

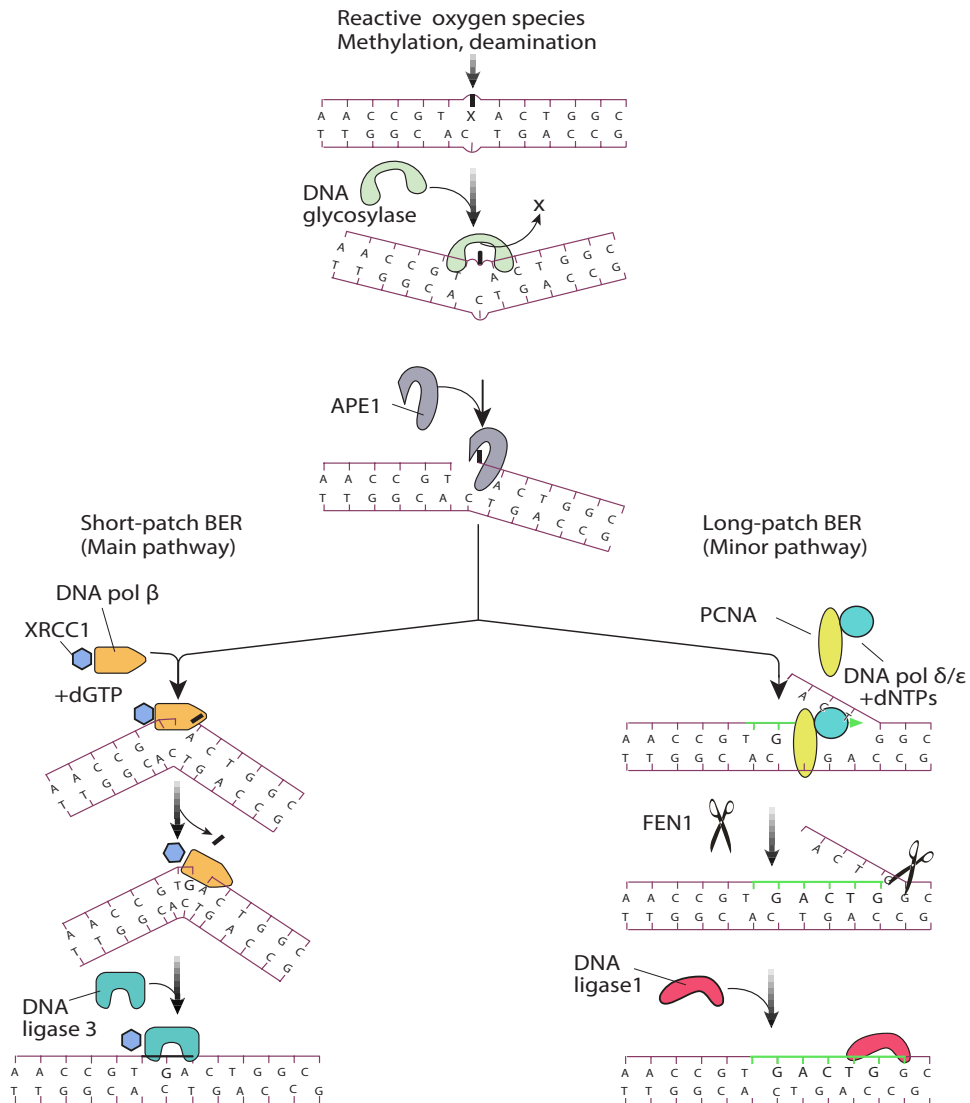


Figure 3. Schematic overview of the base-excision repair (BER) pathway. The lesion is recognized by a lesion type specific glycosylase. This glycosylase flips the damaged base out of the DNA helix by compressing the DNA backbone and driving the base into the active site of the glycosylase. The base is then cleaved from the sugar-phosphate backbone of the DNA double helix. This results in an abasic site which is recognised by the endonuclease APE1. After recognition APE1 incises the strand of DNA leading to one of two possible pathways. In short-patch BER the resulting one nucleotide gap is filled by DNA Pol β and the DNA ends are ligated together by the XRCC1-DNA ligase III α .

If the gap is processed by long patch BER the APE1 induced nick on the 5' end of the AP site leads to recruitment PCNA and DNA Pol δ , causing displacement of the strand and incorporation of 2 to 8 nucleotides of new DNA by Pol δ . This strand displacement produces a DNA flap that is refractory to ligation and needs to be resolved. Flap structure-specific endonuclease 1 (FEN1) is recruited and degrades the displaced DNA fragment, after which DNA ligase 1 can ligate the remaining ends of the newly incorporated nucleotides. Figure adapted from Hoeijmakers, Nature 2001

Mismatch Repair (MMR)

During replication and recombination, erroneous insertion, deletion or mis-incorporation of bases can occur. These spontaneous mutations occur on average at a frequency of 1 per 10^9 - 10^{10} base pairs per cell division in humans (Drake, 1991). To increase the fidelity of the copying process, amongst other measures, the DNA mismatch repair (MMR) pathway is in place. The MMR pathway recognizes and repairs these mismatches and by doing so decreases the frequency of spontaneous mutations 50-1000 fold (Iyer et al., 2006).

MMR is initiated in eukaryotes during replication (Modrich, 2006). There are two possible modes of recognition (Figure 4). In the case of base-base mismatches or when there are one or two base loops, the mismatch is bound by a heterodimer of MutS α homologues (MSH2/MSH6). If there are larger base loops the mismatch is bound by MutS β homologues (MSH2/MSH3) (Acharya and Wilson, 1996). This is followed by an ATP-dependent conformational change of MutS proteins, which results in the recruitment of MutL α homologues (MLH1/PMS2) or MutL β homologues (MLH1/PMS1) heterodimers. The MutL heterodimers then translocate in either direction to search for strand discontinuity and nick the 3' or 5' side of the mismatched base on the orientation of the PCNA clamp. In this way, MMR distinguishes the nascent and the template strands (Pluciennik et al., 2010). The EXO1 exonuclease then degrades the stretch of DNA harbouring the mismatch, leaving a short stretch of ssDNA, which is protected by binding of RPA. The stretch is then filled by the DNA Pol δ and remaining nicks are ligated by DNA ligase I (Iyama and Wilson, 2013).

Defects in the MMR pathway are most known in the context of hereditary nonpolyposis colorectal cancer (HNPCC). In this form of colon cancers mutation of MLH1 and MSH2 cause defective MMR, mostly resulting in changes in the lengths of dinucleotide repeats of the nucleobases cytosine and adenine (Fishel et al., 1993; Papadopoulos et al., 1994). This causes repeats with, amongst others, a CACACACACA... sequence which greatly destabilize the genome and causes mutation of genes.

Interstrand Cross-Link (ICL) repair

Interstrand cross-links (ICLs) are lesions in which two DNA strands in the double helix are covalently linked. ICLs can arise from endogenously produced metabolites from peroxidised lipids and the metabolism of dietary components e.g. coffee, ripe fruit and alcohol (Clouston et al., 2013). Exogenous sources include chemical compounds which are often used as chemotherapeutic drugs, such as mitomycin C (MMC) and cisplatin (Muniandy et al., 2010). Research has shed some light on the repair of ICLs, but the exact molecular components and kinetics are not all identified. Up till now 16 causative proteins have been identified. Repair is performed by a complex combination of these Fanconi Anemia (FA) proteins and factors from nucleotide excision repair (NER), HR, Translesion synthesis (TLS) (Deans and West, 2011).

The FA pathway is initiated by the binding of the ATP-dependent DNA helicase FANCM Fanconi anemia, complementation group M (FANCM) to a stalled replication fork (Kee and D'Andrea, 2012). FANCM then unwinds the DNA, creating ssDNA to which RPA binds (Schwab et al., 2010). The binding of RPA then induces ATR-mediated signalling which leads to activation of the core FA complex. Of this 12 subunit large complex, Fanconi anemia, complementation group L (FANCL) mono-ubiquitylates the Fanconi anemia, complementation group D2 (FANCD2), Fanconi anemia, complementation group L (FANCL) heterodimer (D2/I) (Cole et al., 2010; Garner and Smogorzewska, 2011). Monoubiquitinated D2/I is recruited to the site of damage and functions as a docking site for downstream structure-specific nucleases. These nucleases include endonuclease excision

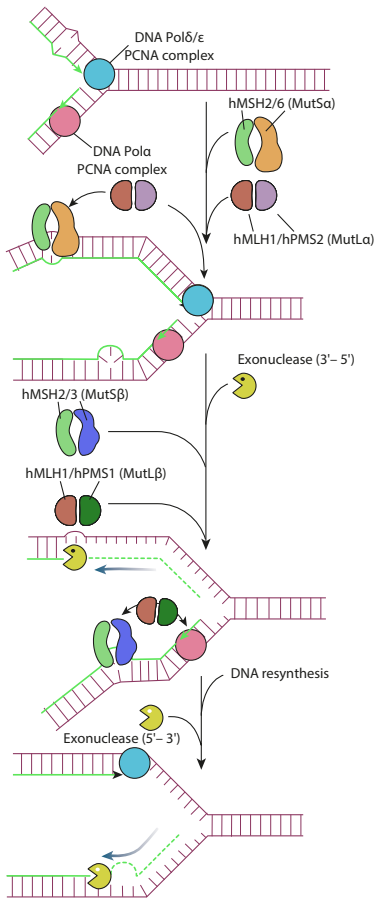


Figure 4. Schematic overview of the mismatch repair (MMR) pathway. There are two possible modes of recognition of nucleotide mismatches or base loops in the double stranded DNA. In the case of base-base mismatches or when there are one or two base loops (bases in one strand of the DNA without a conjugated base), the mismatch is bound by a heterodimer of MutSα homologues (MSH2/MSH6). If the damage consist of larger base loops the mismatch is bound by MutSβ homologues (MSH2/MSH3).

This is followed by an ATP-dependent conformational change of MutS proteins, which results in the recruitment of MutLα homologues (MLH1/PMS2) or MutLβ homologues (MLH1/PMS1) heterodimers. The MutL heterodimers then translocate in either direction to search for strand discontinuity and nick the 3' or 5' side of the mismatched based on the orientation of the PCNA clamp. In this way, MMR distinguishes the nascent and the template strands. The EXO1 exonuclease then degrades the stretch of DNA harbouring the mismatch, leaving a short stretch of ssDNA, which is protected by binding of RPA. The stretch is then filled by the DNA Polδ and remaining nicks are ligated by DNA ligase I. Figure adapted from Hoeijmakers, Nature 2001.

repair cross-complementing protein 1-Xeroderma pigmentosum group F (ERCC1-XPF), the MUS81- Essential Meiotic Endonuclease 1 (EME1) complex, SLX1, and FANCD2/FANCI-associated nuclease 1 (FAN1) (Ciccia et al., 2008). On either side of the covalently linked nucleotides an incision is made by these nucleases. This leaves an unhooked crosslink which is still tethered to the complementary strand. Docking protein SLX4 interacts with all of these nucleases and is thought to coordinate the unhooking reaction, but it is still unknown how this is achieved. To bypass the unhooked crosslink TLS polymerases REV1 and Pol ζ are recruited. HR is then induced by downstream FA proteins initiating RAD51-dependent strand invasion (Kim and D'Andrea, 2012). Subsequently NER removes the remaining unhooked adduct and fills the resulting gap. In a final step the Ubiquitin carboxyl-terminal hydrolase 1 (USP1)/ WD repeat-containing protein 48 (UAF1) complex deubiquitylates D2/I to complete the pathway (Nijman et al., 2005a).

Covalently linked strands of the DNA double helix are extremely hazardous since they block transcription as well as replication, and may disrupt overall chromatin structure. Where other forms of DNA damage are mostly mutagenic, interstrand cross-links (ICLs) are mostly clastogenic, i.e., they give rise to or induce disruption or breakages of chromosomes leading to sections of the chromosome being deleted, added, or rearranged. These damages can produce the gain, loss, or rearrangement of chromosomal segments and/or cause sister chromatid exchanges (Noll et al., 2006).

Nucleotide excision repair (NER)

Nucleotide excision repair (NER) removes a wide variety of structurally unrelated DNA lesions. This wide variety of lesions have in common that they are all, to some degree, helix-distorting and locally impair proper Watson and Crick base pairing. One source which can cause these lesions is the UV-C irradiation which our cells receive from sunlight. This UV-C irradiation leads to the formation of dimeric photoproducts involving two of the adjacent pyrimidine bases. Examples of these lesions are cyclobutane pyrimidine dimers (CPDs) and pyrimidine- (6,4)-pyrimidone photoproducts (6-4PPs). Other known causes for these bulky lesions are certain chemotherapeutic agents such as cisplatin, and chemicals in cigarette smoke (Kim and Choi, 1995; Cadet et al., 2005). Both transcription and replication are severely hampered by these bulky lesions and need to be resolved. An example of a problem in transcription is when RNA polymerase II encounters such a lesion. When this happens the elongation reaction stalls. This unresolved stalling can lead to single or double strand breaks, re-arrangements, mutations and ultimately apoptosis and premature aging (Ljungman and Zhang, 1996). Nucleotide Excision Repair (NER) is the pathway in place to cope with these lesions and it consists of more than 30 highly coordinated proteins performing the multi-step repair process. This process can be divided in the following steps: damage recognition, DNA helix unwinding, damage verification, lesion excision, DNA synthesis and ligation (Figure 5).

Damage recognition:

There are two essentially different mechanisms by which NER recognises damages: transcription-coupled repair (TC-NER) and global genome repair (GG-NER) (Hanawalt and Spivak, 2008; Gillet and Schärer, 2006). In the TC-NER pathway, lesions are detected by the stalling of a RNA polymerase II (RNAP2) when it is actively transcribing a gene. RNAP2-stalling then triggers recruitment of secondary factors, including Cockayne syndrome A and B (CSA, CSB), to initiate the formation of a functional TC-NER complex (Hanawalt, 2002; Foustari et al., 2006).

Lesions in other parts of the genome, including the non-transcribed strands of active genes, are detected by GG-NER. The DNA binding protein Xeroderma pigmentosum group C (XPC) is the main damage sensor in GG-NER (Masutani et al., 1994; Sugawara et al., 1998; Nishi et al., 2005). It forms a complex together with RAD23B and Centrin-2. *In vitro* experiments have shown that XPC binds to a myriad of different DNA structures that cause DNA helix destabilisation and even bind to nucleotide mismatches which do not activate NER *in vivo* (Sugawara et al., 2001). The model proposed for the binding of XPC is based on crystal structures of the yeast XPC homologue RAD4 bound to a DNA molecule containing a CPD (Min and Pavletich, 2007). XPC binds to a small piece of ssDNA opposite of the lesion caused by the disrupted base pairing. This binding is performed by inserting the carboxy-terminal double β -hairpin of XPC at the junction between the dsDNA and the ssDNA. If this is possible, it leads to stable binding of XPC and possibly extending the ssDNA to enable recruitment of downstream NER factors.

Although this binding mechanism works very well in the case of 6-4pps, XPC is not able to recognize a lesion if the distorting effect of the lesion on the DNA helix is too small. This is for instance the case with CPD lesions. These lesions create too little distortion to be efficiently recognized by the XPC-complex alone. Therefore, full function of XPC requires additional factors, like the UV-damaged DNA-binding (UV-DDB) complex (Moser et al., 2005; Chu and Yang, 2008). This heterodimer complex consists of two subunits, DNA damage-binding protein 1 (DDB1) and DNA damage-binding protein 2 (DDB2). This complex directly binds to the CPD lesion and acts as secondary damage-recognition factor by stimulating the binding of XPC (Wakasugi et al., 2002;

Scrima et al., 2008; Groisman et al., 2003). This is achieved by DDB2 directly binding to the lesion, extruding the lesion into its binding pocket and thereby kinking the DNA in such a way that the damage is exposed, thereby facilitating subsequent XPC binding.

DNA helix unwinding and lesion verification:

After lesion recognition has taken place, either by TCR or GGR, the same core NER machinery is recruited. First, the DNA helix is unwound by the general Transcription factor II H (TFIIH) and the lesion is verified. This process makes the lesion accessible for downstream NER proteins (Sugasawa et al., 2009; Volker et al., 2001; Giglia-Mari et al., 2004; Ranish et al., 2004). Unwinding is performed by two subunits, Xeroderma pigmentosum group B (XPB) and Xeroderma pigmentosum group D (XPD), which are ATP dependent helicases that unwind a stretch of 30 nucleotides of the helix containing the lesion (Schaeffer et al., 1993; Coin et al., 1998). Apart from this role of TFIIH during the NER reaction, this ten subunit large protein the helicase capabilities also plays a major role during transcription (Zurita and Merino, 2003).

Although there is still ample discussion about the order of binding in the NER reaction (Luijsterburg et al., 2010), currently it is thought that after opening of the helix, Xeroderma pigmentosum group A (XPA) and RPA get access to the NER complex. The precise role of XPA is not fully understood, but it is regarded the key player in this step of the NER reaction. It is not only associated with stimulating lesion verification by TFIIH but also interacts with almost all other NER proteins. Therefore it is considered to be the central coordinator and directs the precise positioning of the complex before the incision step of the pathway (Sugasawa et al., 2009; Schärer, 2013). After the unwinding of the DNA the undamaged strand needs to be protected from endonucleases. This is achieved by the binding of RPA, which protects the ssDNA and stabilizes the open complex formation together with XPA and TFIIH (Gourdin et al., 2014)

Lesion excision and gap filling:

The heterotrimeric RPA also correctly positions the endonuclease Xeroderma pigmentosum group G (XPG) and the heterodimeric ERCC1-XPF complex (de Laat et al., 1998; Rademakers et al., 2003; O'Donovan et al., 1994; Zotter et al., 2006; Sijbers et al., 1996). When verification of the lesion and proper orientation of the core NER factors is complete the endonucleases XPG and ERCC1-XPF incise the 3' and the 5' side of the damage, respectively. The excised piece of ssDNA containing the lesion is then released and degraded, leaving a RPA protected single-strand gap to be filled. Gap filling is initiated by the replication machinery including DNA polymerases δ , ϵ or κ , Replication factor C (RFC) and Proliferating Cell Nuclear Antigen (PCNA) (Ogi et al., 2010). As a final step, the nick in the DNA backbone is sealed by either DNA ligase I or III (LigI or LigIII) (Moser et al., 2007)

Defects in the NER process are best illustrated by several rare, autosomal recessive disorders. Xeroderma pigmentosum (XP) is one of these disorders. XP is caused by mutations in the XP genes (XPA through XPG). Patients who suffer from this disease show dry skin (xeroderma), abnormal pigmentation in sun exposed skin (pigmentosum), photohypersensitivity of the skin, and an almost 10.000-fold increased risk for skin cancer in patients below 20 years of age (DiGiovanna and Kraemer, 2012). Another disease linked to NER is Cockayne syndrome (CS). CS is caused by mutations in either CSA or CSB, both important proteins needed when RNAP2 stalls at a lesion. Like XP patients, CS patients also show a photohypersensitivity of the skin but they do not harbor the same increased risk for skin cancer (Nance and Berry, 1992; Pines et al., 2010). Furthermore, CS patients show severe developmental, neurological, and premature aging features.

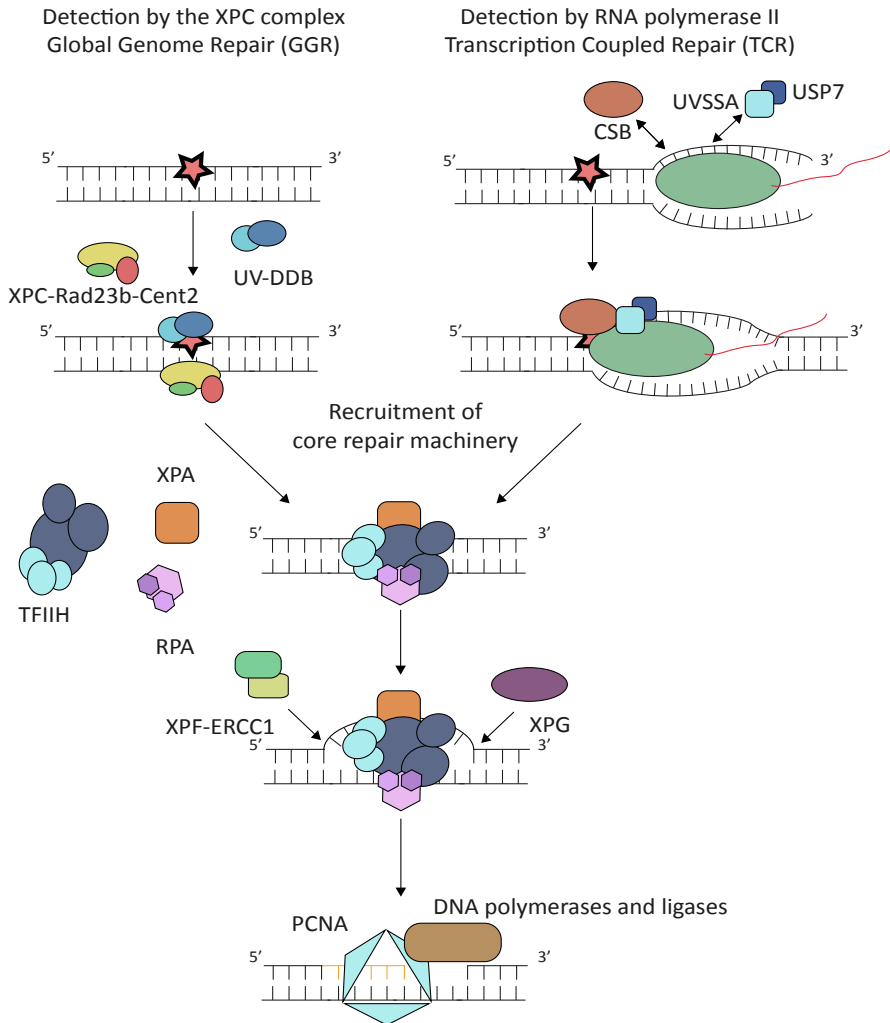


Figure 5. Schematic overview of the nucleotide excision repair pathway (NER). Lesions can be detected by in two different ways. In global genome NER (GG-NER) helix-destabilising lesions are recognised by XPC-RAD23-CETN2 and UV-DDB complexes. In transcription-coupled repair (TC-NER) the lesions is recognised by stalling of a RNA polymerase II (RNA PolII) at the lesion in the transcribed strand of the active gene. Stalling of RNA PolII leads to stable binding of CSB, UVSSA and other proteins. After recognition, either by RNA PolII or XPC, the core NER machinery is recruited. Helicase transcription Factor II H (TFIIH) opens the DNA around the damage and XPA binds to verify the lesion and the orientation of all the repair factors. RPA is recruited to stabilise the ssDNA created by the unwinding of the helix. Subsequently the specific endonucleases XPF-ERCC1 and XPG excise the damaged strand on the 5' and 3' side respectively. This results in a 25-30 nt ssDNA gap which is filled by replication machinery proteins PCNA and several DNA polymerases (δ , ϵ and/or κ). In the final step the remaining nick is sealed by DNA ligase I or IIIa.

Post Translational Modifications (PTMs)

When a protein is translated and correctly folded into its mature form, the cell still controls its behaviour and lifespan. These control levels are largely achieved by post-translational modifications (PTMs). Chemical groups are specifically added to or removed from specific residues of the protein to turn on, turn off, tune, change, or destroy the protein. Tight regulation by PTMs of the concerted actions of proteins is vital in all cellular processes, including the DDR.

The DDR pathways consist of multiple steps in which timing, localisation and availability of involved proteins are key factors to ensure a proper and swift handling of DNA damages. For this reason the importance of the existence of DNA damage signalling pathways cannot be understated. Apart from (de)activating specific proteins, signalling can induce cell cycle arrest in G1/S phase transition, intra S or G2/M phase transition. This arrest gives cells the time to repair the encountered damage. If the damage load is too high and DDR mechanisms cannot cope with the damages in time, signalling persists, which can result in cellular senescence or apoptosis. This ensures that cells do not propagate faulty or broken DNA and aberrant cellular processes in daughter cells do not wreak havoc. The cell has multiple signalling pathways and mechanisms to its disposal, foremost using PTMs to achieve this tight regulation of processes. In the following paragraphs the most important will be discussed.

Phosphorylation

Kinases and phosphatases are well-known (de)activators and regulators of cellular processes and play a major role in several DDR pathways. Three crucial kinases of the phosphatidylinositol 3-kinase-like kinases (PIKKs) family are ataxia telangiectasia-mutated (ATM), ataxia telangiectasia and Rad3-related kinase (ATR) and DNA-dependent protein kinase catalytic subunit (DNA-PKcs) (Falck et al., 2005; Jackson and Bartek, 2009). These kinases induce a signalling cascade by phosphorylating downstream targets, for instance p53 and Checkpoint kinase 1 and 2 (Chk1 and Chk2). Phosphorylation and stabilisation of p53 can occur after UV irradiation which in turn can trigger cell cycle arrest or apoptosis (Mckay et al., 1998; Ljungman et al., 1999). Members of this family are also responsible for one of the most prominent chromatin modifications after DNA damage, namely the phosphorylation of histone variant H2A.X. This phosphorylation is mediated by DSB recognition by the MRN complex which triggers ATM to phosphorylate H2A.X (the phosphorylated variant is therefore often referred to as γ -H2A.X). Another example where phosphorylation plays a role is when the kinase ATR is triggered by replication blockage to phosphorylate downstream repair factors after UV irradiation or hypoxia (Koundrioukoff et al., 2004; Foiani et al., 2000; Abraham, 2004). It has been shown that at least part of this activity in replicating and non-replicating cells is dependent upon GG-NER activity (Marini et al., 2006; Marteijn et al., 2009; Hanasoge and Ljungman, 2007).

PARYlation

Poly(ADP-ribosylation) or PARYlation was discovered in the 1960s and has since been associated with the DDR (Nishizuka et al., 1967; Chambon et al., 1963). PARYlation is the process where an ADP-ribosyl moiety is covalently linked to a target protein. Poly(ADP-ribose)polymerase (PARP) catalyses this process by using NAD⁺ as a substrate and cleaving off the nicotinamide during the covalent linkage. Chains of ADP-ribose units can be formed by elongation of the first unit to create branched polymer structures which are termed poly(ADP-ribose) (PAR) (Bürkle and Virág, 2013). DDB2, the protein aiding XPC in recognizing certain cryptic lesions is an example of a protein

which can be PARylated. UV-dependent PARylation of DDB2 induces chromatin de-condensation. PARylation also suppresses ubiquitylation-dependent degradation and promotes DNA binding (Luijsterburg et al., 2012). In turn, DDB2 promotes the poly(ADP-ribose) polymerase 1 dependent (PARP1) PARylation of chromatin. This PARylation aids the recruitment of the ATP-dependent chromatin remodelling enzyme Amplified in Liver Cancer 1 (ALC1). Although the specific role of ALC1 is unclear it is speculated it is needed to modulate chromatin structure through nucleosome sliding. This in turn would allow for recruitment of XPC on CPDs and stimulates NER (Pines et al., 2012).

Acetylation and Methylation

Modifications which change the structure of chromatin are indicated to have a positive influence on the NER process. Acetylation is typically associated with open chromatin and active transcription (Kuo and Allis, 1998). When this type of chromatin is hyper-acetylated by inhibiting the de-acetylation using de-acetylase inhibitors the repair rate is significantly increased (Ramanathan and Smerdon, 1989). Methylation is also a mark for either active or inactive chromatin, depending on which variant of histones are either mono- or tri-methylated. Studies performed in yeast have for instance shown that histone-3-lysine-79 (H3K79) methylation by Disruptor Of Telomeric silencing 1 (DOT1p) is required for efficient UV damage response. Disruption of this methylation results in UV hypersensitivity and the lack of an intra-S phase checkpoint (Bostelman et al., 2007; Giannattasio et al., 2005).

Ubiquitylation and ubiquitin-like modifications

Protein ubiquitylation is an important PTM in many cellular processes. Ubiquitin (Ub) is a highly conserved 76 amino acid, 8.5 kDa (small) protein. Ubiquitylation of lysine residues controls the localization, activity and stability of almost all proteins (Grabbe and Dikic, 2009). Ub (and Ub-likes) can be covalently attached to the ϵ -amino group of lysine residues or in less frequent cases the N-terminal amino group of the target protein (Ciechanover, 1994; Ciechanover and Ben-Saadon, 2004). Target ubiquitylation is orchestrated by three enzymes: the Ub-activating E1, the Ub-conjugating E2 and the Ub-ligating E3 (Hershko and Ciechanover, 1998) (Figure 6). In the first step the E1 enzyme uses ATP to form an E1-thioester-Ub intermediate. This activated Ub is then in the second step transferred and conjugated from the E1 to the active site E2, hence called the conjugation step. The third, final step involves ligating the Ub to the target protein. In general, the Ub-conjugated E2 binds to a target specific E3 ligase, which in turn covalently couples the C-terminal glycine Ub-residue to a lysine residue of the target protein via an isopeptide bond (Pickart, 2001).

Currently only two E1 enzymes for ubiquitin are identified in the human genome (Jin et al., 2007; Pelzer et al., 2007), while there are over 30 E2 enzymes with which they can interact (Markson et al., 2009; Michelle et al., 2009). Subsequently, E2 enzymes can associate with more than 600 putative E3 ligases known in the human genome (Li et al., 2008). The E3 enzymes can be (sub)divided in 3 families (Berndsen and Wolberger, 2014) depending on one specific characterizing domain: homologues to E6-AP-coxyl-terminus (HECT) domain (Scheffner and Kumar, 2014), Really interesting new gene (RING) domain (Deshaies and Joazeiro, 2009) and the RING-between-RING (RBR) domain ligases (Wenzel and Kleit, 2012). E3s containing a HECT domain and RBR E3s are catalytically active, in contrast to the RING E3s. The HECT domain consists of roughly 350 residues in a bi-lobal conformation. The N-terminal lobe harbours an E2-binding site and the C-terminal lobe contains a cysteine which can accept Ub from the E2 before conjugation and allow for

chain-specific polyubiquitylation of the target (Kim and Huibregtse, 2009). The RBR family has a similar, but subtle different activity. Here an E2 first binds to the first RING domain thereafter transferring the Ub to a cysteine residue in the second RING domain. As a final step, the Ub is then transferred to the target protein. The largest family is that of the RING E3s, which only mediate the direct transfer of the Ub to the target protein.

For the ubiquitin-like proteins Small Ubiquitin-like Modifier (SUMO) and Neural-precursor-cell-Expressed Developmentally Down-regulated 8 (NEDD8) similar mechanisms of conjugation to target proteins have been described (Matunis et al., 1996; Kamitani et al., 1997).

This multistep process seems to ensure a high level of regulation and specificity by increasing the amount of possible combinations in each step. Examples have been found where transfer of the Ub was E3 independent and the E2 directly ligates the Ub to the target protein (van Wijk and Timmers, 2010). Next to the combinations between the E1, E2, and E3 enzymes, the possibility of poly-ubiquitylation discussed in the next section adds even more possible combinations and possibilities for the cell to regulate and fine-tune processes.

Poly-Ubiquitylation

When a single Ub has been conjugated to the target protein at one or more lysines (mono-ubiquitylation) it is also possible to conjugate more Ubs to this first one resulting in a chain of Ubs (poly-ubiquitylation). All the available lysine residues (K6, K11, K29, K33, K48 and K63) of the original conjugated Ub have been reported to be used for this poly-ubiquitylation step, resulting in (branched) chains of either one type of linkage. It is also possible that the chains are comprised of a mix of linkages within the chain.

The best-known and most abundant form of poly-ubiquitylation in the cell is that of K48 chains. This form of ubiquitylation is primarily a signal for degradation by the 26S proteasome (Chau et al., 2014). Another example are K63 chains, which have been found to be involved in ribosomal functioning, endocytosis and DNA repair (Hicke, 1999; Spence et al., 2000; Bergink and Jentsch, 2009). Other chains have been found as secondary degradation signals (K11) or signals preventing degradation (K6) (Kulathu and Komander, 2012).

Mixed poly-ubiquitin chains have not been extensively studied because current techniques poorly discriminate between branched and unbranched chains of Ub, but recently a study tried to shed more light on the subject. In this study it was shown that the specific signalling capabilities of for instance K63 chains and K48 chains are retained. This could indicate that mixed chains can carry multiple signals which can still be discriminated by their receptors (Nakasone et al., 2013). Since these chains are structurally different, this provides the cell with an extensive network of regulation layers. The addition of different Ub-chains to various lysine residues changes the function of the target protein (Li and Ye, 2008; Komander and Rape, 2012).

De-ubiquitylating enzymes (DUBs)

Like all PMTs, ubiquitylation is reversible. As there are specific proteins which can attach one or more Ubs to a target protein there are also specific proteases which can cleave off Ub or even engage in editing of the complete Ub chain (Clague et al., 2012; Komander et al., 2009). These de-ubiquitylating enzymes (DUBs) can be general in their activity, but there are also specialized DUBs known which can be either chain- or substrate-specific (Nijman et al., 2005b). It is interesting

to note that the majority of these DUBs are not specific in their activity. This is very common in biological regulatory systems, where it seems easier to have very specific modifying enzymes for PTMs, but unspecific de-modifiers for these same PTMs.

Ubiquitylation in NER

Lesion recognition by the GG-NER pathway and numerous other steps in the NER pathway have been found to be regulated by (de)ubiquitylation. The UV-DDB associates with the cullin 4A (CUL4A)-regulator of cullins 1 (ROC1) E3-ubiquitin ligase (CTRL) via its conserved C-terminus. The ligase activity of the UV-DDB-E3 complex is inhibited by neddylation of the CUL4a subunit by the COP9 signalosome (CSN). Upon UV irradiation CSN dissociates and allows neddylation after lesion binding (Groisman et al., 2003). This activation leads to poly-ubiquitylation of DDB2 and XPC, but has different effects on both of them. Poly-ubiquitylation of DDB2 upon UV irradiation results in rapid degradation of DDB2 by the 26S proteasome (Yeh et al., 2012; Fitch et al., 2003). However, poly-ubiquitylation of XPC does not lead to its degradation but *in vitro* has shown to increase the affinity for DNA lesions (Sugasawa et al., 2005). Interestingly, *in vivo* the ubiquitylated form of XPC was not only found in the chromatin bound fraction but also in the soluble nuclear fraction of the chromatin immune-precipitation experiments (Wang et al., 2005; Sugasawa et al., 2005). This could indicate that the modification has a trans-effect throughout the nucleus and is not only lesion specific.

RAD23 has been held responsible for the protection against proteasomal degradation of XPC. Cells lacking HR23A and HR23B display dramatic reduction of XPC levels, which can be counteracted by blocking the 26S proteasome (Ng et al., 2003). In contrast it has also been shown RAD23 is essential for binding of XPC to lesions. Experiments in RAD23A and RAD23B double knock-out mouse embryonic fibroblast (MEF) cells reveal that after UV irradiation XPC does not bind to lesions. Intriguingly, RAD23 itself does not accumulate on UV-induced lesions. Fluorescence recovery after photobleaching (FRAP) experiments show that the mobility of RAD23 after UV irradiation is slightly higher than in absence of damage. Therefore it is hypothesized that RAD23 leaves the XPC complex upon lesion recognition and stable binding by XPC (Bergink et al., 2012). This seems to conflict with the earlier mentioned observations that XPC ubiquitylation takes place almost simultaneously with binding (Sugasawa et al., 2005), and suggests that RAD23 is not the factor protecting XPC from degradation. This suggests there is another factor responsible for the ubiquitylated form of XPC not being degraded. A possible explanation to this is offered in chapter 4 where we show that the ubiquitylation of XPC is responsible for a molecular switch needed for binding of XPC to the lesion.

Recently, the ubiquitin E3 ligase ring finger protein 111 (RNF111) was identified as a factor promoting XPC ubiquitylation (Poulsen et al., 2013). RNF111 is a member of the family of SUMO-targeted ubiquitin ligases (STUbLs), which facilitate crosstalk between SUMOylation and ubiquitylation (Prudden et al., 2007; Sun et al., 2007; Uzunova et al., 2007). In chapters 2 and 3 of this thesis we show that RNF111 specifically targets SUMOylated XPC and modifies it with K63-linked ubiquitin chains in a UBC13-dependent manner. We show that although RNF111 is not essential for GG-NER, it strongly enhances the repair reaction by stimulating the release of XPC from damaged DNA, thereby enabling the progress of the NER reaction by recruitment of the endonucleases XPG and XPF/ERCC1.

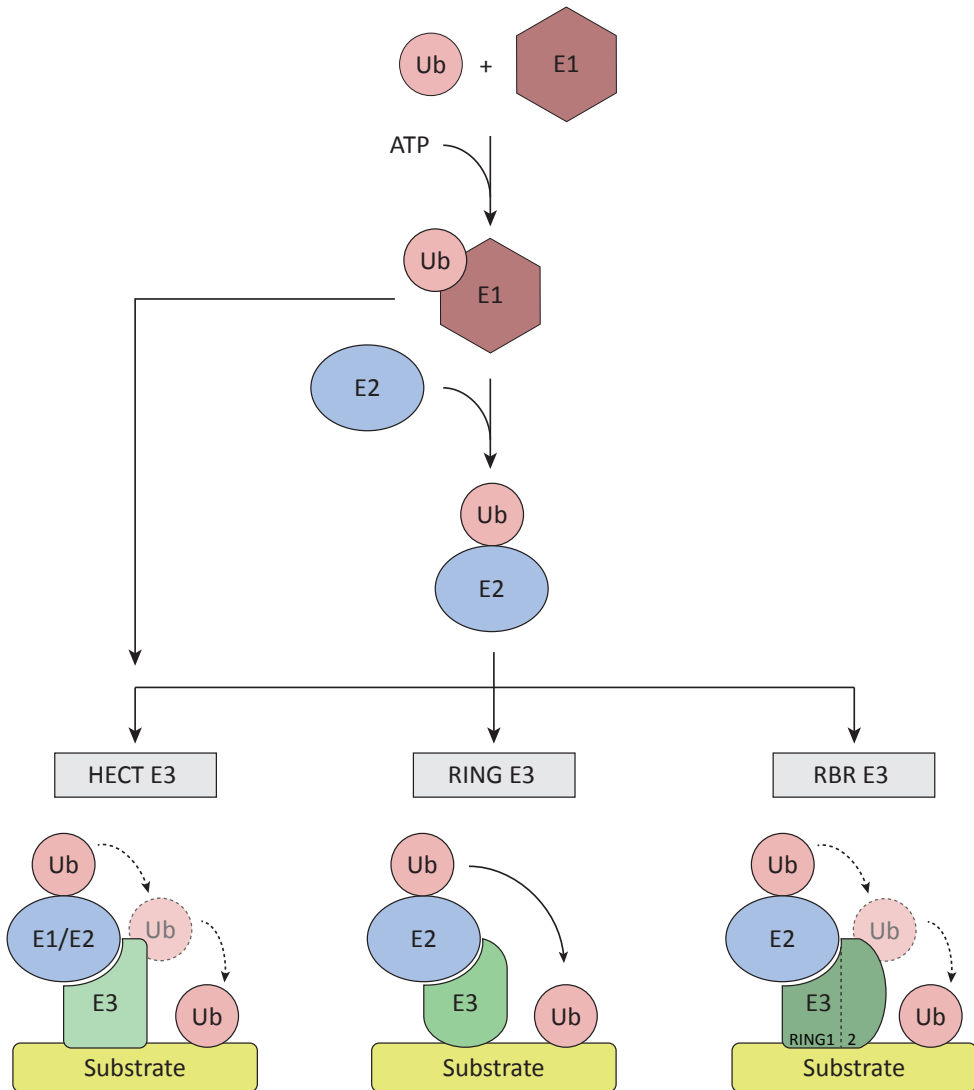


Figure 6. Schematic overview of the ubiquitylation pathway. The covalent binding of a Ubiquitin (Ub) molecule to a lysine residue in a target protein takes place in three distinct enzymatic steps. The Ub is activated by the activating E1 enzyme. A thioester bond is formed between the Ub C-terminus and an internal cysteine residue of the E1. In the next step the activated Ub is transferred to the active-site cysteine of a Ub conjugating E2 enzyme. The final step involves a Ub ligating E3 enzyme which catalyses the formation of an isopeptide bond between the C-terminal glycine residue of the Ub and a lysine of the substrate protein. Currently there are three type of E3 enzymes known: HECT E3s, RING E3s, and RING-between-RING (RBR) E3s. With RING E3s the activated Ub is transferred directly from the E2 to the substrate protein. Both with HECT and RBR E3s the activated Ub is first transferred from the E2 to the E3 and only then to the substrate protein. The difference between the HECT and the RBR E3s is that the first is also catalytically active, meaning that it can also activate a Ub without help from a specific E2. With each step in the processes the specificity is increased by increasing the number of possible pairings. Up till now only two E1s are identified, 30 E2s, and more than 600 putative E3s. (Figure adapted from Schwertman, 2014)

Signalling, feedback loops and bi-stability

In chapter 4 of this thesis we discuss in detail the binding of the damage sensor XPC in GG-NER. We describe how it responds in a bi-stable manner when cells are subjected to certain doses of UV irradiation. This bi-stable response is controlled by a tightly regulated feedback loop system. In this chapter we find that the signalling which controls these feedback loops also operates *in trans* through the whole nucleus. Here these concepts are introduced and explained.

The extensive array of reversible PTMs the cell has at its disposal makes it possible to create highly intricate signalling pathways. Next to their high sensitivity, these signalling pathways are also suitable for relaying rapid messages and cell cycle decision making (Kholodenko, 2006). Positive and negative feedback loops are the bases of this high level of intricacy and sensitivity. Positive feedback loops provide the cell with means to amplify a signal, where negative feedback loops can attenuate signals. These signals can be combined one or several times to provide different outcomes of the signal. One of these outcomes is the phenomenon of bi-stability. The concept of bi-stability says that a dynamic system can be in either of two equilibrium states. Due to this property it can also be regarded as a 'switch' in the system (Tyson et al., 2003). A basic example of a feedback loop system can be found in figure 7A. In this example a balance is preserved between a phosphatase and a kinase, both being stimulated by the resulting protein.

Numerous biological systems are known that are regulated in a switch-like manner by bi-stability. One example is the polarization of budding yeast (Figure 7B). The first rapid loop involves the activity cycling of Cell Division Control protein 42 homolog (CDC42). The second slower loop consists of the actin-mediated transport of CDC42 (Wedlich-Soldner et al., 2004). A system also incorporating a fast positive feedback loop with a slower feedback is the calcium signalling cascade, which is present in many cell types (Figure 6C). This cascade incorporates the induction of a prolonged Ca⁺ signals by using two types of positive feedback loops (Figure 4a). The first loop is centred around rapid release of Ca⁺ which is mediated by inositol 1,4,5-trisphosphate (IP₃). The second loop is slower and induces Ca⁺ influx mediated by the depletion of Ca⁺ stores (Berridge, 2001; Lewis, 2001).

Systems with interacting loops have been identified over the years. One of the examples in this category is the system responsible for the maturation of the *Xenopus* oocyte (Figure 7D). The first rapid acting feedback loop reacts to progesterone maturation stimuli by phosphorylating and dephosphorylating the Cyclin-dependent kinase 1 (CDC2), Cell Division Control protein 25 homolog (CDC25), and Myelin transcription factor 1 (Myt1). In this loop CDC2 promotes the activation of the Cdc2 activator Cdc25, and simultaneously promotes inactivation of the CDC2 inhibitor MYT1. A slower positive feedback loop is active between CDC2, Mitogen-Activated Protein Kinase (MAPK), Mos kinase, and MYT1. In this feedback loop CDC2 stimulates Mos activity, which in turn stimulates MAPK. MAPK in turn stimulates Mos, but inhibits the activity of MYT1. MYT1 is a negative regulator of CDC2, which in turn also is a negative regulator of MYT1 (Xiong and Ferrell, 2003; Brandman et al., 2005). The combination of a slow and a faster loop give rise to certain advantages over single loop systems. In these systems the switch will produce its outcome rapidly due to the rapid activation of the fast loop. Turning this system into its 'off' position goes slower due to the kinetics of the slow loop. By this mechanism the activation and deactivation times can be independently tuned (Brandman et al., 2005).

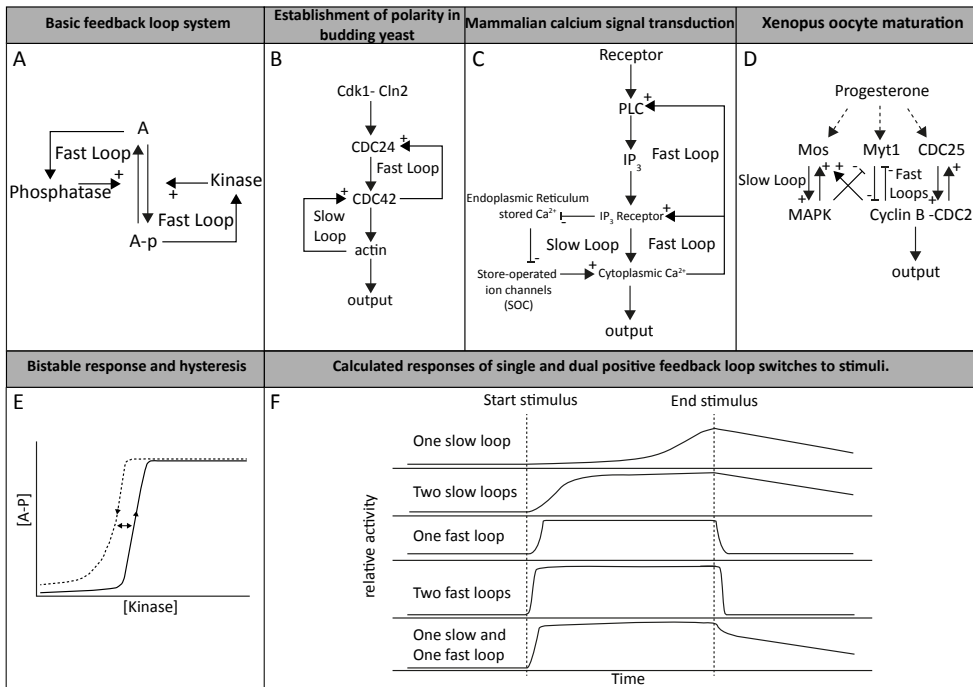


Figure 7. Schematic overview of feedback loops in several cellular systems and possible responses to stimuli. (A) Schematic of a basic feedback loop system. Protein A is phosphorylated by a kinase to form A-p, which on itself stimulates the kinase. In the reverse loop, A-p is dephosphorylated. This process is stimulated by protein A itself. **(B)** Schematic overview of the feedback loops involved in establishing the polarity in budding yeast. **(C)** Schematic overview of the feedback loops involved in mammalian calcium signal transduction. **(D)** Schematic overview of the feedback loops involved in the maturation of the Xenopus oocyte. **(E)** Schematic representation of a bi-stable response. When a the stimulus drops below the level at which the kinase was triggered, the activity of the kinase does not drop immediately. This process is phenomenon is known as hysteresis. **(F)** Overview of activity of a protein over time when a feedback loop system employs one or more loops. Adapted from Brandman et al, 2005

Positive and negative feedback loops have also been proposed to play a role in the DDR. Most of the research is focused on p53 regulatory pathway which controls DNA repair, cell cycle arrest, apoptosis, and cellular senescence. In brief, the p53 protein is considered the master switch of cell cycle fate after DNA damage or other stress: either the cell repairs the damage and continues to live or the cell is incapable of repair and apoptosis is induced. Much research has focused on elucidating the precise mechanism behind this decision making process, but much is still not clear. Many proteins have been found to act in positive and negative feedback loops regulating the stability of p53 and all the effectors in the feedback loops themselves. An added level of complexity is provided by the difference in insults and the effectors playing a role in the specific pathways dealing with them. In the repair of DSBs several feedback loops have been found or proposed (Puszyński et al., 2008; Zhang et al., 2011). The first loop is between p53 and Mouse Double Minute 2 homolog (MDM2). MDM2 binds and degrades p53, which prevents p53 from stabilizing. Upon detection of DSBs the Ataxia Telangiectasia Mutated (ATM) protein inhibits the function of MDM2 and stabilizes p53. ATM itself is inhibited by Protein phosphatase 1D (Wip1). Simultaneously stabilized p53 activates a cascade in which Phosphatase and Tensin Homolog

(PTEN) activates Protein kinase B (Akt), which in turn stimulates MDM2 function. If the signal which stabilizes p53 persists a positive feedback loop involving Cytochrome C (CytoC) and Caspase 3 (Casp3) is activated, leading to apoptosis

As the previous paragraphs illustrates, simple or intricate feedback loop systems are abundant in biological systems. PTMs play a crucial role in regulating decision making process and can have subtle or an 'all or nothing' character. In chapter 5 of this thesis we will use the biological data we obtained and integrate this in models containing these feedback loops to gain better insight into which key players could be interesting targets for biological experiments.

Confocal microscopy and methods

Ever since the development of the first microscopes by Zacharias Jansen (~1585–1632) and Cornelis Drebbel (1572–1633) and the pioneering work of Antoni van Leeuwenhoek (1632–1723), microscopy has been a staple technique in biology. Technical improvements lead to microscopes with higher resolution and combined with new visualization techniques, like phase contrast microscopy (Zernike, 1955), the technique only grew in power. Immuno-histochemical techniques made it possible to specifically stain and visualize protein localisation and structures which could not be seen before. A problem of conventional fluorescence microscopy is the out-of-focus light: besides the in-focus fluorophores, light from fluorophores out of the focal plane of the objective will also be observed and will result in blurred images. To resolve this problem the out-of-focus light was blocked using a pinhole in front of the detector and one in front of the light source (Marvin Minsky, 1961 US patent 3013467) (Davidovits and Egger, 1969, 1971). Confocal setups which were truly usable for biological experimentation were introduced in the 1980s. With the advent of fast computer systems and laser technology, two independent groups managed to set up the first real confocal laser scanning microscope (CLSM) (Cox and Sheppard, 1983; Brakenhoff et al., 1985). These modern confocal microscopes use a laser as a light source. The detection and excitation pinhole are in conjugated focal planes, hence the term confocal. Since only in-focus fluorescence is detected the quality of the image is greatly improved.

Studying the dynamics of cellular processes in general and the work described in this thesis, mostly on damage detection in NER only became possible after the revolution which swept the life science research community: the genetic labelling of proteins with fluorescent proteins. Before this, following specific moieties of proteins inside a living cell was not feasible to the extent where full blown experiments could be designed, and thorough comparison between different proteins under varying conditions could be made, since roughly only two techniques were available: microinjection of fluorescently conjugated antibodies or immune fluorescent techniques. To study the behaviour of proteins over time cells were fixed at different time points, permeabilized and stained using dyes or fluorescent antibodies. With the discovery of the green fluorescent protein (GFP) the dynamic behaviour of proteins could be assessed in living cells in real time. Immune fluorescent techniques also were improved due to the independence of specific labelling antibodies.

GFP is a 27 kDa protein which was initially isolated from the jellyfish *Aequorea Victoria* (Tsien, 1998). The protein absorbs blue light at 395 nm and has one emission peak at a wavelength of 508 nm. Mutagenesis of the wild type GFP resulted in versions of the protein with enhanced characteristics like improved brightness and more efficient expression due to humanised codons

(Heim et al., 1994; Lippincott-Schwartz and Patterson, 2003). Proteins with characteristics similar to GFP were discovered in several other, mostly marine, species. Fluorescent proteins ranging from cyan to red were found in reef Anthozoa greatly broadening the spectrum of available fluorescent proteins (Matz et al., 1999). In the *Discosoma* species an even better red fluorescent protein DsRed was found and using mutagenesis optimized for human expression (Baird et al., 2000). Further improvements in the available colour spectrum of fluorescent proteins came from yellow fluorescent proteins which were either found in other species or created by mutagenesis of GFP (Shagin et al., 2004; Masuda et al., 2006).

Illumination of a chromophore with a specific wavelength can induce conversions between chromophore stereoisomers or induce photochemical reactions. These illumination-dependent changes in spectral properties can be exploited to create fluorescent proteins which can be turned in an on- or off-state by illumination at specific wavelengths (Lukyanov et al., 2005). There are two types of fluorescent proteins of which the properties can be altered, photo-activatable and photo-switchable proteins. Photo-activatable fluorescent proteins only turn fluorescent after having been illuminated at a specific shorter wavelength than their final excitation wavelength, usually 405 nm. Photo-convertible fluorescent proteins can be switched from one emission wavelength to another longer wavelength. Photo-switchable fluorescent proteins can be switched between an active fluorescent state to an inactive state by illuminating with a specific wavelength (Remington, 2006; Shaner et al., 2007). With the growing availability of these tools new applications have been developed. An example is the use of photo-activatable fluorescent proteins to image with sub-diffraction limit resolutions, immensely increasing the resolution with which structures can be visualized (Betzig et al., 2006; Willig et al., 2006).

Fluorescence Recovery After Photobleaching (FRAP)

Next to (confocal) microscopy, methods which are focused on imaging structures in high resolution, other techniques focus on extracting quantitative parameters. FRAP is one of these techniques. FRAP was developed in the 1970s and was mostly focused on the mobility of fluorescently labelled proteins in cellular membranes. With this technique one of the physical properties of fluorescent molecules can be exploited, namely that when the molecule absorbs a very intense light pulse in its excitation spectrum the molecule irreversibly loses its ability to fluoresce (Axelrod et al., 1976; Koppel et al., 1976; Peters et al., 1974). When the technique was introduced one of the biggest drawbacks was that it required custom-built microscopy systems and at the time relied on chemical fluorescently labelled proteins. When commercialized CLSMs were introduced in the 1990s, which were very powerful with respect to resolution, speed, sensitivity and flexibility, FRAP became more popular. This coincided with the discovery of the GFP protein which appeared to be highly suited for FRAP experiments and the field measuring protein dynamics using this technique rapidly expanded (Houtsmuller et al., 1999; Phair and Misteli, 2000; McNally et al., 2000; Stenoien et al., 2001; Mochizuki et al., 2001).

The setup of a FRAP experiment is straightforward: selectively a specific small volume within a larger volume is photobleached, i.e. the fluorescent property of the used tag is irreversibly removed by brief irradiation with a high intensity laser, and the recovery of fluorescence in the bleached area is measured over time (Figure 8). This can be a single spot (spot-FRAP) or a complete strip spanning the entire nucleus of a cell (strip-FRAP) or any other region within a cell of interest (Soumpasis, 1983; Farla et al., 2004; Hoogstraten et al., 2008; van Royen et al., 2009). Depending on the mobility

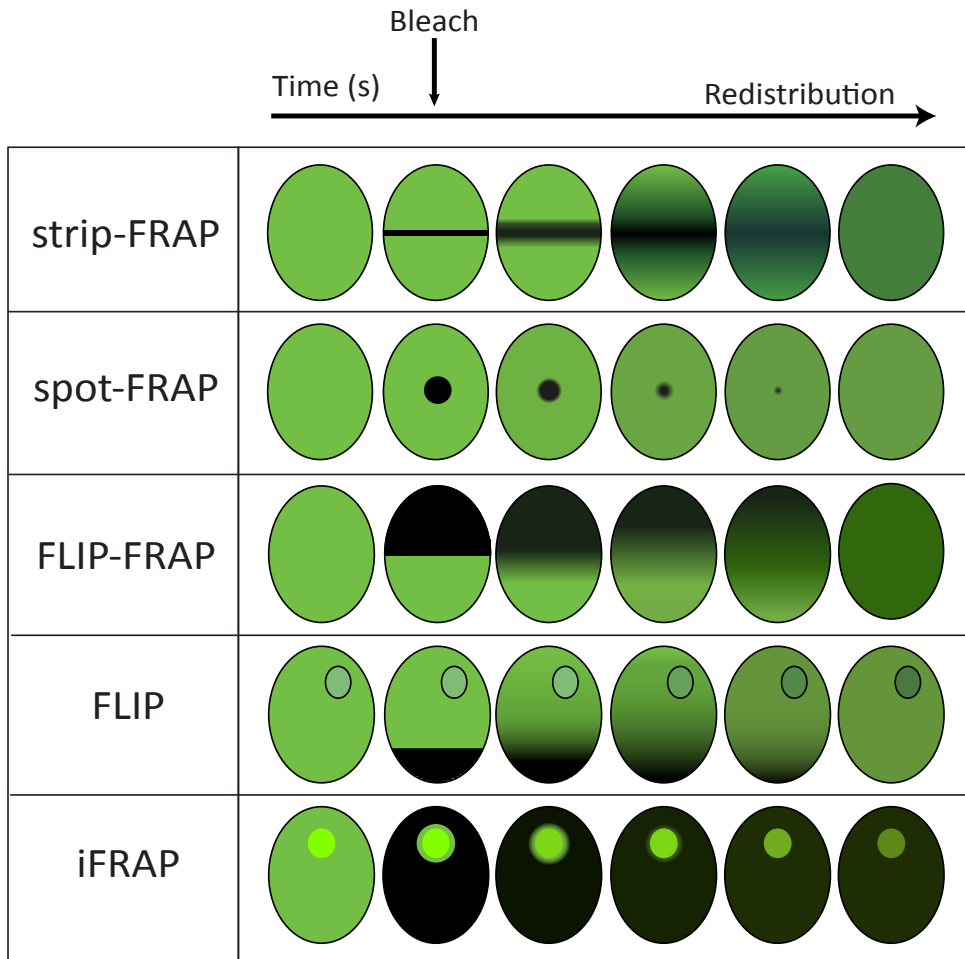


Figure 8. Examples of different FRAP applications that have been developed to study the dynamics of nuclear proteins.

strip-FRAP. Especially useful when signals are relatively low due to low expression of the tagged protein. Here a strip spanning the entire nucleus is bleached and the fluorescence monitored at regular intervals in the bleached strip.

spot-FRAP. Straightforward FRAP experiment based on bleaching only a diffraction limited spot. As with strip-FRAP the recovery of the fluorescence is monitored in the bleached region.

FLIP-FRAP. One half of the nucleus is bleached. Fluorescence is measured in both the bleached and the non-bleached half. Due to the long redistribution time, shorter residence times can be distinguished from longer residence times.

FLIP. An area at a distance of nuclear accumulation is bleached. The velocity at which fluorescence is lost in the distant accumulation is a measure for the residence time at the accumulation. The point in time where a new steady state is reached being a good measure for residence time.

iFRAP. The complete nucleus is bleached, except for a small area around a nuclear accumulation. The loss of fluorescence in the accumulation immediately after bleaching, fully represents the releasing molecules, which is a direct measure for the rate of exchange between the accumulation and the rest of the nucleus.

of the tagged proteins several scenarios can then unfold. If proteins are fully mobile, proteins from outside the bleached area will immediately diffuse into the bleached region and will contribute to the recovery of the fluorescent signal (Figure 9a, green and yellow curves). This recovery will continue until a new equilibrium in fluorescent intensity has been established. If a fraction of the labelled proteins or all the labelled proteins are immobilized, then the labelled proteins will not move into the bleached area and no or an incomplete recovery of the fluorescent signal will occur (Figure 9a, red curve). Finally, transient binding and immobilization of proteins will give rise to a secondary recovery in the bleached region (Figure 9a, blue curve). This secondary recovery occurs due to the release of transiently immobilized labelled proteins during the FRAP experiment. When the volume of the bleached area is relatively large compared to the volume to which labelled proteins are confined, the final recovery of the fluorescence will not be to the pre-bleach level.

FRAP variants

Other variants of the FRAP technique are available to investigate specific research questions. Another technique to study transient or long term immobilisation is the Fluorescence Loss In Photobleaching (FLIP)-FRAP method (Farla et al., 2004) (Figure 8 and Figure 9B and 9C). In a FLIP-FRAP experiment a region distant from the bleach region is monitored simultaneously with the FRAP region. In most experiments a strip at either pole of the nucleus is used for this. The region distant from the bleach region is regarded as the FLIP region. By subtracting the FRAP results from the FLIP results a FLIP-FRAP curve can be obtained which is a measure for the transient and long term immobile fractions.

FLIP can also be used as a stand-alone method: it can be used to study accumulations or fluorescence in small compartments, for instance DNA repair foci or protein binding to telomeres (Essers et al., 2002; Mattern et al., 2004) (Figure 8). An area at a distance of the accumulation is bleached. If there is no drop in fluorescence in the accumulation this means that the bleached molecules do not exchange with the molecules in the accumulation and are permanently immobilized. However, if the fluorescence in the accumulation does decrease the molecules are transiently immobilized. By measuring the velocity at which the fluorescence is lost and a new steady state is reached, the residence time of the molecules can be determined.

The rate of exchange between a compartment or an accumulation can also be determined by using the inverse FRAP (iFRAP) method (Figure 8). The method was introduced to measure the rate at which molecules in the nucleolus exchange with the surrounding nucleoplasm (Dundr et al., 2002). In a typical iFRAP experiment the complete volume of the nucleus is bleached with exception of the accumulation or compartment of interest. The observed loss of fluorescence in the accumulation largely represents the release of labelled proteins. This gives the technique a distinct advantage over the FLIP technique since with iFRAP there hardly is any turnover of fluorescent proteins in the accumulation with non-bleached proteins from the nucleoplasm. As a result no further complicated analytical methods have to be used to determine the rate of exchange (K_{off}).

FRAP curve normalisation

For interpretation and representation of the gathered data several methods of normalisation can be applied. The most straight forward way is to express the data relative to the pre-bleach value: $I_{norm,t} = (I_t - I_{background}) / (I_{pre-bleach} - I_{background})$, where $I_{pre-bleach}$ is the measurement, or preferably the average of a number of measurements before the bleach and $I_{background}$ is the signal level where

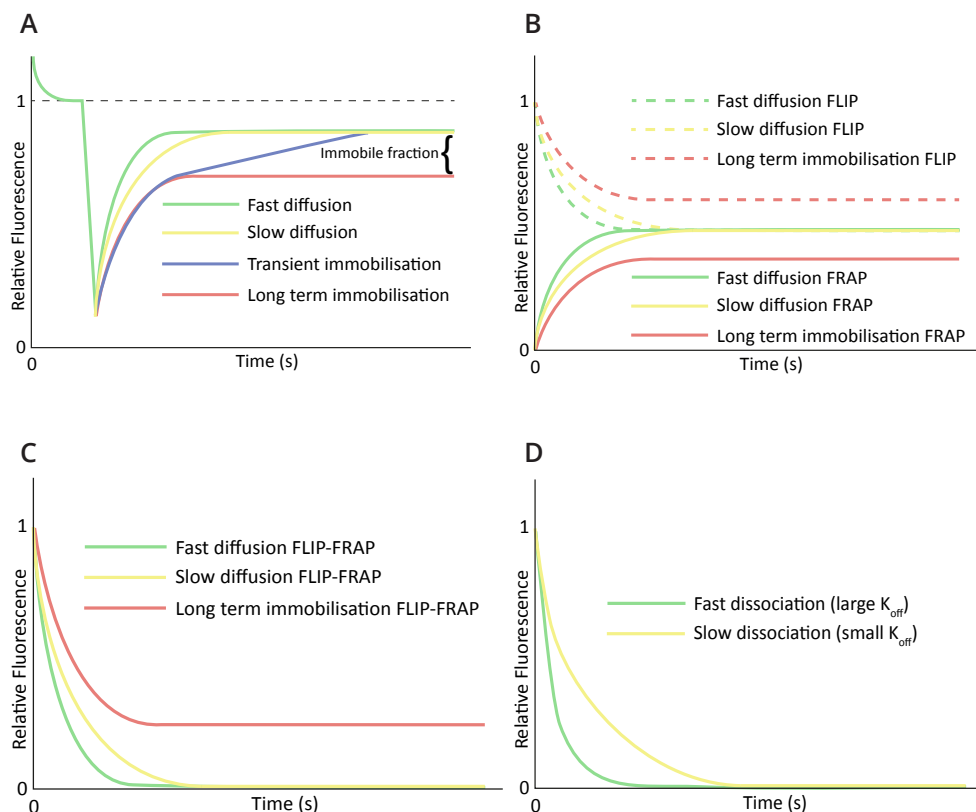


Figure 9. Schematic representation of FRAP curves resulting from different scenarios. (A) spot and strip-FRAP. The curves represent different possible curves resulting from a typical spot- or strip-FRAP experiment (See figure 8). All curves are expressed relative to pre-bleach values. Freely diffusing GFP-tagged molecules can recover completely, but the final fluorescence level will be lower, especially in the case of a strip-FRAP experiment, since a substantial portion of the molecules are bleached (typically 10-20% in an average strip-FRAP experiment). Fast diffusing tagged molecules (green curve) will lead to faster fluorescence recovery faster than slow diffusing tagged molecules (yellow curve). Molecules which are transiently immobilised (blue curve), for instance by brief interactions with chromatin can be identified by the secondary recovery visible in the curve. Long term immobilised tagged molecules show incomplete fluorescence recovery (red curve) compared to the free diffusing molecules. The difference between these curves is a measure for the immobile fraction, but the percentage of bleached molecules should be taken into consideration. **(B)** FLIP and FRAP. The curves represent different possible curves resulting from a typical half-FRAP (FLIP-FRAP) experiment before subtracting either curve from the other (See figure 8). Curves from fast diffusing tagged molecules (green solid and dotted curves) meet after a short period of time. Slower diffusing tagged molecules will take a longer time (yellow solid and dotted lines), but also here the fluorescent signal will recover in both halves of the bleached nucleus. If there is a fraction of the molecules immobilised (red solid and dotted curves), the fluorescence in both halves of the nucleus will not fully recover to the same level and the resulting curves will not meet. **(C)** FLIP-FRAP. When the resulting FRAP curves of a half-FRAP experiment are subtracted from the FLIP curves the time it takes for the system to equilibrate can be read directly, including the potential presence of an immobile fraction: the green and the yellow curves reach 0, where the red curve does not. The difference between the red curve and the x-axis is a measure for the bound fraction of tagged molecules. **(D)** iFRAP. This method has the advantage that the resulting curves only represent the turn over or off-rate (K_{off}) of the tagged molecules. Molecules with a large K_{off} (green curve) will dissociate faster leading to a fast decrease of fluorescence in the measured region. If the K_{off} is lower the time until all molecules have dissociated will take longer (yellow curve).

no fluorescence is present. A second method of normalisation is an extension of the first option, here taking into account the fluorescence intensity directly after bleaching (I_0). This value can be expressed by taking the intensity values relative to the intensity directly after bleaching, as well as to the pre-bleach intensity: $(I_{\text{norm},t}) = (I_t - I_0)/(I_{\text{pre-bleach}} - I_0)$. By doing so, the resulting curves enable a qualitative visual estimate of the size of any potentially present immobile fractions, minus the fraction removed by the bleach pulse. Lastly, the values can be normalized by expressing the intensities relative to the level after complete recovery (I_{final}) and the intensity directly after bleaching (I_0): $I_{t,\text{norm}} = (I_t - I_0)/(I_{\text{final}} - I_0)$. The resulting curve runs from 0 directly after bleaching to 1 after final recovery. This allows for a direct comparison of the diffusion rates without being hampered by the effects of potential immobile fractions. The resulting curves of this method can also be quantitatively analysed by fitting the data to mathematically derived equations representing the diffusion process and the transient immobilization.

FRAP curve analysis using Monte Carlo simulations

Analytical techniques developed for FRAP quantification are mostly based on mathematical analytical models of diffusion of the labelled molecules. These mathematical models are often highly simplified to be able to solve these differential equations describing the model. Photobleaching of the chromophore is often considered as an irreversible process, boundary effects are neglected, a reduced set of spatial dimensions is used, or the full point spread function of the focused laser beam is replaced by a geometrical approximation or even a cylinder. Though, there are several examples of methods which succeed to capture the essence of FRAP experiments (Axelrod et al., 1976; Soumpasis, 1983; Blonk et al., 1993; Carrero et al., 2003). and improvements can be made by incorporating more of the now simplified parameters. Since this can lead to very complex and sometimes unsolvable mathematical problems another approach to analyse FRAP data can be applied: a computer model of the FRAP procedure and the behaviour of (labelled) molecules inside small volumes (Siggia et al., 2000) using a straightforward Monte Carlo method (Houtsmuller et al., 1999; Hoogstraten et al., 2002; Farla et al., 2004). These simulations have the advantage that they can incorporate experimentally obtained parameters. Next to that, properties describing the microscope optical path can be used. This includes, but is not limited to: the shape of the laser beam and the 3D intensity distribution during all the stages of the experiment, the size and shape of the cell nucleus, and the photochemical properties (bleaching and 'blinking' parameters, quantum yield) of the fluorescent label. Simulations can then be run with these fixed parameters in place. By varying the three protein mobility parameters (the diffusion coefficient, the duration of binding of individual molecules, and the immobile fractions) simulated FRAP curves can be generated and subsequently fitted to the original curves. This approach of Monte Carlo simulations provides a very comprehensible, flexible, and scalable tool to analyse FRAP experiments by fitting the *in vivo* obtained FRAP curves to their *in silico* simulated counterparts.

References

- Abraham, R.T. 2004. PI 3-kinase related kinases: "big" players in stress-induced signaling pathways. *DNA Repair (Amst)*. 3:883-7. doi:10.1016/j.dnarep.2004.04.002.
- Acharya, S., and T. Wilson. 1996. hMSH2 forms specific mismatch-binding complexes with hMSH3 and hMSH6. *Proc. Natl. Acad. Sci. U. S. A.* 93:13629-13634.
- Antoniou, A., P.D.P. Pharoah, S. Narod, H.A. Risch, J.E. Eyfjord, J.L. Hopper, N. Loman, H. Olsson, O. Johannsson, A. Borg, B. Pasini, P. Radice, S. Manoukian, D.M. Eccles, N. Tang, E. Olah, H. Anton-Culver, E. Warner, J. Lubinski, J. Gronwald, B. Gorski, H. Tulinius, S. Thorlacius, H. Eerola, H. Nevanlinna, K. Syrjäkoski, O.-P. Kallioniemi, D. Thompson, C. Evans, J. Peto, F. Lalloo, D.G. Evans, and D.F. Easton. 2003. Average risks of breast and ovarian cancer associated with BRCA1 or BRCA2 mutations detected in case Series unselected for family history: a combined analysis of 22 studies. *Am. J. Hum. Genet.* 72:1117-30. doi:10.1086/375033.
- Axelrod, D., D.E. Koppel, J. Schlessinger, E. Elson, and W.W. Webb. 1976. Mobility measurement by analysis of fluorescence photobleaching recovery kinetics. *Biophys. J.* 16:1055-69. doi:10.1016/S0006-3495(76)85755-4.
- Baird, G.S., D. Zacharias, and R.Y. Tsien. 2000. Biochemistry, mutagenesis, and oligomerization of DsRed, a red fluorescent protein from coral. *Proc. Natl. Acad. Sci. U. S. A.* 97:11984-9. doi:10.1073/pnas.97.22.11984.
- Bergink, S., and S. Jentsch. 2009. Principles of ubiquitin and SUMO modifications in DNA repair. *Nature.* 458:461-7. doi:10.1038/nature07963.
- Bergink, S., W. Toussaint, M.S. Lujsterburg, C. Dinant, S. Alekseev, J.H.J. Hoeijmakers, N.P. Dantuma, A.B. Houtsmuller, and W. Vermeulen. 2012. Recognition of DNA damage by XPC coincides with disruption of the XPC-RAD23 complex. *J. Cell Biol.* 196:681-8. doi:10.1083/jcb.201107050.
- Berndsen, C.E., and C. Wolberger. 2014. New insights into ubiquitin E3 ligase mechanism. *Nat. Struct. Mol. Biol.* 21:301-7. doi:10.1038/nsmb.2780.
- Betzig, E., G.H. Patterson, R. Sougrat, O.W. Lindwasser, S. Olenych, J.S. Bonifacio, M.W. Davidson, J. Lippincott-Schwartz, and H.F. Hess. 2006. Imaging intracellular fluorescent proteins at nanometer resolution. *Science.* 313:1642-5. doi:10.1126/science.1127344.
- Blonk, J., A. Don, H. Aalst, and J. Birmingham. 1993. Fluorescence photobleaching recovery in the confocal scanning light microscope. *J. Microsc.* 169:363-374. doi:10.1111/j.1365-2818.1993.tb03312.x.
- De Boer, J., J.O. Andressoo, J. de Wit, J. Huijman, R.B. Beems, H. van Steeg, G. Weeda, G.T.J. van der Horst, W. van Leeuwen, A.P.N. Themmen, M. Meradji, and J.H.J. Hoeijmakers. 2002. Premature aging in mice deficient in DNA repair and transcription. *Science.* 296:1276-9. doi:10.1126/science.1070174.
- Bostelman, L.J., A.M. Keller, A.M. Albrecht, A. Arat, and J.S. Thompson. 2007. Methylation of histone H3 lysine-79 by Dot1p plays multiple roles in the response to UV damage in *Saccharomyces cerevisiae*. *DNA Repair (Amst)*. 6:383-95. doi:10.1016/j.dnarep.2006.12.010.
- Brakenhoff, G.J., H.T. van der Voort, E. van Spronsen, W. a Linnemans, and N. Nanninga. 1985. Three-dimensional chromatin distribution in neuroblastoma nuclei shown by confocal scanning laser microscopy. *Nature.* 317:748-749. doi:10.1038/317748a0.
- Brandman, O., J.E. Ferrell, R. Li, and T. Meyer. 2005. Interlinked fast and slow positive feedback loops drive reliable cell decisions. *Science.* 310:496-8. doi:10.1126/science.1113834.
- Bürkle, A., and L. Virág. 2013. Poly(ADP-ribose): PARadigms and PARadoxes. *Mol. Aspects Med.* 34:1046-65. doi:10.1016/j.mam.2012.12.010.
- Cadet, J., E. Sage, and T. Douki. 2005. Ultraviolet radiation-mediated damage to cellular DNA. *Mutat. Res.* 571:3-17. doi:10.1016/j.mrfmmm.2004.09.012.
- Carrero, G., D. McDonald, E. Crawford, G. de Vries, and M.J. Hendzel. 2003. Using FRAP and mathematical modeling to determine the in vivo kinetics of nuclear proteins. *Methods.* 29:14-28. doi:10.1016/S1046-2023(02)00288-8.
- Chambon, P., J. Weill, and P. Mandel. 1963. Nicotinamide mononucleotide activation of a new DNA-dependent polyadenylic acid synthesizing nuclear enzyme. *Biochem. Biophys. Res. Commun.* 11:39-43.
- Chan, D.W., and S.P. Lees-Miller. 1996. The DNA-dependent protein kinase is inactivated by autophosphorylation of the catalytic subunit. *J. Biol. Chem.* 271:8936-41. doi:10.1074/jbc.271.15.8936.
- Chau, V., J.W. Tobias, A. Bachmair, D. Marriott, D.J. Ecker, D.K. Gonda, A. Varshavsky, and D.J. Eckert. 2014. Multiubiquitin in a Targeted Lysine Specific to Is Confined Short-Lived Protein. 243:1576-1583.
- Chu, G., and W. Yang. 2008. Here comes the sun: recognition of UV-damaged DNA. *Cell.* 135:1172-4. doi:10.1016/j.cell.2008.12.015.
- Ciccia, A., N. McDonald, and S.C. West. 2008. Structural and functional relationships of the XPF/MUS81 family of proteins. *Annu. Rev. Biochem.* 77:259-87. doi:10.1146/annurev.biochem.77.070306.102408.
- Ciechanover, A. 1994. The ubiquitin-proteasome proteolytic pathway. *Cell.* 79:13-21.
- Ciechanover, A., and R. Ben-Saadon. 2004. N-terminal ubiquitination: more protein substrates join in. *Trends Cell Biol.* 14:103-6.
- Clague, M.J., J.M. Coulson, and S. Urbé. 2012. Cellular functions of the DUBs. *J. Cell Sci.* 125:277-86. doi:10.1242/jcs.090985.
- Clauson, C., O.D. Schärer, and L. Niedernhofer. 2013. Advances in understanding the complex mechanisms of DNA interstrand cross-link repair. *Cold Spring Harb. Perspect. Biol.* 5:a012732. doi:10.1101/cshperspect.a012732.
- Coin, F., J.C. Marinoni, C. Rodolfo, S. Fribourg, a M. Pedrini, and J.M. Egly. 1998. Mutations in the XPD helicase gene result in XP and TTD phenotypes, preventing interaction between XPD and the p44 subunit of TFIIH. *Nat. Genet.* 20:184-8. doi:10.1038/2491.
- Cole, A.R., L.P.C. Lewis, and H. Walden. 2010. The structure of the catalytic subunit FANCL of the Fanconi anemia core complex. *Nat. Struct. Mol. Biol.* 17:294-8. doi:10.1038/nsmb.1759.
- Cox, I.J., and C.J. Sheppard. 1983. Scanning optical microscope incorporating a digital framestore and microcomputer. *Appl. Opt.* 22:1474. doi:10.1364/AO.22.001474.
- Davidovits, P., and M.D. Egger. 1969. Scanning laser microscope. *Nature.* 223:831.
- Davidovits, P., and M.D. Egger. 1971. Scanning laser microscope for biological investigations. *Appl. Opt.* 10:1615-9.
- Deans, A.J., and S.C. West. 2011. DNA interstrand crosslink repair and cancer. *Nat. Rev. Cancer.* 11:467-80. doi:10.1038/nrc3088.
- Demple, B., and J.-S. Sung. 2005. Molecular and biological roles of Ape1 protein in mammalian base excision repair. *DNA Repair (Amst)*. 4:1442-9. doi:10.1016/j.dnarep.2005.09.004.

- Deshaies, R.J., and C. a P. Joazeiro. 2009. RING domain E3 ubiquitin ligases. *Annu. Rev. Biochem.* 78:399–434. doi:10.1146/annurev.biochem.78.101807.093809.
- Dianov, G.L., and U. Hübscher. 2013. Mammalian base excision repair: the forgotten archangel. *Nucleic Acids Res.* 41:3483–90. doi:10.1093/nar/gkt076.
- DiGiovanna, J.J., and K.H. Kraemer. 2012. Shining a light on xeroderma pigmentosum. *J. Invest. Dermatol.* 132:785–96. doi:10.1038/jid.2011.426.
- Drake, J.W. 1991. Spontaneous mutation. *Annu. Rev. Genet.* 25:125–46. doi:10.1146/annurev.ge.25.120191.001013.
- Dundr, M., U. Hoffmann-Rohrer, Q. Hu, I. Grummt, L.I. Rothblum, R.D. Phair, and T. Misteli. 2002. A kinetic framework for a mammalian RNA polymerase *in vivo*. *Science.* 298:1623–6. doi:10.1126/science.1076164.
- Engelward, B.P., G. Weeda, M.D. Wyatt, J.L. Broekhof, J. de Wit, I. Donker, J.M. Allan, B. Gold, J.H. Hoeijmakers, and L.D. Samson. 1997. Base excision repair deficient mice lacking the Aag alkyladenine DNA glycosylase. *Proc. Natl. Acad. Sci. U. S. A.* 94:13087–92.
- Essers, J., A. Houtsmuller, L. van Veelen, C. Paulusma, A.L. Nigg, A. Pastink, W. Vermeulen, J.H.J. Hoeijmakers, and R. Kanaar. 2002. Nuclear dynamics of RAD52 group homologous recombination proteins in response to DNA damage. *EMBO J.* 21:2030–2037.
- Falck, J., J. Coates, and S.P. Jackson. 2005. Conserved modes of recruitment of ATM, ATR and DNA-PKcs to sites of DNA damage. *Nature.* 434:605–11. doi:10.1038/nature03442.
- Farla, P., R. Hersmus, B. Geverts, P.O. Mari, A.L. Nigg, H.J. Dubbink, J. Trapman, and A.B. Houtsmuller. 2004. The androgen receptor ligand-binding domain stabilizes DNA binding in living cells. *J. Struct. Biol.* 147:50–61. doi:10.1016/j.jsb.2004.01.002.
- Finkel, T. 2011. Signal transduction by reactive oxygen species. *J. Cell Biol.* 194:7–15. doi:10.1083/jcb.201102095.
- Fishel, R., M.K. Lescoe, M.R. Rao, N.G. Copeland, N.A. Jenkins, J. Garber, M. Kane, and R. Kolodner. 1993. The human mutator gene homolog MSH2 and its association with hereditary nonpolyposis colon cancer. *Cell.* 75:1027–38.
- Fitch, M.E., I. V. Cross, S.J. Turner, S. Adimoolam, C.X. Lin, K.G. Williams, and J.M. Ford. 2003. The DDB2 nucleotide excision repair gene product p48 enhances global genomic repair in p53 deficient human fibroblasts. *DNA Repair (Amst).* 2:819–826. doi:10.1016/S1568-7864(03)00066-1.
- Foiani, M., A. Pelliccioli, M. Lopes, C. Lucca, M. Ferrari, G. Liberi, M.M. Falconi, and P. Plevani. 2000. DNA damage checkpoints and DNA replication controls in *Saccharomyces cerevisiae*.
- Fousteri, M., W. Vermeulen, A. van Zeeland, and L.H.F. Mullenders. 2006. Cockayne syndrome A and B proteins differentially regulate recruitment of chromatin remodeling and repair factors to stalled RNA polymerase II *in vivo*. *Mol. Cell.* 23:471–82. doi:10.1016/j.molcel.2006.06.029.
- Fulford, J., H. Nikjoo, D.T. Goodhead, and P. O'Neill. 2001. Yields of SSB and DSB induced in DNA by Al(K) ultrasoft X-rays and alpha-particles: comparison of experimental and simulated yields. *Int. J. Radiat. Biol.* 77:1053–66. doi:10.1080/09553000110069308.
- Garner, E., and A. Smogorzewska. 2011. Ubiquitylation and the Fanconi anemia pathway. *FEBS Lett.* 585:2853–60. doi:10.1016/j.febslet.2011.04.078.
- Van Gent, D.C., J.H. Hoeijmakers, and R. Kanaar. 2001. Chromosomal stability and the DNA double-stranded break connection. *Nat. Rev. Genet.* 2:196–206. doi:10.1038/35056049.
- Giannattasio, M., F. Lazzaro, P. Plevani, and M. Muzi-Falconi. 2005. The DNA damage checkpoint response requires histone H2B ubiquitination by Rad6-Bre1 and H3 methylation by Dot1. *J. Biol. Chem.* 280:9879–86. doi:10.1074/jbc.M414453200.
- Giglia-Mari, G., F. Coin, J. a Ranish, D. Hoogstraten, A. Theil, N. Wijgers, N.G.J. Jaspers, A. Raams, M. Argentini, P.J. van der Spek, E. Botta, M. Stefanini, J.-M. Egly, R. Aebersold, J.H.J. Hoeijmakers, and W. Vermeulen. 2004. A new, tenth subunit of TFIIH is responsible for the DNA repair syndrome trichothiodystrophy group A. *Nat. Genet.* 36:714–9. doi:10.1038/ng1387.
- Gillet, L.C.J., and O.D. Schärer. 2006. Molecular mechanisms of mammalian global genome nucleotide excision repair. *Chem. Rev.* 106:253–76. doi:10.1021/cr040483f.
- Gottlieb, T., and S. Jackson. 1993. The DNA-dependent protein kinase: requirement for DNA ends and association with Ku antigen. *Cell.* 72:131–42. doi:10.1016/0092-8674(93)90057-W.
- Gourdin, A.M., L. van Cuijk, M. Tresini, M.S. Luijsterburg, A.L. Nigg, G. Giglia-Mari, A.B. Houtsmuller, W. Vermeulen, and J. a Martein. 2014. Differential binding kinetics of replication protein A during replication and the pre- and post-incision steps of nucleotide excision repair. *DNA Repair (Amst).* 24C:46–56. doi:10.1016/j.dnarep.2014.09.013.
- Grabbe, C., and I. Dikic. 2009. Functional roles of ubiquitin-like domain (ULD) and ubiquitin-binding domain (UBD) containing proteins. *Chem. Rev.* 109:1481–94. doi:10.1021/cr800413p.
- Grawunder, U., M. Wilm, X. Wu, and P. Kulesza. 1997. Activity of DNA ligase IV stimulated by complex formation with XRCC4 protein in mammalian cells. *Nature.* 388:492–5. doi:10.1038/41358.
- Groisman, R., J. Polanowska, I. Kuraoka, J. Sawada, M. Saijo, R. Drapkin, A.F. Kisselev, K. Tanaka, and Y. Nakatani. 2003. The ubiquitin ligase activity in the DDB2 and CSA complexes is differentially regulated by the COP9 signalosome in response to DNA damage. *Cell.* 113:357–67.
- Hanasoge, S., and M. Ljungman. 2007. H2AX phosphorylation after UV irradiation is triggered by DNA repair intermediates and is mediated by the ATR kinase. *Carcinogenesis.* 28:2298–304. doi:10.1093/carcin/bgm157.
- Hanawalt, P.C. 2002. Subpathways of nucleotide excision repair and their regulation. *Oncogene.* 21:8949–56. doi:10.1038/sj.onc.1206096.
- Hanawalt, P.C., and G. Spivak. 2008. Transcription-coupled DNA repair: two decades of progress and surprises. *Nat. Rev. Mol. Cell Biol.* 9:958–70. doi:10.1038/nrm2549.
- Hang, B., B. Singer, G.P. Margison, and R.H. Elder. 1997. Targeted deletion of alkylpurine-DNA-N-glycosylase in mice eliminates repair of 1,N6-ethenoadenine and hypoxanthine but not of 3,N4-ethenocytosine or 8-oxoguanine. *Proc. Natl. Acad. Sci. U. S. A.* 94:12869–74.
- Hegde, M.L., T.K. Hazra, and S. Mitra. 2008. Early steps in the DNA base excision/single-strand interruption repair pathway in mammalian cells. *Cell Res.* 18:27–47. doi:10.1038/cr.2008.8.
- Heim, R., D.C. Prasher, and R.Y. Tsien. 1994. Wavelength mutations and posttranslational autoxidation of green fluorescent protein. *Proc. Natl. Acad. Sci. U. S. A.* 91:12501–4.
- Hershko, A., and A. Ciechanover. 1998. The ubiquitin system. *Annu. Rev. Biochem.* 67:425–79. doi:10.1146/annurev.biochem.67.1.425.
- Hicke, L. 1999. Gettin' down with ubiquitin: turning off cell-surface receptors, transporters and channels. *Trends Cell Biol.* 9:107–12.

- Hoogstraten, D., S. Bergink, J.M.Y. Ng, V.H.M. Verbiest, M.S. Luijsterburg, B. Geverts, A. Raams, C. Dinant, J.H.J. Hoeijmakers, W. Vermeulen, and A.B. Houtsmuller. 2008. Versatile DNA damage detection by the global genome nucleotide excision repair protein XPC. *J. Cell Sci.* 121:2850–9. doi:10.1242/jcs.031708.
- Hoogstraten, D., A.L. Nigg, H. Heath, L.H.F. Mullenders, R. van Driel, J.H.J. Hoeijmakers, W. Vermeulen, and A.B. Houtsmuller. 2002. Rapid switching of TFIIH between RNA polymerase I and II transcription and DNA repair in vivo. *Mol. Cell.* 10:1163–74.
- Houtsmuller, A.B., S. Rademakers, A. Nigg, D. Hoogstraten, J.H. Hoeijmakers, and W. Vermeulen. 1999. Action of DNA repair endonuclease ERCC1/XPF in living cells. *Science.* 284:958–61.
- Huang, N., N.K. Banavali, and A.D. MacKerell. 2003. Protein-facilitated base flipping in DNA by cytosine-5-methyltransferase. *Proc. Natl. Acad. Sci. U. S. A.* 100:68–73. doi:10.1073/pnas.0135427100.
- Inagaki, A., S. Schoenmakers, and W.M. Baarends. 2010. and transcriptional silencing in meiosis. 255–266.
- Iyama, T., and D.M. Wilson. 2013. DNA repair mechanisms in dividing and non-dividing cells. *DNA Repair (Amst).* 12:620–36. doi:10.1016/j.dnarep.2013.04.015.
- Iyer, R.R., A. Pluciennik, V. Burdett, and P.L. Modrich. 2006. DNA mismatch repair: functions and mechanisms. *Chem. Rev.* 106:302–23. doi:10.1021/cr0404794.
- Jackson, S.P., and J. Bartek. 2009. The DNA-damage response in human biology and disease. *Nature.* 461:1071–8. doi:10.1038/nature08467.
- De Jager, M., J. van Noort, D.C. van Gent, C. Dekker, R. Kanaar, and C. Wyman. 2001. Human Rad50/Mre11 is a flexible complex that can tether DNA ends. *Mol. Cell.* 8:1129–35. doi:10.1016/S1097-2765(01)00381-1.
- Jin, J., X. Li, S.P. Gygi, and J.W. Harper. 2007. Dual E1 activation systems for ubiquitin differentially regulate E2 enzyme charging. *Nature.* 447:1135–8. doi:10.1038/nature05902.
- Kamitani, T., K. Kito, H.P. Nguyen, and E.T.H. Yeh. 1997. Characterization of NEDD8, a Developmentally Down-regulated Ubiquitin-like Protein. *J. Biol. Chem.* 272:28557–28562. doi:10.1074/jbc.272.45.28557.
- Kanaar, R., J.H. Hoeijmakers, and D.C. van Gent. 1998. Molecular mechanisms of DNA double strand break repair. *Trends Cell Biol.* 8:483–9.
- Kee, Y., and A.D. D'Andrea. 2012. Molecular pathogenesis and clinical management of Fanconi anemia. *J. Clin. Invest.* 122:3799–806. doi:10.1172/JCI58321.
- Kholodenko, B. 2006. Cell-signalling dynamics in time and space. *Nat. Rev. Mol. Cell Biol.* 7:165–176.
- Kim, H., and A.D. D'Andrea. 2012. Regulation of DNA cross-link repair by the Fanconi anemia/BRCA pathway. *Genes Dev.* 26:1393–408. doi:10.1101/gad.195248.112.
- Kim, H.C., and J.M. Huibregtse. 2009. Polyubiquitination by HECT E3s and the determinants of chain type specificity. *Mol. Cell. Biol.* 29:3307–18. doi:10.1128/MCB.00240-09.
- Kim, J., and B. Choi. 1995. The Solution Structure of DNA Duplex-Decamer Containing the (6-4) Photoproduct of Thymidyl[3'(to)5']Thymidine by NMR and Relaxation Matrix Refinement. *Eur. J. Biochem.* 228:849–854.
- Kim, Y.-J., and D.M. Wilson. 2012. Overview of base excision repair biochemistry. *Curr. Mol. Pharmacol.* 5:3–13.
- Kisby, G.E., J. Milne, and C. Sweatt. 1997. Evidence of reduced DNA repair in amyotrophic lateral sclerosis brain tissue. *Neuroreport.* 8:1337–40. doi:10.1097/00001756-199704140-00004.
- Klungland, a., I. Rosewell, S. Hollenbach, E. Larsen, G. Daly, B. Epe, E. Seeberg, T. Lindahl, and D.E. Barnes. 1999. Accumulation of premutagenic DNA lesions in mice defective in removal of oxidative base damage. *Proc. Natl. Acad. Sci. U. S. A.* 96:13300–5. doi:10.1073/pnas.96.23.13300.
- Komander, D., M.J. Clague, and S. Urbé. 2009. Breaking the chains: structure and function of the deubiquitinases. *Nat. Rev. Mol. Cell Biol.* 10:550–63. doi:10.1038/nrm2731.
- Komander, D., and M. Rape. 2012. The ubiquitin code. *Annu. Rev. Biochem.* 81:203–29. doi:10.1146/annurev-biochem-060310-170328.
- Koppel, D.E., D. Axelrod, J. Schlessinger, E.L. Elson, and W.W. Webb. 1976. Dynamics of fluorescence marker concentration as a probe of mobility. *Biophys. J.* 16:1315–29. doi:10.1016/S0006-3495(76)85776-1.
- Koundrioukoff, S., S. Polo, and G. Almouzni. 2004. Interplay between chromatin and cell cycle checkpoints in the context of ATR/ATM-dependent checkpoints. *DNA Repair (Amst).* 3:969–78. doi:10.1016/j.dnarep.2004.03.010.
- Kulathu, Y., and D. Komander. 2012. Atypical ubiquitylation - the unexplored world of polyubiquitin beyond Lys48 and Lys63 linkages. *Nat. Rev. Mol. Cell Biol.* 13:508–23. doi:10.1038/nrm3394.
- Kuo, M.H., and C.D. Allis. 1998. Roles of histone acetyltransferases and deacetylases in gene regulation. *Bioessays.* 20:615–26. doi:10.1002/(SICI)1521-1878(199808)20:8<615::AID-BIES4>3.0.CO;2-H.
- De Laat, W.L., E. Appeldoorn, K. Sugawara, E. Weterings, N.G. Jaspers, and J.H. Hoeijmakers. 1998. DNA-binding polarity of human replication protein A positions nucleases in nucleotide excision repair. *Genes Dev.* 12:2598–609.
- Lavin, M.F. 2008. Ataxia-telangiectasia: from a rare disorder to a paradigm for cell signalling and cancer. *Nat. Rev. Mol. Cell Biol.* 9:759–69. doi:10.1038/nrm2514.
- Lee, S., J. Moore, A. Holmes, and K. Umezū. 1998. Saccharomyces Ku70, Mre11/Rad50, and RPA Proteins Regulate Adaptation to G2/M Arrest after DNA Damage. *Cell.* 94:399–409. doi:10.1016/S0092-8674(00)81482-8.
- Li, W., M.H. Bengtson, A. Ulbrich, A. Matsuda, V. a Reddy, A. Orth, S.K. Chanda, S. Batalov, and C. a P. Joazeiro. 2008. Genome-wide and functional annotation of human E3 ubiquitin ligases identifies MULAN, a mitochondrial E3 that regulates the organelle's dynamics and signaling. *PLoS One.* 3:e1487. doi:10.1371/journal.pone.0001487.
- Li, W., and Y. Ye. 2008. Polyubiquitin chains: functions, structures, and mechanisms. *Cell. Mol. Life Sci.* 65:2397–406. doi:10.1007/s00018-008-8090-6.
- Lippincott-Schwartz, J., and G.H. Patterson. 2003. Development and use of fluorescent protein markers in living cells. *Science.* 300:87–91. doi:10.1126/science.1082520.
- Lisby, M., and R. Rothstein. 2009. Choreography of recombination proteins during the DNA damage response. *DNA Repair (Amst).* 8:1068–76. doi:10.1016/j.dnarep.2009.04.007.
- Ljungman, M., and F. Zhang. 1996. Blockage of RNA polymerase as a possible trigger for u.v. light-induced apoptosis. *Oncogene.* 13:823–31.
- Ljungman, M., F. Zhang, F. Chen, a J. Rainbow, and B.C. McKay. 1999. Inhibition of RNA polymerase II as a trigger for the p53 response. *Oncogene.* 18:583–92. doi:10.1038/sj.onc.1202356.

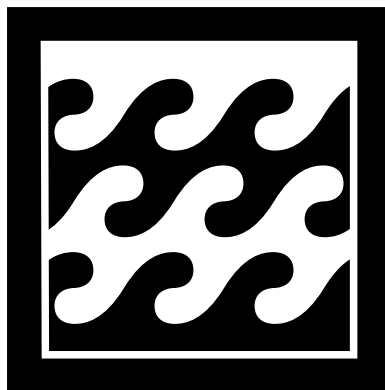
- Luijsterburg, M.S., M. Lindh, K. Acs, M.G. Vrouwe, A. Pines, H. van Attikum, L.H. Mullenders, and N.P. Dantuma. 2012. DDB2 promotes chromatin decondensation at UV-induced DNA damage. *J. Cell Biol.* 197:267–81. doi:10.1083/jcb.201106074.
- Lukyanov, K., D. Chudakov, S. Lukyanov, and V. V. Verkhusha. 2005. Photoactivatable fluorescent proteins. *Nat. Rev. Mol. Cell Biol.* 6:885–891.
- Ma, Y., U. Pannicke, K. Schwarz, and M.R. Lieber. 2002. Hairpin opening and overhang processing by an Artemis/DNA-dependent protein kinase complex in nonhomologous end joining and V(D)J recombination. *Cell.* 108:781–94. doi:10.1016/S0092-8674(02)00671-2.
- Mahaney, B.L., K. Meek, and S.P. Lees-Miller. 2009. Repair of ionizing radiation-induced DNA double-strand breaks by non-homologous end-joining. *Biochem. J.* 417:639–50. doi:10.1042/bj20080413.
- Mari, P.-O., B.I. Florea, S.P. Persengiev, N.S. Verkaik, H.T. Brüggewirth, M. Modesti, G. Giglia-Mari, K. Bezstarosti, J.A.A. Demmers, T.M. Luijck, A.B. Houtsmuller, and D.C. van Gent. 2006. Dynamic assembly of end-joining complexes requires interaction between Ku70/80 and XRCC4. *Proc. Natl. Acad. Sci. U. S. A.* 103:18597–18602. doi:10.1073/pnas.0609061103.
- Marini, F., T. Nardo, M. Giannattasio, M. Minuzzo, M. Stefanini, P. Plevani, and M. Muzi Falconi. 2006. DNA nucleotide excision repair-dependent signaling to checkpoint activation. *Proc. Natl. Acad. Sci. U. S. A.* 103:17325–30. doi:10.1073/pnas.0605446103.
- Markson, G., C. Kiel, R. Hyde, S. Brown, P. Charalabous, A. Bremm, J. Semple, J. Woodsmith, S. Duley, K. Salehi-Ashtiani, M. Vidal, D. Komander, L. Serrano, P. Lehner, and C.M. Sanderson. 2009. Analysis of the human E2 ubiquitin conjugating enzyme protein interaction network. *Genome Res.* 19:1905–11. doi:10.1101/gr.093963.109.
- Marteijn, J. a. S. Bekker-Jensen, N. Mailand, H. Lans, P. Schwertman, A.M. Gourdin, N.P. Dantuma, J. Lukas, and W. Vermeulen. 2009. Nucleotide excision repair-induced H2A ubiquitination is dependent on MDC1 and RNF8 and reveals a universal DNA damage response. *J. Cell Biol.* 186:835–47. doi:10.1083/jcb.200902150.
- Masuda, H., Y. Takenaka, A. Yamaguchi, S. Nishikawa, and H. Mizuno. 2006. A novel yellowish-green fluorescent protein from the marine copepod, *Chiridius poppei*, and its use as a reporter protein in HeLa cells. *Gene.* 372:18–25. doi:10.1016/j.gene.2005.11.031.
- Masutani, C., K. Sugasawa, J. Yanagisawa, T. Sonoyama, M. Uli, T. Enomoto, K. Takio, K. Tanaka, P.J. van der Spek, and D. Bootsma. 1994. Purification and cloning of a nucleotide excision repair complex involving the xeroderma pigmentosum group C protein and a human homologue of yeast RAD23. *EMBO J.* 13:1831–43.
- Mattern, K.A., S.J.J. Swiggers, A.L. Nigg, B. Löwenbreg, A.B. Houtsmuller, and J. Zijlmans. 2004. Dynamics of Protein Binding to Telomeres in Living Cells: Implications for Telomere Structure and Function Dynamics of Protein Binding to Telomeres in Living Cells: Implications for Telomere Structure and Function. *Mol. Cell Biol.* 24:5589–5594. doi:10.1128/MCB.24.12.5587.
- Matunis, M.J., E. Coutavas, and G. Blobel. 1996. A novel ubiquitin-like modification modulates the partitioning of the RanGTPase-activating protein RanGAP1 between the cytosol and the nuclear pore complex. *J. Cell Biol.* 135:1457–70.
- Matz, M. V, a F. Fradkov, Y. a Labas, a P. Savitsky, a G. Zarasky, M.L. Markelov, and S. a Lukyanov. 1999. Fluorescent proteins from nonbioluminescent Anthozoa species. *Nat. Biotechnol.* 17:969–73. doi:10.1038/13657.
- Maynard, S., S.H. Schurman, C. Harboe, N.C. de Souza-Pinto, and V. a Bohr. 2009. Base excision repair of oxidative DNA damage and association with cancer and aging. *Carcinogenesis.* 30:2–10. doi:10.1093/carcin/bgn250.
- Mckay, B.C., M. Ljungman, and A.J. Rainbow. 1998. Persistent DNA damage induced by ultraviolet light inhibits p21 waf1 and bax expression: implications for DNA repair, UV sensitivity and the induction of apoptosis.
- McNally, J.G., W.G. Müller, D. Walker, R. Wolford, and G.L. Hager. 2000. The Glucocorticoid Receptor: Rapid Exchange with Regulatory Sites in Living Cells. *Science (80-.).* 287:1262–1265. doi:10.1126/science.287.5456.1262.
- Michelle, C., P. Vourc'h, L. Mignon, and C.R. Andres. 2009. What was the set of ubiquitin and ubiquitin-like conjugating enzymes in the eukaryote common ancestor? *J. Mol. Evol.* 68:616–28. doi:10.1007/s00239-009-9225-6.
- Min, J.-H., and N.P. Pavletich. 2007. Recognition of DNA damage by the Rad4 nucleotide excision repair protein. *Nature.* 449:570–5. doi:10.1038/nature06155.
- Mochizuki, N., S. Yamashita, K. Kurokawa, Y. Ohba, T. Nagai, A. Miyawaki, and M. Matsuda. 2001. Spatio-temporal images of growth-factor-induced activation of Ras and Rap1. *Nature.* 411:1065–1068.
- Modrich, P. 2006. Mechanisms in eukaryotic mismatch repair. *J. Biol. Chem.* 281:30305–9. doi:10.1074/jbc.R600022200.
- Moser, J., H. Kool, I. Giakzidis, K. Caldecott, L.H.F. Mullenders, and M.I. Foustier. 2007. Sealing of chromosomal DNA nicks during nucleotide excision repair requires XRCC1 and DNA ligase III alpha in a cell-cycle-specific manner. *Mol. Cell.* 27:311–23. doi:10.1016/j.molcel.2007.06.014.
- Moser, J., M. Volker, H. Kool, S. Alekseev, H. Vrieling, A. Yasui, A. van Zeeland, and L.H.F. Mullenders. 2005. The UV-damaged DNA binding protein mediates efficient targeting of the nucleotide excision repair complex to UV-induced photo lesions. *DNA Repair (Amst).* 4:571–82. doi:10.1016/j.dnarep.2005.01.001.
- Muniandy, P.A., J. Liu, A. Majumdar, S. Liu, and M.M. Seidman. 2010. DNA interstrand crosslink repair in mammalian cells: step by step. *Crit. Rev. Biochem. Mol. Biol.* 45:23–49. doi:10.3109/10409230903501819.
- Nakasone, M.A., N. Livnat-Levanon, M.H. Glickman, R.E. Cohen, and D. Fushman. 2013. Mixed-linkage ubiquitin chains send mixed messages. *Structure.* 21:727–40. doi:10.1016/j.str.2013.02.019.
- Nance, M. a, and S. a Berry. 1992. Cockayne syndrome: review of 140 cases. *Am. J. Med. Genet.* 42:68–84. doi:10.1002/ajmg.1320420115.
- Ng, J.M.Y., W. Vermeulen, G.T.J. van der Horst, S. Bergink, K. Sugasawa, H. Vrieling, and J.H.J. Hoeijmakers. 2003. A novel regulation mechanism of DNA repair by damage-induced and RAD23-dependent stabilization of xeroderma pigmentosum group C protein. *Genes Dev.* 17:1630–45. doi:10.1101/gad.260003.
- Niedernhofer, L.J., V. a Bohr, M. Sander, and K.H. Kraemer. 2011. Xeroderma pigmentosum and other diseases of human premature aging and DNA repair: molecules to patients. *Mech. Ageing Dev.* 132:340–7. doi:10.1016/j.mad.2011.06.004.
- Niedernhofer, L.J., G. a Garinis, A. Raams, A.S. Lalai, A.R. Robinson, E. Appeldoorn, H. Odiijk, R. Oostendorp, A. Ahmad, W. van Leeuwen, A.F. Theil, W. Vermeulen, G.T.J. van der Horst, P. Meinecke, W.J. Kleijer, J. Vlij, N.G.J. Jaspers, and J.H.J. Hoeijmakers. 2006. A new progeroid syndrome reveals that genotoxic stress suppresses the somatotroph axis. *Nature.* 444:1038–43. doi:10.1038/nature05456.
- Nijman, S.M.B., T.T. Huang, A.M.G. Dirac, T.R. Brummelkamp, R.M. Kerkhoven, A.D. D'Andrea, and R. Bernards. 2005a. The deubiquitinating enzyme USP1 regulates the Fanconi anemia pathway. *Mol. Cell.* 17:331–9. doi:10.1016/j.molcel.2005.01.008.

- Nijman, S.M.B., M.P. a Luna-Vargas, A. Velds, T.R. Brummelkamp, A.M.G. Dirac, T.K. Sixma, and R. Bernards. 2005b. A genomic and functional inventory of deubiquitinating enzymes. *Cell*. 123:773–86. doi:10.1016/j.cell.2005.11.007.
- Nishi, R., Y. Okuda, E. Watanabe, T. Mori, S. Iwai, C. Masutani, K. Sugawara, and F. Hanaoka. 2005. Centrin 2 stimulates nucleotide excision repair by interacting with xeroderma pigmentosum group C protein. *Mol. Cell Biol.* 25:5664–74. doi:10.1128/MCB.25.13.5664-5674.2005.
- Nishizuka, Y., K. Ueda, K. Nakazawa, and O. Hayaishi. 1967. Studies on the Polymer of Adenosine Diphosphate Ribose I. ENZYMIC FORMATION FROM NICOTINAMIDE ADENINE DINUCLEOTIDE IN MAMMALIAN NUCLEI. *J. Biol. Chem.* 242:3164–3171.
- Noll, D.M., T.M. Mason, and P.S. Miller. 2006. Formation and repair of interstrand cross-links in DNA. *Chem. Rev.* 106:277–301. doi:10.1021/cr040478b.
- O'Donovan, A., A. Davies, and J. Moggs. 1994. XPG endonuclease makes the 3' incision in human DNA nucleotide excision repair. *Zhurnal Eksp. i Teor. Fiz.* 371:1994.
- Ogi, T., S. Limsirichaikul, R.M. Overmeer, M. Volker, K. Takenaka, R. Cloney, Y. Nakazawa, A. Niimi, Y. Miki, N.G. Jaspers, L.H.F. Mullenders, S. Yamashita, M.I. Foustari, and A.R. Lehmann. 2010. Three DNA polymerases, recruited by different mechanisms, carry out NER repair synthesis in human cells. *Mol. Cell.* 37:714–27. doi:10.1016/j.molcel.2010.02.009.
- Papadopoulos, N., N.C. Nicolaides, Y.F. Wei, S.M. Ruben, K.C. Carter, C.A. Rosen, W.A. Haseltine, R.D. Fleischmann, C.M. Fraser, and M.D. Adams. 1994. Mutation of a mutL homolog in hereditary colon cancer. *Science*. 263:1625–9.
- Pelzer, C., I. Kassner, K. Matentzoglou, R.K. Singh, H.-P. Wollscheid, M. Scheffner, G. Schmidtke, and M. Groettrup. 2007. UBE1L2, a novel E1 enzyme specific for ubiquitin. *J. Biol. Chem.* 282:23010–4. doi:10.1074/jbc.C700111200.
- Peters, R., J. Peters, K.H. Tews, and W. Bähr. 1974. A microfluorimetric study of translational diffusion in erythrocyte membranes. *Biochim. Biophys. Acta.* 367:282–94.
- Phair, R., and T. Misteli. 2000. High mobility of proteins in the mammalian cell nucleus. *Nature*. 404:604–9. doi:10.1038/35007077.
- Pickart, C.M. 2001. Mechanisms underlying ubiquitination. *Annu. Rev. Biochem.* 70:503–33. doi:10.1146/annurev.biochem.70.1.503.
- Pines, A., L. Hameetman, J. de Wilde, S. Alekseev, F.R. de Grijijl, H. Vrieling, and L.H.F. Mullenders. 2010. Enhanced global genome nucleotide excision repair reduces UV carcinogenesis and nullifies strand bias in p53 mutations in Csb^{-/-} mice. *J. Invest. Dermatol.* 130:1746–9. doi:10.1038/jid.2010.18.
- Pines, A., M.G. Vrouwe, J. a Martijn, D. Typas, M.S. Luijsterburg, M. Cansoy, P. Hensbergen, A. Deelder, A. de Groot, S. Matsumoto, K. Sugawara, N. Thoma, W. Vermeulen, H. Vrieling, and L. Mullenders. 2012. PARP1 promotes nucleotide excision repair through DDB2 stabilization and recruitment of ALC1. *J. Cell Biol.* 199:235–49. doi:10.1083/jcb.201112132.
- Pluciennik, A., L. Dzantiev, R.R. Iyer, N. Constantin, F.A. Kadyrov, and P. Modrich. 2010. PCNA function in the activation and strand direction of MutLα endonuclease in mismatch repair. *Proc. Natl. Acad. Sci. U. S. A.* 107:16066–71. doi:10.1073/pnas.1010662107.
- Poulsen, S.L., R.K. Hansen, S. a Wagner, L. van Cuijk, G.J. van Belle, W. Streicher, M. Wikström, C. Choudhary, A.B. Houtsmuller, J. a Martijn, S. Bekker-Jensen, and N. Mailand. 2013. RNF111/Arkadia is a SUMO-targeted ubiquitin ligase that facilitates the DNA damage response. *J. Cell Biol.* 201:797–807. doi:10.1083/jcb.201212075.
- Prudden, J., S. Pebernard, G. Raffa, D. a Slavin, J.J.P. Perry, J. a Tainer, C.H. McGowan, and M.N. Boddy. 2007. SUMO-targeted ubiquitin ligases in genome stability. *EMBO J.* 26:4089–101. doi:10.1038/sj.emboj.7601838.
- Puszyński, K., B. Hat, and T. Lipniacki. 2008. Oscillations and bistability in the stochastic model of p53 regulation. *J. Theor. Biol.* 254:452–65. doi:10.1016/j.jtbi.2008.05.039.
- Rademakers, S., M. Volker, D. Hoogstraten, A.L. Nigg, M.J. Moné, A.A. Van Zeeland, J.H.J. Hoeijmakers, A.B. Houtsmuller, and W. Vermeulen. 2003. Xeroderma pigmentosum group A protein loads as a separate factor onto DNA lesions. *Mol. Cell Biol.* 23:5755–67. doi:10.1128/MCB.23.16.5755.
- Ramanathan, B., and M.J. Smerdon. 1989. Enhanced DNA repair synthesis in hyperacetylated nucleosomes. *J. Biol. Chem.* 264:11026–34.
- Ranish, J.A., S. Hahn, Y. Lu, E.C. Yi, X. Li, J. Eng, and R. Aebersold. 2004. Identification of TFB5, a new component of general transcription and DNA repair factor IIH. *Nat. Genet.* 36:707–13. doi:10.1038/ng1385.
- Ravanat, J.L., T. Douki, and J. Cadet. 2001. Direct and indirect effects of UV radiation on DNA and its components. *J. Photochem. Photobiol. B.* 63:88–102.
- Remington, S.J. 2006. Fluorescent proteins: maturation, photochemistry and photophysics. *Curr. Opin. Struct. Biol.* 16:714–21. doi:10.1016/j.sbi.2006.10.001.
- Robertson, a B., a Klungland, T. Rognes, and I. Leiros. 2009. DNA repair in mammalian cells: Base excision repair: the long and short of it. *Cell. Mol. Life Sci.* 66:981–93. doi:10.1007/s00018-009-8736-z.
- Van Royen, M.E., P. Farla, K. a Mattern, B. Geverts, J. Trapman, and A.B. Houtsmuller. 2009. Fluorescence recovery after photobleaching (FRAP) to study nuclear protein dynamics in living cells. *Methods Mol. Biol.* 464:363–85. doi:10.1007/978-1-60327-461-6_20.
- Ryan, D.P., T.S. Hong, and N. Bardeesy. 2014. Pancreatic adenocarcinoma. *N. Engl. J. Med.* 371:1039–49. doi:10.1056/NEJMr1404198.
- Sancar, A. 1996. DNA excision repair. *Annu. Rev. Biochem.* 65:43–81. doi:10.1146/annurev.bi.65.070196.000355.
- Schaeffer, L., R. Roy, S. Humbert, V. Moncollin, W. Vermeulen, J.H. Hoeijmakers, P. Chambon, and J.M. Egly. 1993. DNA repair helicase: a component of BTF2 (TFIIH) basic transcription factor. *Science*. 260:58–63.
- Schärer, O.D. 2013. Nucleotide excision repair in eukaryotes. *Cold Spring Harb. Perspect. Biol.* 5:a012609. doi:10.1101/cshperspect.a012609.
- Scheffner, M., and S. Kumar. 2014. Mammalian HECT ubiquitin-protein ligases: biological and pathophysiological aspects. *Biochim. Biophys. Acta.* 1843:61–74. doi:10.1016/j.bbamcr.2013.03.024.
- Schwab, R. a, A.N. Blackford, and W. Niedzwiedz. 2010. ATR activation and replication fork restart are defective in FANCM-deficient cells. *EMBO J.* 29:806–18. doi:10.1038/emboj.2009.385.
- Scrima, A., R. Konicková, B.K. Czyzewski, Y. Kawasaki, P.D. Jeffrey, R. Groisman, Y. Nakatani, S. Iwai, N.P. Pavletich, and N.H. Thomá. 2008. Structural basis of UV DNA-damage recognition by the DDB1–DDB2 complex. *Cell*. 135:1213–23. doi:10.1016/j.cell.2008.10.045.
- Shagin, D. a, E. V Barsova, Y.G. Yanushevich, A.F. Fradkov, K. a Lukyanov, Y. a Labas, T.N. Semenova, J. a Ugalde, A. Meyers, J.M. Nunez, E. a Widder, S. a Lukyanov, and M. V Matz. 2004. GFP-like proteins as ubiquitous metazoan superfamily: evolution of functional features and structural complexity. *Mol. Biol. Evol.* 21:841–50. doi:10.1093/molbev/msh079.

- Shaner, N.C., G.H. Patterson, and M.W. Davidson. 2007. Advances in fluorescent protein technology. *J. Cell Sci.* 120:4247–60. doi:10.1242/jcs.005801.
- Siggia, E.D., J. Lippincott-schwartz, and S. Bekiranov. 2000. Diffusion in Inhomogeneous Media: Theory and Simulations Applied to. *Biophys. J.* 79:1761–1770.
- Sijbers, A.M., W.L. de Laat, R.R. Ariza, M. Biggerstaff, Y.F. Wei, J.G. Moggs, K.C. Carter, B.K. Shell, E. Evans, M.C. de Jong, S. Rademakers, J. de Rooij, N.G. Jaspers, J.H. Hoeijmakers, and R.D. Wood. 1996. Xeroderma pigmentosum group F caused by a defect in a structure-specific DNA repair endonuclease. *Cell.* 86:811–22.
- Soumpasis, D. 1983. Theoretical analysis of fluorescence photobleaching recovery experiments. *Biophys. J.* 41:95–97.
- Spence, J., R.R. Gali, G. Dittmar, F. Sherman, M. Karin, D. Finley, and N. York. 2000. Cell Cycle – Regulated Modification of the Ribosome by a Variant Multiubiquitin Chain University of California at San Diego. 102:67–76.
- Starcevic, D., S. Dalal, and J.B. Sweasy. 2004. Is there a link between DNA polymerase beta and cancer? *Cell Cycle.* 3:998–1001. doi:10.4161/cc.3.8.1062.
- Stenoien, D.L., K. Patel, M.G. Mancini, M. Dutertre, C.L. Smith, B.W. O'Malley, and M. a Mancini. 2001. FRAP reveals that mobility of oestrogen receptor-alpha is ligand- and proteasome-dependent. *Nat. Cell Biol.* 3:15–23. doi:10.1038/35050515.
- Struewing, J.P., P. Hartge, S. Wacholder, S.M. Baker, M. Berlin, M. McAdams, M.M. Timmerman, L.C. Brody, and M.A. Tucker. 1997. The risk of cancer associated with specific mutations of BRCA1 and BRCA2 among Ashkenazi Jews. *N. Engl. J. Med.* 336:1401–8. doi:10.1056/NEJM199705153362001.
- Sugasawa, K., J. Akagi, R. Nishi, S. Iwai, and F. Hanaoka. 2009. Two-step recognition of DNA damage for mammalian nucleotide excision repair: Directional binding of the XPC complex and DNA strand scanning. *Mol. Cell.* 36:642–53. doi:10.1016/j.molcel.2009.09.035.
- Sugasawa, K., J.M. Ng, C. Masutani, S. Iwai, P.J. van der Spek, A.P. Eker, F. Hanaoka, D. Bootsma, and J.H. Hoeijmakers. 1998. Xeroderma pigmentosum group C protein complex is the initiator of global genome nucleotide excision repair. *Mol. Cell.* 2:223–32. doi:10.1016/S1097-2765(00)80132-X.
- Sugasawa, K., T. Okamoto, Y. Shimizu, C. Masutani, S. Iwai, and F. Hanaoka. 2001. A multistep damage recognition mechanism for global genomic nucleotide excision repair. *Genes Dev.* 15:507–21. doi:10.1101/gad.866301.
- Sugasawa, K., Y. Okuda, M. Saijo, R. Nishi, N. Matsuda, G. Chu, T. Mori, S. Iwai, K. Tanaka, K. Tanaka, and F. Hanaoka. 2005. UV-induced ubiquitylation of XPC protein mediated by UV-DDB-ubiquitin ligase complex. *Cell.* 121:387–400. doi:10.1016/j.cell.2005.02.035.
- Sun, H., J.D. Levenson, and T. Hunter. 2007. Conserved function of RNF4 family proteins in eukaryotes: targeting a ubiquitin ligase to SUMOylated proteins. *EMBO J.* 26:4102–12. doi:10.1038/sj.emboj.7601839.
- Sung, P., and H. Klein. 2006. Mechanism of homologous recombination: mediators and helicases take on regulatory functions. *Nat. Rev. Mol. Cell Biol.* 7:739–50. doi:10.1038/nrm2008.
- Tauchi, H., J. Kobayashi, and K. Morishima. 2002. Nbs1 is essential for DNA repair by homologous recombination in higher vertebrate cells. *Nature.* 420:93–8. doi:10.1038/nature01125.
- Tsien, R.Y. 1998. The green fluorescent protein. *Annu. Rev. Biochem.* 67:509–544. doi:10.1146/annurev.biochem.67.1.509.
- Tyson, J.J., K.C. Chen, and B. Novak. 2003. Sniffers, buzzers, toggles and blinkers: dynamics of regulatory and signaling pathways in the cell. *Curr. Opin. Cell Biol.* 15:221–231. doi:10.1016/S0955-0674(03)00017-6.
- Uzunova, K., K. Götttsche, M. Miteva, S.R. Weisshaar, C. Glanemann, M. Schnellhardt, M. Niessen, H. Scheel, K. Hofmann, E.S. Johnson, G.J.K. Praefcke, and R.J. Dohmen. 2007. Ubiquitin-dependent proteolytic control of SUMO conjugates. *J. Biol. Chem.* 282:34167–75. doi:10.1074/jbc.M706505200.
- Volker, M., M.J. Moné, P. Karmakar, a van Hoffen, W. Schul, W. Vermeulen, J.H. Hoeijmakers, R. van Driel, a a van Zeeland, and L.H. Mullenders. 2001. Sequential assembly of the nucleotide excision repair factors in vivo. *Mol. Cell.* 8:213–24.
- Wakasugi, M., A. Kawashima, H. Morioka, S. Linn, A. Sancar, T. Mori, O. Nikaïdo, and T. Matsunaga. 2002. DDB accumulates at DNA damage sites immediately after UV irradiation and directly stimulates nucleotide excision repair. *J. Biol. Chem.* 277:1637–40. doi:10.1074/jbc.C100610200.
- Walker, J., R. Corpina, and J. Goldberg. 2001. Structure of the Ku heterodimer bound to DNA and its implications for double-strand break repair. *Nature.* 412:607–14. doi:10.1038/35088000.
- Wang, Q.-E., Q. Zhu, G. Wani, M. a El-Mahdy, J. Li, and A. a Wani. 2005. DNA repair factor XPC is modified by SUMO-1 and ubiquitin following UV irradiation. *Nucleic Acids Res.* 33:4023–34. doi:10.1093/nar/gki684.
- Waris, G., and H. Ahsan. 2006. Reactive oxygen species: role in the development of cancer and various chronic conditions. *J. Carcinog.* 5:14. doi:10.1186/1477-3163-5-14.
- Wenzel, D.M., and R.E. Kleivt. 2012. Following Ariadne's thread: a new perspective on RBR ubiquitin ligases. *BMC Biol.* 10:24. doi:10.1186/1741-7007-10-24.
- Weterings, E., and D.C. van Gent. 2004. The mechanism of non-homologous end-joining: a synopsis of synapsis. *DNA Repair (Amst).* 3:1425–35. doi:10.1016/j.dnarep.2004.06.003.
- Van Wijk, S.J.L., and H.T.M. Timmers. 2010. The family of ubiquitin-conjugating enzymes (E2s): deciding between life and death of proteins. *FASEB J.* 24:981–93. doi:10.1096/fj.09-136259.
- Willig, K.I., R.R. Kellner, R. Medda, B. Hein, S. Jakobs, and S.W. Hell. 2006. Nanoscale resolution in GFP-based microscopy. *Nat. Methods.* 3:721–3. doi:10.1038/nmeth922.
- Xiong, W., and J.E. Ferrell. 2003. A positive-feedback-based bistable "memory module" that governs a cell fate decision. *Nature.* 426:460–5. doi:10.1038/nature02089.
- Yeh, J.I., A.S. Levine, S. Du, U. Chinte, H. Ghodke, H. Wang, H. Shi, C.L. Hsieh, J.F. Conway, B. Van Houten, and V. Rapić-Otrin. 2012. Damaged DNA induced UV-damaged DNA-binding protein (UV-DDB) dimerization and its roles in chromatinized DNA repair. *Proc. Natl. Acad. Sci. U. S. A.* 109:E2737–46. doi:10.1073/pnas.1110067109.
- Zhang, X.-P., F. Liu, and W. Wang. 2011. Two-phase dynamics of p53 in the DNA damage response. *Proc. Natl. Acad. Sci. U. S. A.* 108:8990–5. doi:10.1073/pnas.1100600108.
- Zotter, A., M.S. Luijsterburg, D.O. Warmerdam, S. Ibrahim, A. Nigg, W. a van Cappellen, J.H.J. Hoeijmakers, R. van Driel, W. Vermeulen, and A.B. Houtsmuller. 2006. Recruitment of the nucleotide excision repair endonuclease XPG to sites of UV-induced dna damage depends on functional TFIIH. *Mol. Cell. Biol.* 26:8868–79. doi:10.1128/MCB.00695-06.
- Zurita, M., and C. Merino. 2003. The transcriptional complexity of the TFIIH complex. *Trends Genet.* 19:578–84. doi:10.1016/j.tig.2003.08.005.

Chapter II

RNF111/Arkadia is a SUMO-targeted ubiquitin ligase that facilitates the DNA damage response




Sara L. Poulsen¹, Rebecca K. Hansen¹, Sebastian A. Wagner², Loes van Cuijk⁴, Gijsbert J. van Belle⁵, Werner Streicher³, Mats Wikström³, Chunaram Choudhary², Adriaan B. Houtsmuller⁵, Jurgan A. Marteijn⁴, Simon Bekker-Jensen¹, and Niels Mailand¹

¹Ubiquitin Signaling Group, Department of Disease Biology, ²Department of Proteomics, and ³Protein Function and Interactions Group, The Novo Nordisk Foundation Center for Protein Research, University of Copenhagen, DK-2200 Copenhagen, Denmark ⁴Department of Genetics and ⁵Department of Pathology, Josephine Nefkens Institute, Erasmus Medical Center, 3015 GE Rotterdam, Netherlands

Published in Journal of Cell Biology 2013 Jun 10; 201(6):797-807

Abstract



Protein modifications by ubiquitin and small ubiquitin-like modifier (SUMO) play key roles in cellular signaling pathways. SUMO-targeted ubiquitin ligases (STUbLs) directly couple these modifications by selectively recognizing SUMOylated target proteins through SUMO-interacting motifs (SIMs), promoting their K48-linked ubiquitylation and degradation. Only a single mammalian STUbL, RNF4, has been identified. We show that human RNF111/Arkadia is a new STUbL, which used three adjacent SIMs for specific recognition of poly-SUMO2/3 chains, and used Ubc13–Mms2 as a cognate E2 enzyme to promote non-proteolytic, K63-linked ubiquitylation of SUMOylated target proteins. We demonstrate that RNF111 promoted ubiquitylation of SUMOylated XPC (xeroderma pigmentosum C) protein, a central DNA damage recognition factor in nucleotide excision repair (NER) extensively regulated by ultraviolet (UV)-induced SUMOylation and ubiquitylation. Moreover, we show that RNF111 facilitated NER by regulating the recruitment of XPC to UV-damaged DNA. Our findings establish RNF111 as a new STUbL that directly links non-proteolytic ubiquitylation and SUMOylation in the DNA damage response.

Introduction

Protein modification by ubiquitin and the small ubiquitin-like modifier (SUMO) play important, often interconnected, regulatory roles in numerous signaling pathways in eukaryotic cells (Kerscher et al., 2006; Gareau and Lima, 2010; Komander and Rape, 2012). Similar enzymatic cascades involving activating (E1), conjugating (E2), and ligase (E3) enzymes underlie protein modification by ubiquitin and SUMO (Kerscher et al., 2006). Although no consensus sequences surrounding ubiquitylation sites have been described, SUMOylation is frequently, but not always, targeted to K-X-E/D motifs or an inverted version of this sequence (Matic et al., 2010). Three different SUMO isoforms, SUMO1–3, are expressed in cells, and although SUMO2 and SUMO3 are 97% identical and thus often referred to as SUMO2/3, SUMO1 and SUMO2/3 only share ~50% sequence identity (Gareau and Lima, 2010). Both ubiquitin and SUMO can be attached to target proteins as single moieties but additionally share the ability to form chains via internal lysine residues. Unlike ubiquitin, only a single lysine residue in SUMO that conforms to the SUMO consensus sequence is used for chain formation, and this ability is exclusive to SUMO2/3 (Tatham et al., 2001; Komander and Rape, 2012).

Different polyubiquitin chains have distinct cellular functions (Komander and Rape, 2012). Although most of the known ubiquitylation processes generate K48-linked chains, which target substrates for degradation by the 26S proteasome, protein ubiquitylation does not always promote destruction; in particular, K63-linked polyubiquitylation, catalyzed by the E2 enzyme Ubc13 in conjunction with its partner proteins Mms2 or Uev1, is a non-degradative modification used in a range of signaling pathways, including cellular stress responses such as DNA damage and inflammatory responses (Chen and Sun, 2009; Al-Hakim et al., 2010; Komander and Rape, 2012). The function of poly-SUMO chains is less well understood, but roles in processes such as chromosome segregation, DNA damage, and heat shock responses have been described (Schwartz et al., 2007; Golebiowski et al., 2009; Yin et al., 2012). Several cellular processes, including the DNA damage response, are intimately co-regulated by ubiquitin- and SUMO-mediated signaling (Kerscher et al., 2006; Bergink and Jentsch, 2009; Bekker-Jensen and Mailand, 2011). The discovery of SUMO-targeted ubiquitin ligases (STUbLs) revealed a further, direct interplay between these modifications. By means of tandem SUMO-interacting motifs (SIMs) (Hecker et al., 2006), STUbLs recognize poly-SUMOylated proteins and target them for K48-linked polyubiquitylation and degradation via their E3 ubiquitin ligase activities (Prudden et al., 2007; Sun et al., 2007). Accordingly, although SUMOylation is not a degradative modification per se, it can indirectly promote proteasomal destruction via STUbLs. Only a few STUbLs have been identified so far, including Slx5-Slx8 in *Saccharomyces cerevisiae*, Rfp1/Rfp2-Slx8 in *Schizosaccharomyces pombe*, and RNF4 in mammalian cells. All of these enzymes play important roles in maintenance of genome stability (Prudden et al., 2007; Sun et al., 2007; Galanty et al., 2012; Yin et al., 2012), consistent with the extensive involvement of both ubiquitin and SUMO in cellular responses to DNA damage.

In a search for new SUMO-binding proteins, we discovered that the human RNF111 ubiquitin ligase (also known as Arkadia) is a STUbL, which can promote non-proteolytic ubiquitylation of target proteins through cognate E2 enzymes such as Ubc13. We demonstrate that RNF111 has a physiological role in nucleotide excision repair (NER), catalyzing DNA damage-induced ubiquitylation of SUMOylated XPC (xeroderma pigmentosum C). Our findings reveal direct coupling between non-proteolytic ubiquitylation and SUMOylation in the DNA damage response.



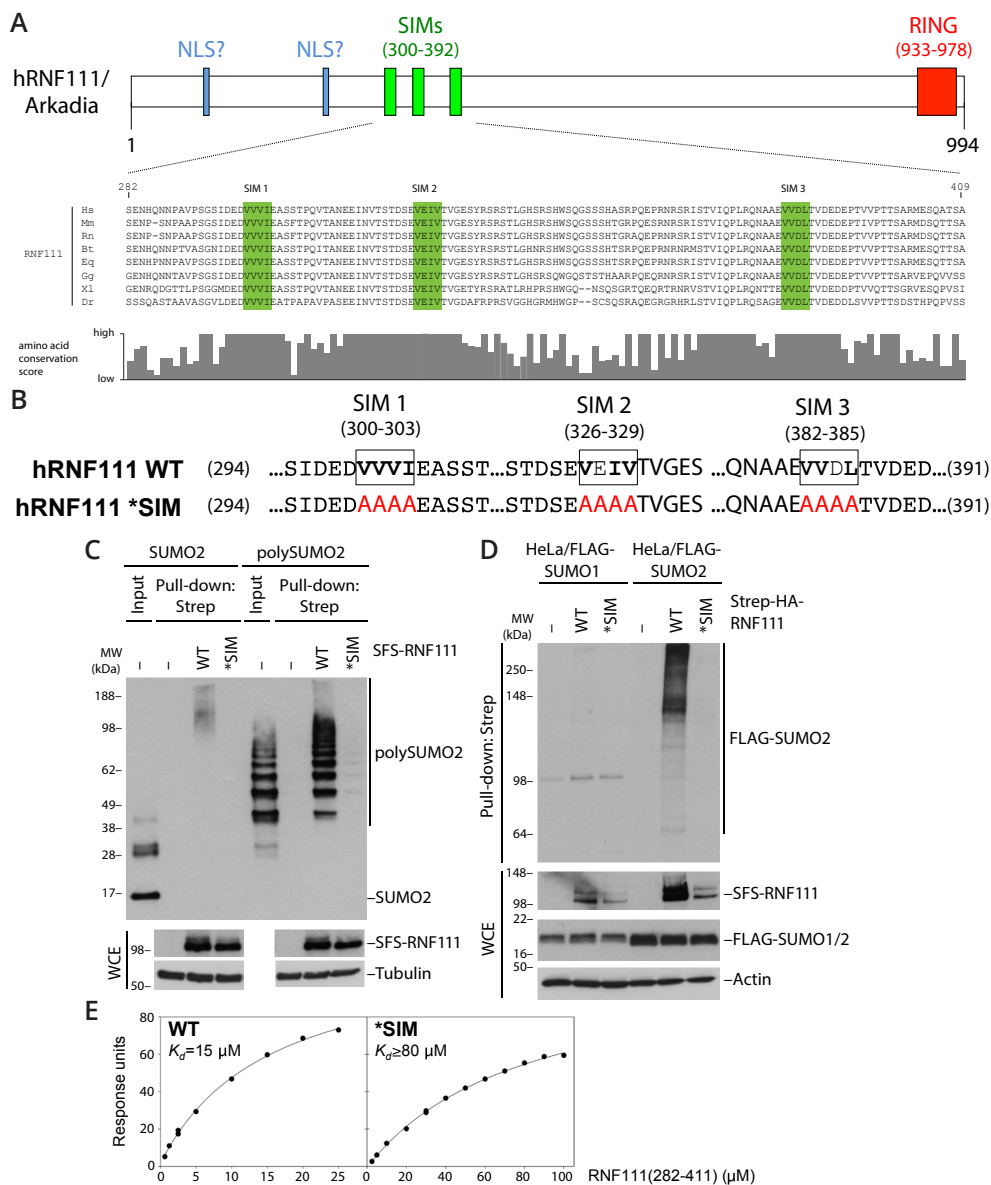


Figure 1. Human RNF111 binds to poly-SUMOylated proteins via an N-terminal SIM region. (A) Schematic of human RNF111/Arkadia. The RING domain, two putative NLSs (Episkopou et al., 2001), and three SUMO-interacting motifs (SIMs; top), conserved in higher vertebrates (bottom), are shown. Core hydrophobic SIM residues are highlighted in green. (B) Amino acid substitutions (highlighted in red) in the RNF111 SIM region to disrupt its SUMO-binding ability (*SIM). (C) S-FLAG-Strep-tagged RNF111 (SFS-RNF111) proteins expressed in U2OS cells were purified on Strep-Tactin Sepharose, incubated with purified SUMO2 or poly-SUMO2 (3–8), and washed extensively. Bound complexes were immunoblotted with the SUMO2 antibody. WCE, whole-cell extract. (D) HeLa cells stably expressing FLAG-SUMO isoforms were transfected with Strep-HA-RNF111 plasmids as indicated. Whole-cell extracts were subjected to Strep-Tactin pull-down and immunoblotting with the FLAG antibody. (E) Plasmon surface resonance analysis of poly-SUMO2 binding kinetics of RNF111 fragments spanning the SIMs. Data shown are from a single representative experiment out of three repeats. MW, molecular weight.

Results and discussion

RNF111 recognizes poly-SUMO chains via tandem SIMs

In a search for proteins containing SIMs, we noted that the human RNF111/Arkadia E3 ubiquitin ligase, which has been shown to function in amplification of TGF- β signaling pathways (Miyazono and Koinuma, 2011) contains three highly conserved, potential SIMs in its N-terminal region (Fig. 1, A and B). To test whether these putative SIMs are functional SUMO-binding modules, we generated an RNF111 mutant (*SIM) in which the core hydrophobic residues in each of the three SIMs were mutated to alanines, predicted to disrupt their SUMO-binding ability (Fig. 1 B)(Hecker et al., 2006). We first assessed the SUMO-binding ability of ectopically expressed Strep-tagged forms of RNF111 wild type (WT) or *SIM purified on Strep-Tactin agarose. We found that RNF111 bound purified poly-SUMO2 chains with high affinity *in vitro* but was virtually unable to bind free SUMO2 (Fig. 1 C). This was fully dependent on the integrity of the SIM motifs, as the RNF111 *SIM mutant did not interact with poly-SUMO2 (Fig. 1 C). To test whether RNF111 binds to SUMOylated proteins in cells, we overexpressed RNF111 WT or *SIM in cells stably expressing FLAG-SUMO1 or 2 and analyzed their interactions in immunoprecipitation (IP) experiments. Consistent with *in vitro* binding experiments, RNF111 interacted with high-molecular weight SUMOylated species, but not free SUMO2, in a SIM-dependent manner (Fig. 1 D and not depicted). Moreover, RNF111 selectively interacted with proteins modified with SUMO2 but not SUMO1 (Fig. 1 D), in agreement with the notion that SUMO2, but not SUMO1, forms poly-SUMO chains *in vivo* (Tatham et al., 2001). Surface plasmon resonance analysis showed that the RNF111 SIM region bound directly to poly-SUMO2 with a K_d of $\sim 15 \mu\text{M}$, whereas the *SIM mutations reduced binding to a $K_d > 80 \mu\text{M}$ (Fig. 1 E). These data demonstrate that RNF111 interacts with poly-SUMOylated proteins via three N-terminal SIM motifs, in accordance with recent findings that showed an additive contribution of each SIM to poly-SUMO binding (Sun and Hunter, 2012).

RNF111 promotes Ubc13-Mms2-dependent ubiquitylation

To gain insight into the functional significance of RNF111 SUMO binding, we performed quantitative mass spectrometry (MS)-based analysis of cellular RNF111-interacting proteins (Fig. 2 A and Fig. S1 A). Several potential RNF111-binding factors were identified by this approach, including components of the AP2 (clathrin adaptor 2) complex, consistent with the known role of RNF111 in regulating endocytosis via interaction with this complex (Fig. S1, A and B)(Miyazono and Koinuma, 2011). Among the RNF111-associated proteins, we also found two E2 ubiquitin-conjugating enzymes: Ubc13-Mms2, which specifically catalyzes K63-linked ubiquitin chain formation, and UBE2O, a large E2 enzyme of unknown function (Fig. 2 A and Fig. S1 B). The presence of both Ubc13 and Mms2 lends strong support to the possibility that this complex is a physiological E2 partner for RNF111. We validated the interactions between RNF111 and Ubc13 or UBE2O by reciprocal co-IP analysis (Fig. 2 B and Fig. S2, A and B). In contrast, we did not observe binding of RNF4, the known mammalian STUbL, to Ubc13 under a range of conditions (Fig. S2, C and D). Because RNF111 promotes degradation of factors in TGF- β signaling pathways, the interaction with Ubc13-Mms2 was unexpected, and we set out to investigate its physiological relevance. We noted that endogenous RNF111 is primarily localized in the nucleus (Fig. 2 C), suggesting that in addition to facilitating amplification of TGF- β signaling and endocytosis, RNF111 might have other important nuclear functions. To test whether RNF111 has E3 ligase activity in the presence of Ubc13-Mms2, we performed *in vitro* ubiquitylation assays using ectopic RNF111 immunopurified from cells. Because RNF111 appeared to form homodimers in cells (unpublished data), we depleted endogenous RNF111 to remove background E3 ligase

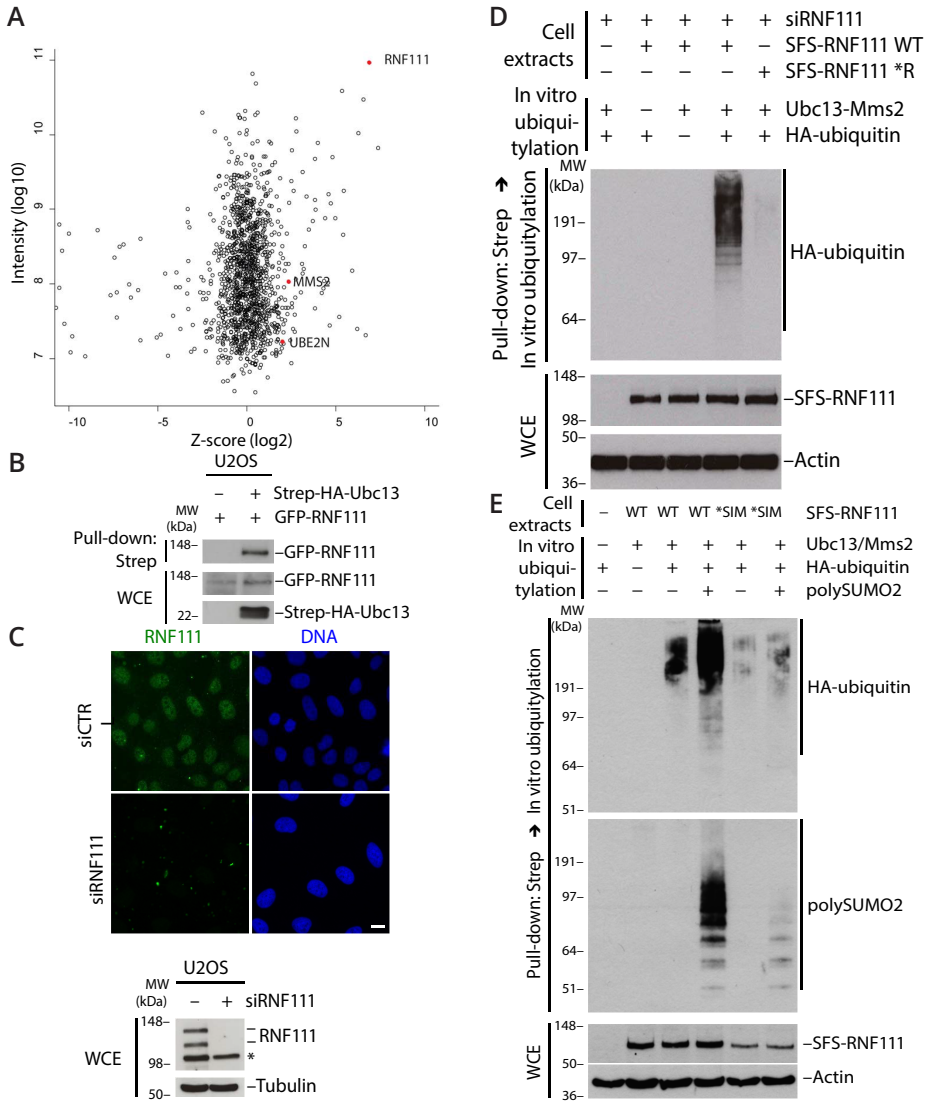


Figure 2. RNF111 has STUbL activity in the presence of Ubc13-Mms2. (A) MS-based analysis of RNF111-interacting proteins. U2OS and U2OS/GFP- RNF111 cells were grown in light and heavy SILAC medium, respectively. GFP-RNF111 and associated proteins enriched on GFP-Trap resin were analyzed by MS. Plot shows z scores (from SILAC heavy/light ratios) and total intensity of identified proteins. RNF111, Ubc13 (UBE2N), and Mms2 (MMS2) are highlighted. See also Fig. S1 (A and B). (B) U2OS cells were co-transfected with indicated combinations of GFP-RNF111 and Strep-HA-Ubc13 plasmids. Whole-cell extracts (WCE) were subjected to Strep-Tactin pull-down followed by immunoblotting with GFP and HA antibodies. (C) U2OS cells transfected with non-targeting (control [CTRL]) or RNF111 siRNAs were collected 72 h later and processed for immunostaining (top) or immunoblot (bottom) with RNF111 antibody. Asterisk indicates a nonspecific band. Bar, 10 μ m. (D) Extracts of U2OS cells sequentially transfected with RNF111 siRNA and S-FLAG- Strep-tagged RNF111 (SFS-RNF111) plasmids were subjected to Strep-Tactin pull-down. Bound complexes were incubated with ubiquitylation reaction mixture containing E1, Ubc13-Mms2 complex, and HA-ubiquitin as indicated and washed extensively, and RNF111 E3 ligase activity was analyzed by immunoblotting with the HA antibody. (E) As in D, except that ubiquitylation reactions were performed in the presence or absence of poly-SUMO2 (3-8) chains followed by immunoblotting with HA and SUMO2 antibodies. MW, molecular weight.

activity of co-purifying endogenous RNF111. We found that RNF111 was highly active as an E3 ligase in the presence of purified Ubc13–Mms2, as judged from its auto-ubiquitylation (Fig. 2 D). As expected, this required the integrity of the RNF111 RING domain (Fig. 2 D), whereas mutation of the SIMs did not impair intrinsic RNF111 E3 ligase activity (Fig. S2 E). In addition to Ubc13–Mms2, RNF111 was active with more generic E2 enzymes, such as UbcH5, as expected (Fig. S2 F). To test whether RNF111 has STUbL activity in the presence of Ubc13–Mms2, we analyzed the impact of SUMO2 on RNF111 E3 ligase activity. Strikingly, we found that poly-SUMO2 chains, but not free SUMO2, were efficiently targeted for Ubc13–Mms2-dependent ubiquitylation by RNF111 in a manner fully dependent on the integrity of the SIMs (Fig. 2 E and not depicted). We conclude from these experiments that RNF111 functions as a STUbL that employs Ubc13–Mms2 and likely other cognate E2 partners in ubiquitylation of SUMOylated substrates.

RNF111 promotes UV-induced ubiquitylation of XPC

We next attempted to identify physiological substrates for the STUbL activity of RNF111. The NER factor XPC is known to undergo both SUMOylation and ubiquitylation in response to UV radiation, and the UV-induced ubiquitin chains on XPC do not appear to destine XPC for proteasomal destruction (Sugasawa et al., 2005; Wang et al., 2005). We reasoned that SUMOylated XPC might be a candidate target of the Ubc13–Mms2-dependent E3 ligase activity of RNF111. Indeed, knockdown of RNF111 by any of several independent siRNAs impaired UV-induced ubiquitylation but not SUMOylation of XPC (Fig. 3, A and B; and Fig. S3, A and B), suggesting that XPC is SUMOylated before ubiquitylation by RNF111. The slow-migrating, UV-inducible XPC species seen in immunoblots represent a mixture of ubiquitin- and SUMO-modified forms; hence, the dramatic decrease in XPC ubiquitylation but not SUMOylation in RNF111-depleted cells manifests less prominently in total XPC blots (Fig. 3 A). Consistent with a direct role of RNF111 in ubiquitylating XPC after UV, we found that elevated levels of RNF111 augmented the UV-induced increase in XPC-GFP ubiquitylation (Fig. 3 C). In contrast, depletion of RNF4, the known STUbL in mammalian cells, had no effect on UV-induced XPC ubiquitylation (Fig. S3 C). The ability of RNF111 to promote Ubc13–Mms2-dependent ubiquitylation prompted us to test whether UV-induced XPC ubiquitylation required Ubc13 function. Like RNF111 knockdown, depletion of Ubc13 decreased UV-induced XPC ubiquitylation substantially (Fig. 3 D and Fig. S3 D), suggesting that RNF111-dependent XPC ubiquitylation after UV exposure was, at least partially, mediated by Ubc13-dependent, non-proteolytic ubiquitylation. To further probe the basis of RNF111-dependent XPC ubiquitylation in response to UV, we asked whether RNF111 and XPC interact in cells. Indeed, UV induced prominent, but transient, interaction between RNF111 and XPC at early time points after UV (Fig. 3 E). Interestingly, like several known NER factors, both endogenous and ectopic RNF111 underwent partial degradation after UV in a proteasome-dependent manner, which, however, did not require the intrinsic E3 ligase activity of RNF111 (Fig. 3, E and F; and Fig. S3 E). In general, the kinetics of UV-induced RNF111 interaction with XPC and degradation correlated with that of XPC ubiquitylation after UV exposure (Fig. 3, E and F; and Fig. S3 F).

RNF111 selectively ubiquitylates SUMOylated XPC

The aforementioned findings suggested that RNF111 targets SUMOylated XPC for ubiquitylation in response to UV. Hence, we tested whether RNF111 specifically interacts with SUMO-modified XPC via its SIMs, using a strategy wherein GFP-tagged XPC immunopurified from cells was SUMOylated *in vitro* and then incubated with extracts of cells transfected with WT or mutant forms of ectopic RNF111 (Fig. 4 A). Under these conditions, RNF111 efficiently interacted with XPC, but only if XPC had been pre-SUMOylated, and this required the integrity of the RNF111



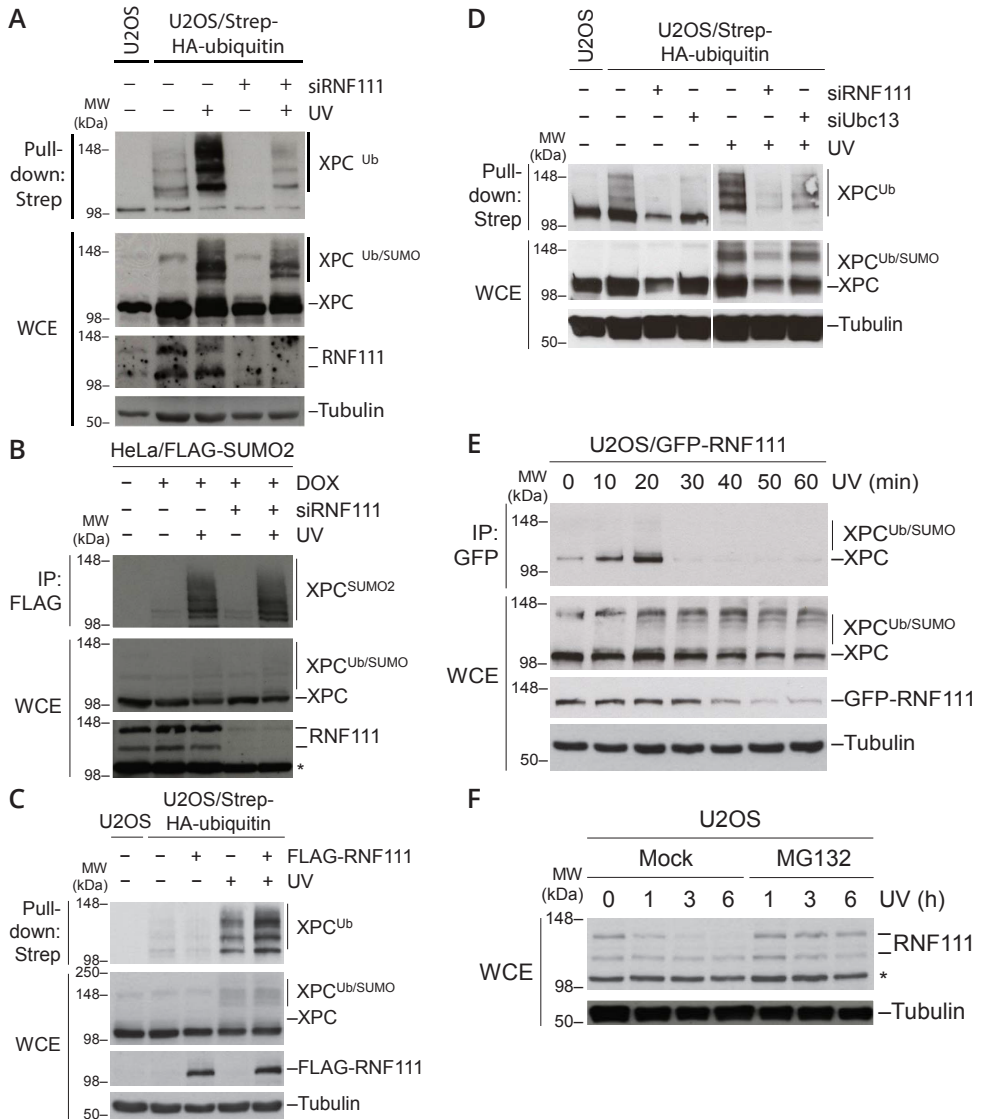


Figure 3. RNF111 promotes UV-induced ubiquitylation of XPC. (A) U2OS or U2OS/Strep-HA-ubiquitin cells transfected with control (-) or RNF111 siRNAs were exposed or not exposed to UV and collected 1 h later, and XPC ubiquitylation was analyzed by immunoblotting Strep-Tactin pull-downs of whole-cell extracts (WCE) with the XPC antibody. (B) HeLa/FLAG-SUMO2 cells transfected with control (-) or RNF111 siRNAs and left untreated or induced to express FLAG-SUMO2 by addition of doxycycline (DOX) were exposed or not exposed to UV and collected 1 h later. Cells were lysed under denaturing conditions, and XPC SUMOylation was analyzed by immunoblotting FLAG IPs with XPC antibody. (C) U2OS/Strep-HA-ubiquitin cells transfected with empty vector (-) or FLAG-RNF111 plasmid were exposed or not exposed to UV and collected 1 h later. XPC ubiquitylation was analyzed as in A. (D) XPC ubiquitylation in U2OS/Strep-HA-ubiquitin cells depleted of RNF111 or Ubc13 was analyzed as in A. Ubc13 knockdown efficiency is shown in Fig. S3 D. (E) Extracts of U2OS/GFP-RNF111 cells collected at the indicated times after UV radiation were subjected to GFP IP followed by immunoblotting with XPC antibody. (F) Extracts of U2OS cells incubated with or without MG132, exposed to UV 30 min later, and collected at the indicated times after UV were analyzed by immunoblotting with the RNF111 antibody. Asterisks denote a nonspecific band. MM, molecular mass.

SIMs (Fig. 4 B), in agreement with the notion that RNF111 specifically recognizes SUMOylated XPC. We next tested whether RNF111 functions as a STUbL for XPC. To do this, we extended the setup to monitor SUMO- dependent RNF111-XPC binding, by subjecting the bound complexes to an *in vitro* ubiquitylation assay in the presence of Ubc13–Mms2 as an E2 (Fig. 4 A). Although a background level of Ubc13–Mms2-dependent ubiquitylation of XPC-GFP could be seen in the absence of ectopically expressed RNF111 (Fig. 4 C, compare lanes 1–6), the addition of RNF111 WT markedly enhanced XPC ubiquitylation (Fig. 4 C, compare lanes 6 and 7) but only if XPC had been pre-SUMOylated (Fig. 4 C, compare lanes 2, 3, and 7). Importantly, this increase in RNF111-dependent XPC ubiquitylation required the functional integrity of both the RNF111 RING and SIM domains (Fig. 4 C, compare lanes 7–9). These data suggest that RNF111 acts as a STUbL for XPC, catalyzing its non-proteolytic ubiquitylation in response to UV damage.

RNF111 promotes NER by regulating the interaction of XPC with damaged DNA

Because RNF111 promotes ubiquitylation of XPC after UV, we asked whether RNF111 regulates NER. Although UV- induced ubiquitylation of XPC has been suggested to increase its DNA-binding affinity (Sugasawa et al., 2005), the exact role of this modification in NER is unclear. Previous work suggested that XPC is ubiquitylated by CRL4DDB2, an E3 ligase complex functioning as a proximal sensor of UV lesions in DNA (Sugasawa et al., 2005). It is possible that XPC is ubiquitylated by both CRL4DDB2 and RNF111 in response to UV. Indeed, using MS, we found that XPC ubiquitylation involves a variety of ubiquitin chains and ≥ 15 individual ubiquitylation sites (unpublished data) (Povlsen et al., 2012); hence, the nature and regulation of XPC ubiquitylation appears to be highly complex, likely involving several E3 ligases. To determine whether RNF111 loss affects NER, we measured UV-induced DNA repair synthesis (UDS) in RNF111^{-/-} mouse embryonic fibroblasts (MEFs)(Mavrakis et al., 2007). Strikingly, these MEFs showed a marked reduction in UDS, as was also observed in XPC^{-/-} MEFs (Fig. 5 A). Moreover, using two independent siRNAs, we found that RNF111 knockdown resulted in increased accumulation of XPC-GFP to locally UV-irradiated chromatin, whereas knockdown of DDB2 had the opposite effect, as previously observed (Fig. 5, B and C)(Nishi et al., 2009). Hence, although DDB2 and RNF111 have opposing effects on XPC accumulation at UV lesions, interfering with the proper kinetics of XPC interaction with damaged chromatin by inactivation of either E3 reduces the efficiency of NER. These data suggest that RNF111 has a physiological role in promoting NER by regulating ubiquitylation of XPC and its association with damaged DNA.

Our findings show that RNF111 is a STUbL that promotes non-proteolytic ubiquitylation of at least a subset of its substrates, including XPC, implying that STUbL activity is not confined to RNF4 in higher vertebrates and that STUbLs do not always target substrates for proteasomal degradation. Although Ubc13–Mms2 appears to be a major cognate E2 enzyme for RNF111 in cells, RNF111 also interacts with other E2 enzymes and is known to promote ubiquitin-dependent degradation of TGF- β signaling factors (Koinuma et al., 2003; Levy et al., 2007; Nagano et al., 2007). Hence, depending on the context, RNF111 may work with different E2s to promote degradative or non-proteolytic ubiquitylation of SUMOylated substrate proteins. Despite the fact that both RNF4 and RNF111 interact with poly-SUMOylated proteins through tandem SIMs, they appear to have largely non-overlapping roles in the cell. For instance, RNF4, but not RNF111, was dispensable for UV-induced ubiquitylation of XPC, whereas RNF111 was not recruited to laser micro-irradiation-induced DNA double-strand breaks, unlike RNF4 (unpublished data)(Galanty et al., 2012; Yin et al., 2012). This distribution of labor between RNF4 and RNF111 in targeting distinct subsets of SUMOylated factors may reflect differences in the SUMO-binding properties of their tandem SIMs,

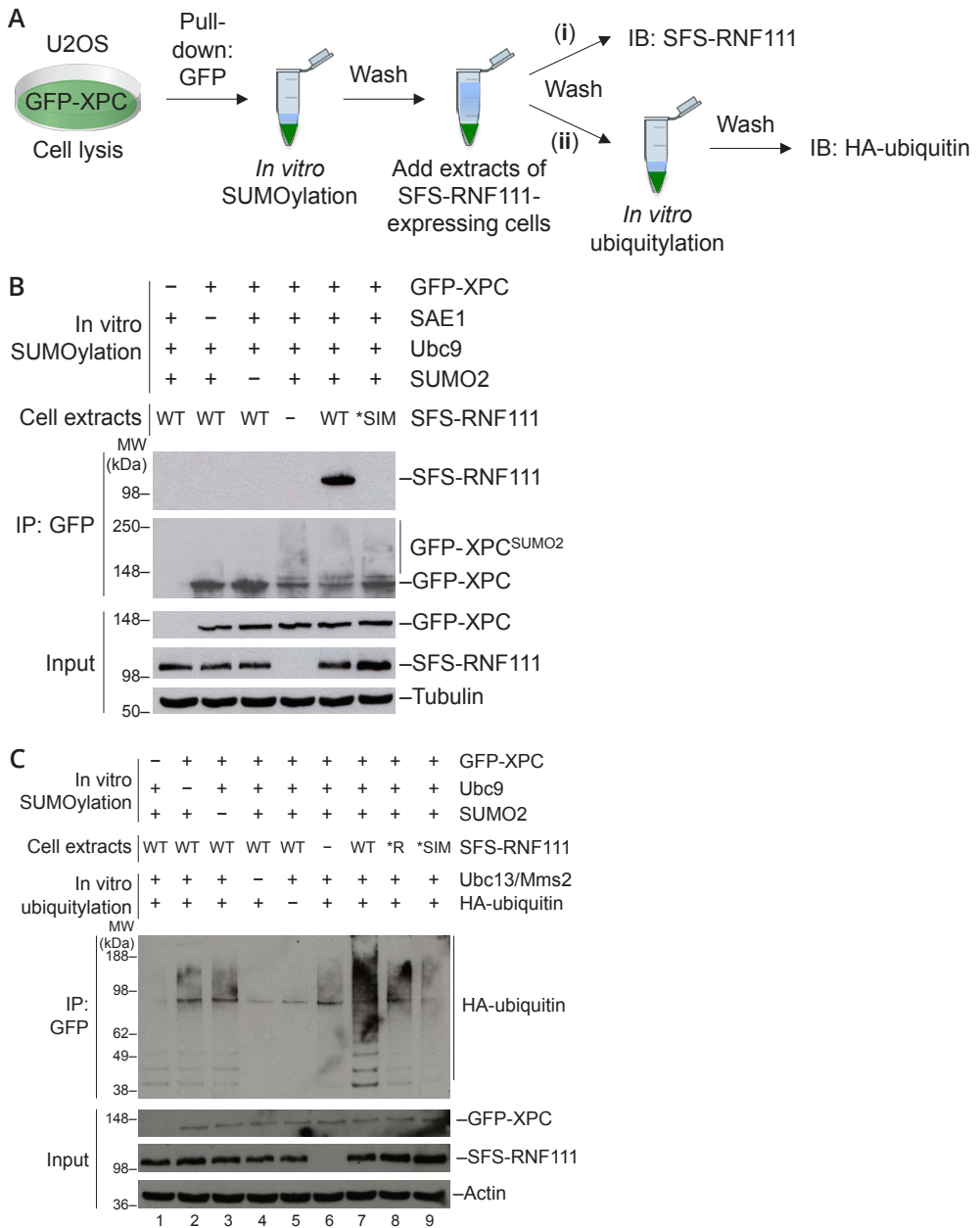


Figure 4. RNF111 ubiquitylates XPC in a SUMOylation-dependent manner. (A) Outline of *in vitro* SUMO-binding and STUBL assays. XPC-GFP expressed in U2OS cells was immunopurified on GFP-Trap resin and subjected to *in vitro* SUMOylation. After washing, the XPC-GFP-containing beads were incubated with extracts of cells transfected or not transfected with S-FLAG-Strep-RNF111 (SFS-RNF111) constructs, washed again, and processed for immunoblotting (IB) of bound SFS-RNF111 with FLAG antibody (i) or subjected to *in vitro* ubiquitylation followed by washing and immunoblotting with the HA antibody to analyze ubiquitin ligase activity (ii). **(B)** SUMOylation-dependent binding of RNF111 to XPC, analyzed as described in A. **(C)** Analysis of SUMOylation-dependent XPC ubiquitylation by RNF111 was performed as described in A. MW, molecular weight.

which have a distinct configuration, as well as differential target-binding specificity contributed by other domains in these proteins.

Although our comprehensive analysis of RNF111-binding factors in unperturbed cells uncovered several E2 partner proteins, we did not detect any known components of TGF- β signaling pathways, nor XPC. Given the involvement of RNF111 in regulating these proteins, we speculate that processes mediated by the RNF111 STUbL activity may, in many cases, be induced by stimuli such as TGF- β or UV treatment, which may promote SUMOylation of specific factors and thus trigger their RNF111-mediated ubiquitylation. This is consistent with previous findings that elevated levels of RNF111 only cause degradation of SnoN in TGF- β -stimulated cells (Levy et al., 2007). Based on the large and heterogeneous group of proteins identified by MS as putative RNF111-interacting proteins, we propose that RNF111, like RNF4, is a multi-functional STUbL regulating a diverse range of cellular signaling processes, determined to a large extent by the SUMOylation state of target proteins. This scenario reconciles the involvement of RNF111 in radically different cellular processes, such as TGF- β signaling and endocytosis (Miyazono and Koinuma, 2011), and NER. Whether the ability of RNF111 to ubiquitylate proteins in the former processes involves its STUbL activity remains to be addressed. Our findings shed further light on how STUbLs directly couple ubiquitylation and SUMOylation in important cellular signaling pathways.

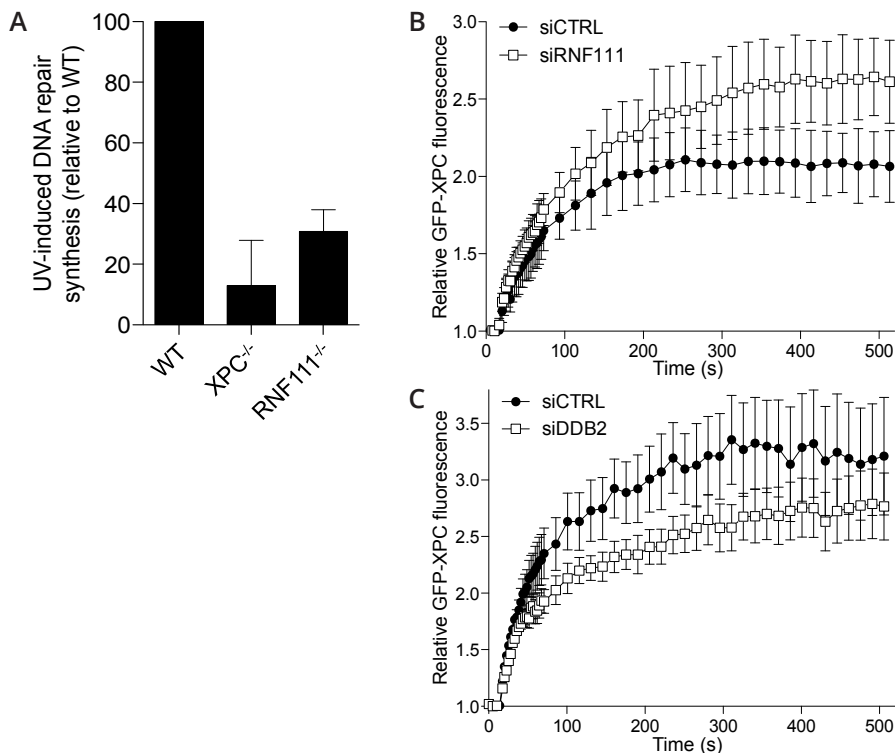


Figure 5. RNF111 promotes NER by regulating XPC recruitment to UV-damaged DNA. (A) UDS of the indicated MEF cell lines, determined by EdU incorporation for 3 h after exposure to 16 J/m² UV-C. Error bars indicate SDs of three independent experiments. (B) Cells stably expressing XPC-GFP were transfected with indicated siRNAs and locally exposed to laser-induced UV-C damage. XPC-GFP fluorescence intensity at the damaged area relative to pre-damage intensity was recorded in time using live-cell confocal imaging (mean of three independent experiments, n = 8 cells per experiment, \pm SD). (C) As in B, except that cells were transfected with control (CTRL) or DDB2 siRNA. Results of a representative experiment (n = 8 cells per sample, \pm SEM) are shown.

Materials and methods

Plasmids and siRNA

Full-length human RNF111 cDNA was amplified by PCR and inserted into pEGFP-C1 (Takara Bio Inc.) and pcDNA4/TO (Invitrogen) containing N-terminal Strep-HA or S-FLAG-Strep tags to generate mammalian expression constructs for GFP-, Strep-HA-, and S-FLAG-Strep-tagged RNF111, respectively. The RNF111 *RING (W963A) point mutation was introduced using the site-directed mutagenesis kit (QuikChange; Agilent Technologies). The RNF111 *SIM mutations (VVI(300–303) AAAA, VEIV(326–329)AAAA, and VVDL(382–385)AAAA) were introduced by replacing part of the coding sequence of human RNF111 (nucleotides 665–1,677 of the RNF111 ORF) with a synthetic gene spanning this region and containing the mutated *SIM sequence using the unique KpnI and EcoNI sites in RNF111. All constructs were verified by sequencing. Constructs expressing Strep-HA-tagged Ubc13 and GFP-XPC were described previously (Bekker-jensen et al., 2010). Plasmid transfections were performed using GeneJuice (EMD Millipore) according to the manufacturer's instructions. siRNA transfections were performed with Lipofectamine RNAiMAX (Invitrogen) as described. siRNA target sequences used in this study were control, 5'-GGGAUACCUGACGUUCUA-3'; RNF111 (#1), 5'-GGAUUUUAAUGCAGAGGAA-3'; RNF111 (#4), 5'-GGAUUAUGAAGAGUGAGAUU-3'; Ubc13, 5'-GAGCAUGGACUAGGCCUAUA-3'; XPC, 5'-GCAAAUGGCUUCUAUCGAAUU-3'; DDB2, 5'-CCCAGAUCUAAUUUCAA-3'; RNF4 (#1), 5'-GCUAUAUCUUGCCCAACUU-3'; and RNF4 (#2), 5'-GACAGAGACGUUAUUCUGA-3'.

Cell culture

Human U2OS and HeLa cells were cultured in DMEM containing 10% fetal bovine serum. SV40-immortalized XP4PA cells stably expressing XPC- GFP (Hoogstraten et al., 2008) were cultured in DMEM containing 5% fetal bovine serum and 2 mM L-glutamine. RNF111^{-/-} primary mouse fibroblasts of mixed 129Sv/MF1 genetic backgrounds (provided by V. Episkopou, Imperial College London, London, England, UK) (Mavrakis et al., 2007), and XPC^{-/-} MEFs in which exons 4–7 of the XPC gene were deleted (Sands et al., 1995) were cultured in a 1:1 ratio of Ham's F10 and DMEM supplemented with 10% fetal calf serum and 1% nonessential amino acids. To generate cell lines stably expressing GFP-tagged WT and mutant RNF111 alleles, U2OS cells were co-transfected with GFP-RNF111 constructs and pBabe-puromycin plasmid, and positive clones were selected with 1 µg/ml puromycin. A stable U2OS/ Strep-HA-ubiquitin cell line (Danielsen et al., 2011) was generated by selecting cells transfected with Strep-HA-ubiquitin expression plasmid in medium containing 400 µg/ml G418 until resistant clones grew out. Stable HeLa cell lines expressing FLAG-SUMO1/2 in a doxycycline-inducible manner (Danielsen et al., 2012) were generated by co-transfection of HeLa/FRT/TRex cells (Invitrogen) with pcDNA5/FRT/TO-3×FLAG-SUMO1/2 and pOG44 followed by selection with 200 µg/ml Hygromycin B. Unless stated otherwise, cells were exposed to 30 J/m² UV and collected 1 h later.

MS-based analysis of RNF111-interacting proteins

For stable isotope labeling by amino acids in cell culture (SILAC) labeling, U2OS or U2OS/GFP-RNF111 cells were cultured for 14 d in Eagle's minimum essential medium (Sigma-Aldrich) supplemented with L-arginine and L-lysine or L-arginine-U-13C6-15N4 and L-lysine-U-13C6-15N2 (Cambridge Isotope Laboratories), respectively (Ong, 2002). Cells were lysed in EBC buffer supplemented with protease and phosphatase inhibitor cocktail (Roche), and GFP-RNF111 and its interacting proteins were enriched using GFP-Trap resin. Proteins were resolved by SDS-PAGE and in-gel digested with trypsin. Peptide fractions were analyzed on a quadrupole mass spectrometer

(Q Exactive; Orbitrap; Thermo Fisher Scientific) equipped with a nanoflow HPLC system (Thermo Fisher Scientific)(Michalski et al., 2011). Raw data files were analyzed using MaxQuant software (version 1.2.2.9;)(Cox and Mann, 2008). Parent ion and MS2 spectra were searched against protein sequences obtained from the UniProt knowledge base using the Andromeda search engine (Cox et al., 2011). Spectra were searched with a mass tolerance of 6 ppm in MS mode and 20 ppm in higher-energy C-trap dissociation MS2 mode, strict trypsin specificity, and allowing up to two missed cleavage sites. Cysteine carbamidomethylation was included as a fixed modification, and N-terminal protein acetylation was included as variable modification. The dataset was filtered based on posterior error probability to arrive at a false discovery rate <1% for peptide spectrum matches and protein groups. For calculation of z scores, the protein group ratios were logarithmized, and the standard deviation was estimated separately for ratios below and above 0 based on the 0.159 and 0.841 quantile (Cox and Mann, 2008).

Immunochemical methods and antibodies

Immunoblotting, IP, and Strep-Tactin pull-downs were performed as previously described (Poulsen et al., 2012). In brief, cells were lysed in EBC buffer (50 mM Tris, pH 7.5, 150 mM NaCl, 1 mM EDTA, 1 mM DTT, and 0.5% NP-40) or denaturing buffer (20 mM Tris, pH 7.5, 50 mM NaCl, 1 mM EDTA, 1 mM DTT, 0.5% NP-40, 0.5% sodium deoxycholate, and 0.5% SDS) supplemented with protease and phosphatase inhibitors and incubated on ice for 10 min, and lysates were cleared by centrifugation for 10 min at 20,000 rpm. Lysates were incubated with FLAG agarose (Sigma-Aldrich), GFP-Trap agarose (ChromoTek), or Strep-Tactin Sepharose (IBA BioTAGnology) for 1.5 h on an end-over-end rotator at 4°C, washed five times with EBC buffer or denaturing buffer, and re-suspended in 2× Laemmli sample buffer.

Antibodies used in this study included mouse monoclonals to RNF111 (M05; Abnova), GFP (sc-9996) and β -actin (sc-130301; Santa Cruz Bio- technology, Inc.), and FLAG (F1804; Sigma-Aldrich), rat monoclonal to HA (Roche), and rabbit polyclonals to XPC (Bethyl Laboratories, Inc.), SUMO1 (ab32058), SUMO2/3 (ab3742), β -tubulin (ab6046; Abcam), and Ubc13 (4919; Cell Signaling Technology). Rabbit polyclonal RNF4 antibody was a gift of J. Palvimo (University of Eastern Finland, Kuopio, Finland).

Immunofluorescence staining, microscopy, and laser microirradiation

Cells were fixed in 4% formaldehyde, permeabilized with PBS containing 0.2% Triton X-100 for 5 min, and incubated with primary antibodies diluted in DMEM for 1 h at room temperature. After staining with secondary anti- bodies (Alexa Fluor 488 and 568; Life Technologies) for 30 min, coverslips were mounted in Vectashield mounting medium (Vector Laboratories) containing nuclear stain DAPI. Confocal images were acquired on a microscope (LSM 510; Carl Zeiss) mounted on a confocal laser-scanning microscope (Axiovert 100M; Carl Zeiss) equipped with Plan-Neofluar 40×/1.3 NA oil immersion objective. Dual-color confocal images were acquired with standard settings using laser lines 488 and 543 nm for excitation of Alexa Fluor 488 and Alexa Fluor 568 dyes (Molecular Probes/Invitrogen), respectively. Band pass filters 505–530 and 560–615 nm were used to collect the emitted fluorescence signals. Image acquisition and analysis was performed with LSM ZEN software (Carl Zeiss). Raw images were exported as TIF files, and if adjustments in image contrast and brightness were applied, identical set- tings were used on all images of a given experiment.

In vitro ubiquitylation, SUMOylation, and binding experiments

To analyze *in vitro* binding of RNF111 to SUMO, S-FLAG-Strep-RNF111 constructs were

overexpressed in U2OS cells, purified on Strep-Tactin Sepharose, and incubated with purified free SUMO1, SUMO2, or poly-SUMO chains (3–8; all obtained from Boston Biochem) for 2 h at 4°C. Bound complexes were washed extensively in EBC buffer (50 mM Tris, pH 7.5, 150 mM NaCl, 1 mM EDTA, 1 mM DTT, and 0.5% NP-40), and immobilized material was resolved by SDS-PAGE and analyzed by immunoblotting.

For *in vitro* RNF111 ubiquitylation assays, S-FLAG-Strep-RNF111 purified from cells as described in the previous section and incubated in 20 μ l ubiquitylation assay buffer (50 mM Tris, pH 7.5, 5 mM MgCl₂, 2 mM NaF, 2 mM ATP, and 0.6 mM DTT) supplemented with 60 ng E1, 300 ng E2 (Ubc13–Mms2 complex or UbcH5c), and 5 μ g HA-ubiquitin (all obtained from Boston Biochem) for 1 h at 37°C. Reactions were stopped by addition of Laemmli sample buffer, resolved by SDS-PAGE, and immunoblotted with the HA antibody.

For *in vitro* SUMOylation and STUbL assays, XPC-GFP ectopically expressed in U2OS cells was captured on GFP-Trap resin and incubated with 100 ng SAE1/2, 200 ng Ubc9, and 3 μ g SUMO2 (all obtained from Boston Biochem) in ubiquitylation assay buffer for 1 h at 37°C. The beads were washed extensively in EBC buffer and incubated with extracts of U2OS cells transfected with WT or mutant versions of S-FLAG-Strep-RNF111 for 2 h at 4°C. The immobilized material was then washed in EBC and processed for immunoblotting or subjected to *in vitro* ubiquitylation assay as described in the previous section.

For surface plasmon resonance analysis, recombinant His6-tagged fragments (WT and *SIM) of human RNF111 (encompassing amino acids 282–411) were expressed in Escherichia coli and purified on an ÄKTexpress system (GE Healthcare). The His6 tag was removed with tobacco etch virus protease, and the RNF111 fragments were further purified using reverse-phase chromatography on an UltiMate 3000 system (Dionex), using C18 columns (Phenomenex). Eluted proteins were lyophilized, and their masses were verified by SDS-PAGE and MS. Poly-SUMO2 chains (3–8) were immobilized on a CM5 sensor chip using standard amine-coupling chemistry. Before titration experiments, the RNF111(282–411) fragments were dialyzed in running buffer (10 mM Hepes, pH 7.4, 150 mM NaCl, and 0.005% P20). After each titration point, the surface was regenerated using 10 mM glycine, pH 2.5. All data were collected on an instrument (T200; Biacore) at 25°C and analyzed using the T200 evaluation software (Biacore), in which the data were fitted to a steady-state model.

UDS and XPC-GFP accumulation kinetics assays

UDS was performed as described previously (Limsirichaikul et al., 2009; Schwertman et al., 2012). In brief, MEFs were seeded on coverslips 3 d before the UDS assay and cultured in medium without serum to reduce the number of S-phase cells. Cells were exposed to 16 J/m² UV-C and labeled with 5-ethynyl,2'-deoxyuridine (EdU) for 3 h. Subsequently, cells were fixed with 3.7% formaldehyde, and EdU incorporation was visualized using Alexa Fluor 594 nm (Click-iT) according to manufacturer's protocol (Invitrogen). UDS was quantified in ≥ 75 cells by measuring the overall nuclear fluorescence using ImageJ software (National Institutes of Health). Images were obtained using a microscope (LSM-700; Carl Zeiss). Kinetic study of XPC-GFP accumulation was performed in SV40-transformed XP4PA cells stably expressing XPC-GFP as described previously (Dinant et al., 2007). In brief, cells were cultured on 25-mm quartz coverslips (SPI Supplies) and imaged on a laser-scanning confocal microscope (SP5; Leica) using an Ultrafluar quartz 100 \times , 1.35 NA glycerol immersion lens (Carl Zeiss) at 37°C and 5% CO₂. Imaging medium was the same as culture medium. For UV laser irradiation, a 2-mW pulsed (7.8 kHz) diode pumped solid-state laser emitting

at 266 nm (DPSL; Rapp OptoElectronic) was connected to the microscope (SP5) with all-quartz optics. Treated nuclei were imaged using the same scanning speed, zoom factor, and laser power. Images were acquired using the LAS AF software (Leica). Data analysis was performed using the ImageJ software package. Measured fluorescence levels were determined in the specific region of the damage in the nucleus over time and corrected for background values. Resulting curves show the relative amount of protein in the damaged area over time and were normalized to 1 for the data points before damage.



Supplemental figures

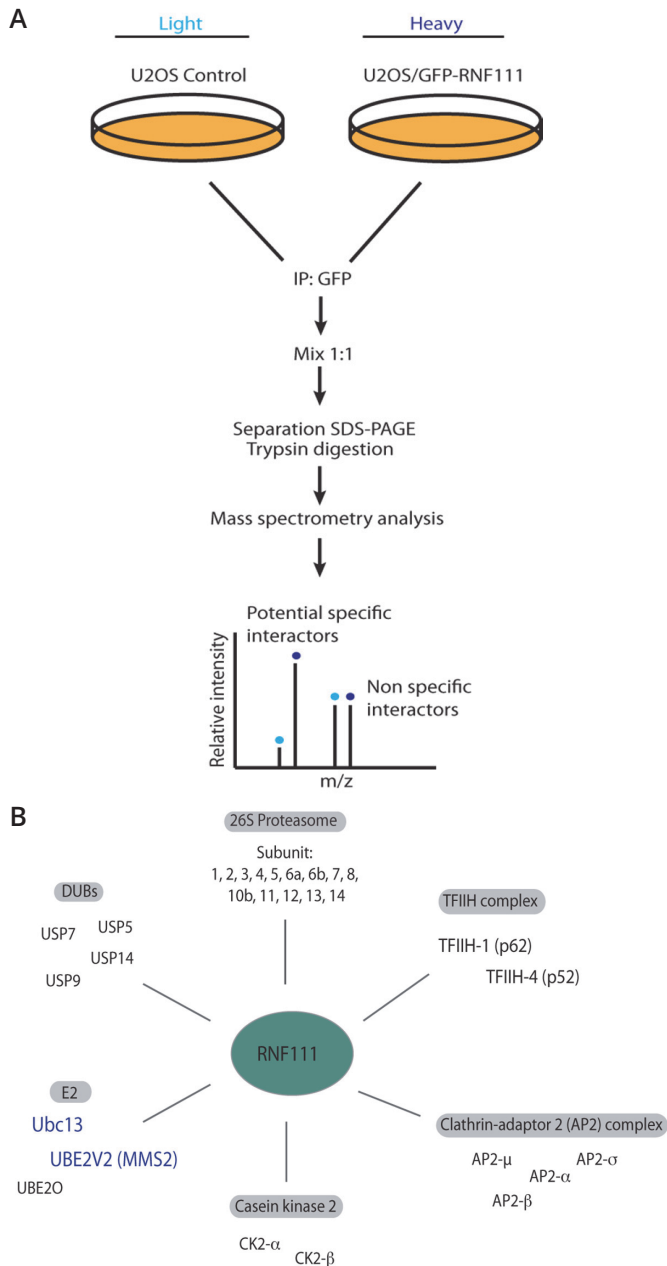


Figure S1. Analysis of cellular RNF111- interacting proteins. (A) MS-based analysis of RNF111-interacting proteins. U2OS or U2OS/GFP-RNF111 cells grown in light or heavy SILAC medium, respectively, were lysed and subjected to GFP IP. Subsequently, samples were combined, resolved by SDS-PAGE, and analyzed by MS. SILAC (heavy/light) ratios for individual proteins were determined. m/z, mass per charge. **(B)** Overview of selected proteins with high SILAC (heavy/light) ratios identified by the experimental approach outlined in A. DUB, deubiquitylating enzyme.

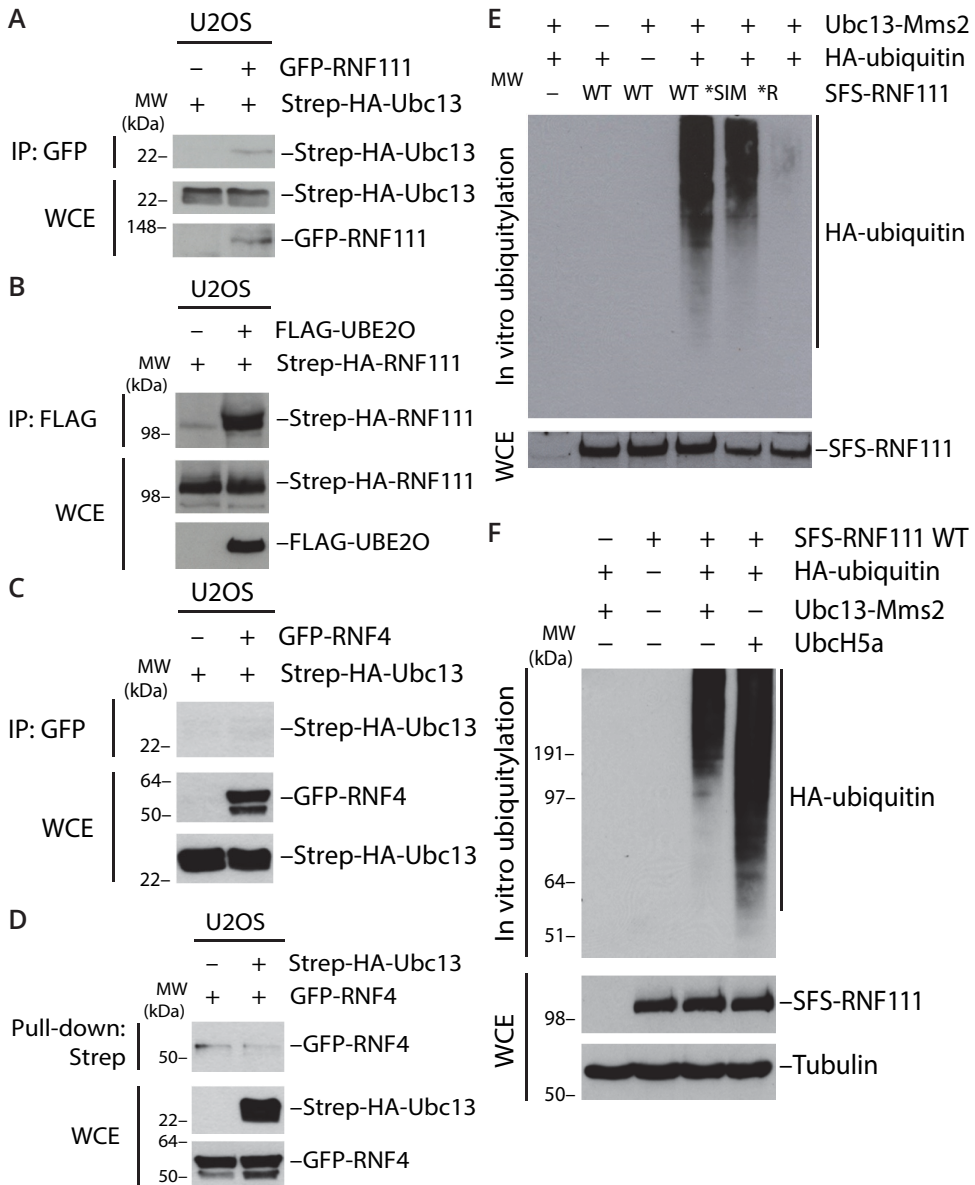


Figure S2. RNF111 promotes Ubc13-Mms2-dependent ubiquitylation. (A) U2OS cells were cotransfected with indicated combinations of GFP-RNF111 and Strep-HA-Ubc13 plasmids. Whole-cell extracts (WCE) were subjected to GFP IP followed by immunoblotting with HA antibody. (B) U2OS cells were cotransfected with the indicated combinations of FLAG-UBE2O and Strep-HA-RNF111 plasmids. Whole-cell extracts were subjected to FLAG IP followed by immunoblotting with HA antibody. (C) As in A, except that cells were transfected with combinations of GFP-RNF4 and Strep-HA-Ubc13 antibodies. (D) As in C, except that extracts were subjected to Strep-Tactin pull-down followed by immunoblotting with the GFP antibody. (E) Extracts of U2OS cells sequentially transfected with RNF111 siRNA and S-FLAG-Strep-tagged RNF111 (SFS-RNF111) plasmids as indicated were subjected to Strep-Tactin pull-down. Bound complexes were incubated with ubiquitylation reaction mixture containing E1, Ubc13-Mms2 complex, and HA-ubiquitin as indicated and washed extensively, and RNF111 auto-ubiquitylation activity was analyzed by immunoblotting with HA antibody. (F) As in E, except that UbcH5a was used as an E2 enzyme instead of Ubc13-Mms2 where indicated. MW, molecular weight.

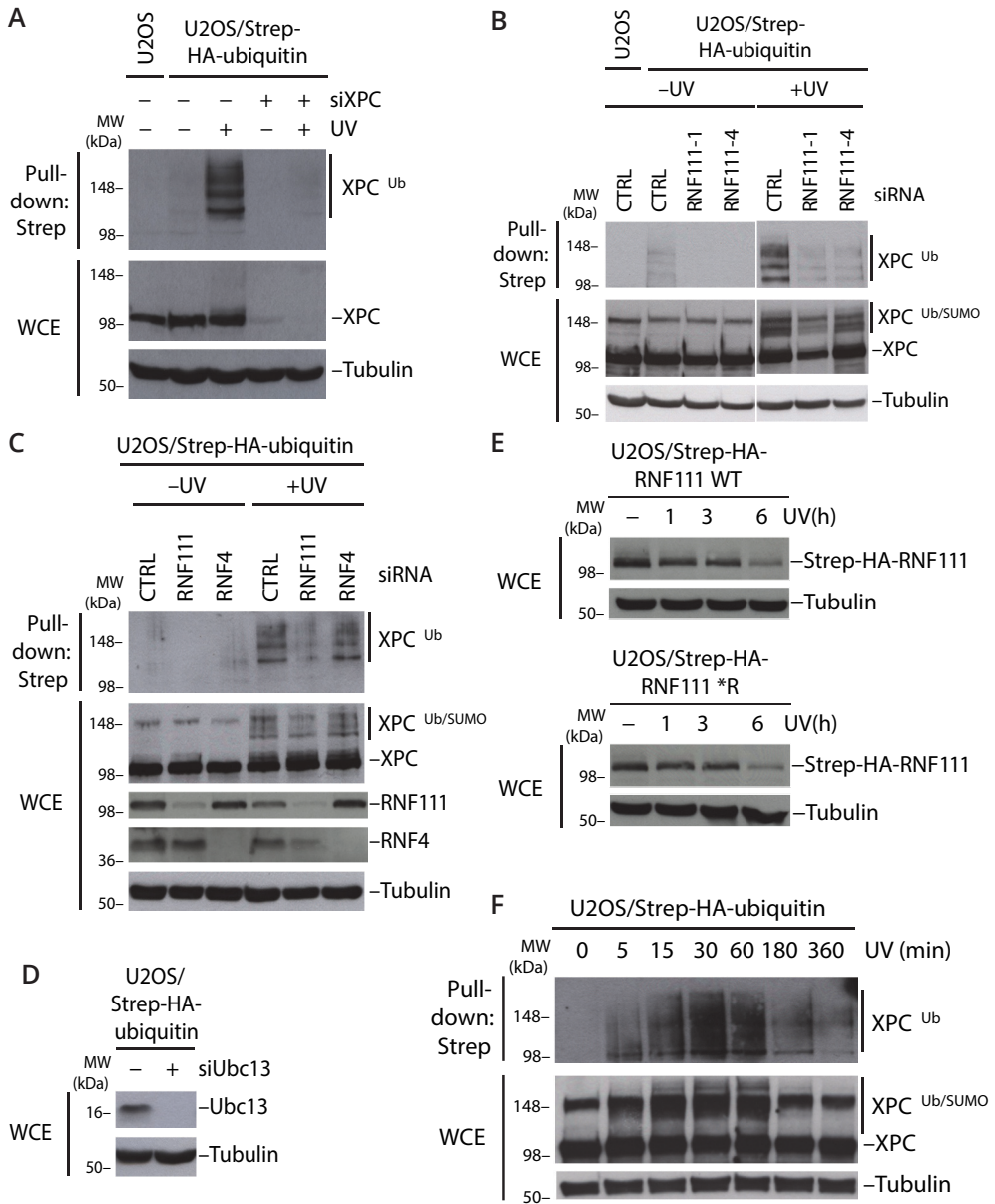


Figure S3. RNF111 promotes UV-induced ubiquitylation of XPC. (A) U2OS or U2OS/Strep-HA-ubiquitin cells transfected with control (?) or XPC siRNAs were exposed or not exposed to UV as indicated and collected 1 h later, and XPC ubiquitylation was analyzed by immunoblotting Strep-Tactin pull-downs of whole-cell extracts (WCE) with XPC antibody. (B) As in A, except that cells were transfected with indicated control (CTRL) or RNF111 siRNAs. (C) As in A, except that cells were transfected with indicated control, RNF111, or RNF4 siRNAs. (D) Knockdown efficiency of Ubc13 siRNA. U2OS/Strep-HA-ubiquitin cells were transfected with control (-) or Ubc13 siRNAs, collected 72 h later, and analyzed by immunoblotting with the Ubc13 antibody. (E) U2OS cell lines stably expressing Strep-HA-tagged RNF111 WT or *R mutant were collected at the indicated times after exposure to UV and analyzed by immunoblotting with HA antibody. (F) Time course analysis of UV-induced XPC ubiquitylation. U2OS/Strep-HA-ubiquitin cells were collected at the indicated times after exposure to UV, and XPC ubiquitylation was analyzed as in A. MW, molecular weight.

References

- Al-Hakim, A., C. Escribano-Diaz, M.-C. Landry, L. O'Donnell, S. Panier, R.K. Szilard, and D. Durocher. 2010. The ubiquitous role of ubiquitin in the DNA damage response. *DNA Repair (Amst)*. 9:1229–40. doi:10.1016/j.dnarep.2010.09.011.
- Bekker-jensen, S., J.R. Danielsen, K. Fugger, I. Gromova, A. Nerstedt, C. Lukas, J. Bartek, J. Lukas, and N. Mailand. 2010. HERC2 coordinates ubiquitin-dependent assembly of DNA repair factors on damaged chromosomes. *12*. doi:10.1038/ncb2008.80.
- Bekker-jensen, S., and N. Mailand. 2011. The ubiquitin- and SUMO-dependent signaling response to DNA double-strand breaks. *FEBS Lett*. 585:2914–9. doi:10.1016/j.febslet.2011.05.056.
- Bergink, S., and S. Jentsch. 2009. Principles of ubiquitin and SUMO modifications in DNA repair. *Nature*. 458:461–7. doi:10.1038/nature07963.
- Chen, Z.J., and L.J. Sun. 2009. Nonproteolytic functions of ubiquitin in cell signaling. *Mol. Cell*. 33:275–86. doi:10.1016/j.molcel.2009.01.014.
- Cox, J., and M. Mann. 2008. MaxQuant enables high peptide identification rates, individualized p.p.b.-range mass accuracies and proteome-wide protein quantification. *Nat. Biotechnol.* 26:1367–72. doi:10.1038/nbt.1511.
- Cox, J., N. Neuhauser, A. Michalski, R. a Scheltema, J. V Olsen, and M. Mann. 2011. Andromeda: a peptide search engine integrated into the MaxQuant environment. *J. Proteome Res*. 10:1794–805. doi:10.1021/pr101065j.
- Danielsen, J.M.R., K.B. Sylvestersen, S. Bekker-Jensen, D. Szklarczyk, J.W. Poulsen, H. Horn, L.J. Jensen, N. Mailand, and M.L. Nielsen. 2011. Mass spectrometric analysis of lysine ubiquitylation reveals promiscuity at site level. *Mol. Cell. Proteomics*. 10:M1110.003590. doi:10.1074/mcp.M110.003590.
- Danielsen, J.R., L.K. Povlsen, B.H. Villumsen, W. Streicher, J. Nilsson, M. Wikström, S. Bekker-Jensen, and N. Mailand. 2012. DNA damage-inducible SUMOylation of HERC2 promotes RNF8 binding via a novel SUMO-binding Zinc finger. *J. Cell Biol.* 197:179–87. doi:10.1083/jcb.201106152.
- Dinant, C., M. de Jager, J. Essers, W. a van Cappellen, R. Kanaar, A.B. Houtsmuller, and W. Vermeulen. 2007. Activation of multiple DNA repair pathways by sub-nuclear damage induction methods. *J. Cell Sci.* 120:2731–40. doi:10.1242/jcs.004523.
- Episkopou, V., R. Arkell, P.M. Timmons, J.J. Walsh, R.L. Andrew, and D. Swan. 2001. Induction of the mammalian node requires Arkadia function in the extraembryonic lineages. *Nature*. 410:825–30. doi:10.1038/35071095.
- Galanty, Y., R. Belotserkovskaya, J. Coates, and S.P. Jackson. 2012. RNF4, a SUMO-targeted ubiquitin E3 ligase, promotes DNA double-strand break repair. *Genes Dev*. 26:1179–95. doi:10.1101/gad.188284.112.
- Gareau, J.R., and C.D. Lima. 2010. The SUMO pathway: emerging mechanisms that shape specificity, conjugation and recognition. *Nat. Rev. Mol. Cell Biol.* 11:861–71. doi:10.1038/nrm3011.
- Golebiowski, F., I. Matic, M.H. Tatham, C. Cole, Y. Yin, A. Nakamura, J. Cox, G.J. Barton, M. Mann, and R.T. Hay. 2009. System-wide changes to SUMO modifications in response to heat shock. *Sci. Signal*. 2:ra24. doi:10.1126/scisignal.2000282.
- Hecker, C.-M., M. Rabiller, K. Haglund, P. Bayer, and I. Dikic. 2006. Specification of SUMO1- and SUMO2-interacting motifs. *J. Biol. Chem.* 281:16117–27. doi:10.1074/jbc.M512757200.
- Hoogstraten, D., S. Bergink, J.M.Y. Ng, V.H.M. Verbiest, M.S. Luijsterburg, B. Geverts, A. Raams, C. Dinant, J.H.J. Hoeijmakers, W. Vermeulen, and A.B. Houtsmuller. 2008. Versatile DNA damage detection by the global genome nucleotide excision repair protein XPC. *J. Cell Sci.* 121:2850–9. doi:10.1242/jcs.031708.
- Kerscher, O., R. Felberbaum, and M. Hochstrasser. 2006. Modification of proteins by ubiquitin and ubiquitin-like proteins. *Annu. Rev. Cell Dev. Biol.* 22:159–80. doi:10.1146/annurev.cellbio.22.010605.093503.
- Koinuma, D., M. Shinozaki, A. Komuro, K. Goto, M. Saitoh, A. Hanyu, M. Ebina, T. Nukiwa, K. Miyazawa, and T. Imamura. 2003. Arkadia ampli @ es TGF- β superfamily signalling through degradation of Smad7. *22:6458–6470*.
- Komander, D., and M. Rape. 2012. The ubiquitin code. *Annu. Rev. Biochem.* 81:203–29. doi:10.1146/annurev-biochem-060310-170328.
- Levy, L., M. Howell, D. Das, S. Harkin, V. Episkopou, and C.S. Hill. 2007. Arkadia activates Smad3/Smad4-dependent transcription by triggering signal-induced SnO degradation. *Mol. Cell Biol.* 27:6068–83. doi:10.1128/MCB.00664-07.
- Limsirichaikul, S., A. Niimi, H. Fawcett, A. Lehmann, S. Yamashita, and T. Ogi. 2009. A rapid non-radioactive technique for measurement of repair synthesis in primary human fibroblasts by incorporation of ethynyl deoxyuridine (EdU). *Nucleic Acids Res.* 37:e31. doi:10.1093/nar/gkp023.
- Matic, I., J. Schimmel, I. a Hendriks, M. a van Santen, F. van de Rijke, H. van Dam, F. Gnad, M. Mann, and A.C.O. Vertegaal. 2010. Site-specific identification of SUMO-2 targets in cells reveals an inverted SUMOylation motif and a hydrophobic cluster SUMOylation motif. *Mol. Cell*. 39:641–52. doi:10.1016/j.molcel.2010.07.026.
- Mavrikis, K.J., R.L. Andrew, K.L. Lee, C. Petropoulou, J.E. Dixon, N. Navaratnam, D.P. Norris, and V. Episkopou. 2007. Arkadia enhances Nodal/TGF- β signaling by coupling phospho-Smad2/3 activity and turnover. *PLoS Biol.* 5:e67. doi:10.1371/journal.pbio.0050067.
- Michalski, A., E. Damoc, J.-P. Hauschild, O. Lange, A. Wiegand, A. Makarov, N. Nagaraj, J. Cox, M. Mann, and S. Horning. 2011. Mass spectrometry-based proteomics using Q Exactive, a high-performance benchtop quadrupole Orbitrap mass spectrometer. *Mol. Cell. Proteomics*. 10:M1111.011015. doi:10.1074/mcp.M111.011015.
- Miyazono, K., and D. Koinuma. 2011. Arkadia—beyond the TGF- β pathway. *J. Biochem.* 149:1–3. doi:10.1093/jb/mvq133.
- Nagano, Y., K.J. Mavrikis, K.L. Lee, T. Fujii, D. Koinuma, H. Sase, K. Yuki, K. Isogaya, M. Saitoh, T. Imamura, V. Episkopou, K. Miyazono, and K. Miyazawa. 2007. Arkadia induces degradation of SnO and c-Ski to enhance transforming growth factor- β signaling. *J. Biol. Chem.* 282:20492–501. doi:10.1074/jbc.M701294200.
- Nishi, R., S. Alekseev, C. Dinant, D. Hoogstraten, A.B. Houtsmuller, J.H.J. Hoeijmakers, W. Vermeulen, F. Hanaoka, and K. Sugawara. 2009. UV-DDB-dependent regulation of nucleotide excision repair kinetics in living cells. *DNA Repair (Amst)*. 8:767–76. doi:10.1016/j.dnarep.2009.02.004.
- Ong, S.-E. 2002. Stable Isotope Labeling by Amino Acids in Cell Culture, SILAC, as a Simple and Accurate Approach to Expression Proteomics. *Mol. Cell. Proteomics*. 1:376–386. doi:10.1074/mcp.M200025-MCP200.
- Poulsen, M., C. Lukas, J. Lukas, S. Bekker-Jensen, and N. Mailand. 2012. Human RNF169 is a negative regulator of the ubiquitin-dependent response to DNA double-strand breaks. *J. Cell Biol.* 197:189–99. doi:10.1083/jcb.201109100.
- Povlsen, L.K., P. Beli, S. a Wagner, S.L. Poulsen, K.B. Sylvestersen, J.W. Poulsen, M.L. Nielsen, S. Bekker-Jensen, N. Mailand, and C. Choudhary. 2012. Systems-wide analysis of ubiquitylation dynamics reveals a key role for PAF15 ubiquitylation in DNA-damage bypass. *Nat. Cell Biol.* 14:1089–98. doi:10.1038/ncb2579.

- 
- Prudden, J., S. Pebernard, G. Raffa, D. a Slavin, J.J.P. Perry, J. a Tainer, C.H. McGowan, and M.N. Boddy. 2007. SUMO-targeted ubiquitin ligases in genome stability. *EMBO J.* 26:4089–101. doi:10.1038/sj.emboj.7601838.
- Sands, A.T., A. Abuin, A. Sanchez, C.J. Conti, and A. Bradley. 1995. High susceptibility to ultraviolet-induced carcinogenesis in mice lacking XPC. *Nature.* 377:162–5. doi:10.1038/377162a0.
- Schwartz, D.C., R. Felberbaum, and M. Hochstrasser. 2007. The Ulp2 SUMO protease is required for cell division following termination of the DNA damage checkpoint. *Mol. Cell. Biol.* 27:6948–61. doi:10.1128/MCB.00774-07.
- Schwertman, P., A. Lagarou, D.H.W. Dekkers, A. Raams, A.C. van der Hoek, C. Laffeber, J.H.J. Hoeijmakers, J. a a Demmers, M. Fouteri, W. Vermeulen, and J. a Martein. 2012. UV-sensitive syndrome protein UVSSA recruits USP7 to regulate transcription-coupled repair. *Nat. Genet.* 44:598–602. doi:10.1038/ng.2230.
- Sugasawa, K., Y. Okuda, M. Saijo, R. Nishi, N. Matsuda, G. Chu, T. Mori, S. Iwai, K. Tanaka, K. Tanaka, and F. Hanaoka. 2005. UV-induced ubiquitylation of XPC protein mediated by UV-DDB-ubiquitin ligase complex. *Cell.* 121:387–400. doi:10.1016/j.cell.2005.02.035.
- Sun, H., and T. Hunter. 2012. Poly-small ubiquitin-like modifier (PolySUMO)-binding proteins identified through a string search. *J. Biol. Chem.* 287:42071–83. doi:10.1074/jbc.M112.410985.
- Sun, H., J.D. Levenson, and T. Hunter. 2007. Conserved function of RNF4 family proteins in eukaryotes: targeting a ubiquitin ligase to SUMOylated proteins. *EMBO J.* 26:4102–12. doi:10.1038/sj.emboj.7601839.
- Tatham, M.H., E. Jaffray, O. a Vaughan, J.M. Desterro, C.H. Botting, J.H. Naismith, and R.T. Hay. 2001. Polymeric chains of SUMO-2 and SUMO-3 are conjugated to protein substrates by SAE1/SAE2 and Ubc9. *J. Biol. Chem.* 276:35368–74. doi:10.1074/jbc.M104214200.
- Wang, Q.-E., Q. Zhu, G. Wani, M. a El-Mahdy, J. Li, and A. a Wani. 2005. DNA repair factor XPC is modified by SUMO-1 and ubiquitin following UV irradiation. *Nucleic Acids Res.* 33:4023–34. doi:10.1093/nar/gki684.
- Yin, Y., A. Seifert, J.S. Chua, J.-F. Maure, F. Golebiowski, and R.T. Hay. 2012. SUMO-targeted ubiquitin E3 ligase RNF4 is required for the response of human cells to DNA damage. *Genes Dev.* 26:1196–208. doi:10.1101/gad.189274.112.

Chapter III

SUMO and ubiquitin-dependent XPC exchange drives nucleotide excision repair



Loes van Cuijk^{1*}, Gijsbert J. van Belle^{2*}, Yasemin Turkyilmaz¹, Sara L. Poulsen³, Roel C. Janssens¹, Arjan F. Theil, Mariangela Sabatella¹, Hannes Lans¹, Niels Mailand³, Adriaan B. Houtsmuller², Wim Vermeulen¹, Jurgen A. Marteijn¹

¹Department of Genetics, Cancer Genomics Netherlands Erasmus MC, Wytemaweg 80, 3015 CN Rotterdam, The Netherlands; ²Department of Pathology, Josephine Nefkens Institute, Erasmus MC, Dr. Molewaterplein 50, 3015 GE Rotterdam, The Netherlands; ³Ubiquitin Signaling Group, Department of Disease Biology, The Novo Nordisk Foundation Center for Protein Research, University of Copenhagen, Blegdamsvej 3B, DK-2200 Copenhagen, Denmark

Published in Nature Communications 2015 Jul 7; 6(1):8499

*These authors contributed equally

Abstract

XPC recognizes UV-induced DNA lesions and initiates their removal by Nucleotide Excision Repair (NER). Damage recognition in NER is tightly controlled by ubiquitin and SUMO modifications. Recent studies have shown that the SUMO-targeted ubiquitin ligase RNF111 promotes K63-linked ubiquitylation of SUMOylated XPC after DNA damage. However, the exact regulatory function of these modifications *in vivo* remains elusive. Here we show that RNF111 is required for efficient repair of UV-induced DNA lesions. RNF111-mediated ubiquitylation promotes the release of XPC from damaged DNA after NER initiation, and is needed for stable incorporation of the NER endonucleases XPG and ERCC1/XPF. Our data suggest that RNF111, together with the CRL4^{DD^{B2}} ubiquitin ligase complex, is responsible for sequential XPC ubiquitylation, which regulates the recruitment and release of XPC and is crucial for efficient progression of the NER reaction, thereby providing an extra layer of quality control of NER.



Introduction

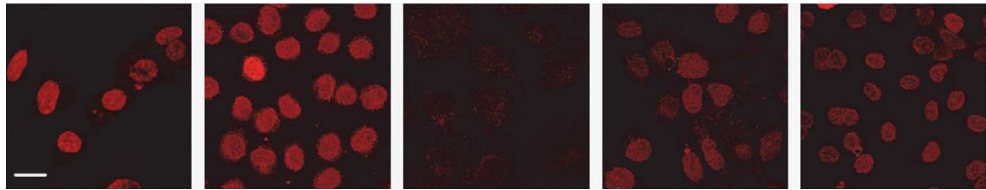
DNA integrity is constantly challenged by internal and external DNA-damaging agents that induce DNA lesions. When not properly repaired, DNA lesions may result in malignant transformation or accelerated ageing. Different DNA repair mechanisms exist that collectively remove most lesions and safeguard genome stability. Nucleotide excision repair (NER) is one of these mechanisms, which removes - in a multi step process - a wide variety of helix-distorting lesions, including UV-induced cyclobutane pyrimidine dimers (CPDs) and 6-4 pyrimidine-pyrimidone photoproducts (6-4PPs) (Marteijn et al., 2014). Lesions located in the transcribed strand of active genes block elongating RNA polymerase II and are specifically processed by a dedicated transcription-coupled NER (TC-NER) sub-pathway. However, the vast majority of helix-distorting DNA lesions located anywhere in the genome are targeted by the global genome NER sub-pathway (GG-NER) (Marteijn et al., 2014). After damage recognition by one of these sub-pathways, the 10 subunit TFIIH complex is recruited (Volker et al., 2001; Yokoi et al., 2000) to unwind the DNA around the lesion. TFIIH and XPA, which also bind the damaged strand (Camenisch et al., 2006), verify the presence of lesions (Sugasawa et al., 2009). Next, RPA binds the undamaged strand and plays a role in correct positioning of the structure-specific endonucleases XPG and ERCC1/XPF to excise a ~25 nt stretch of single-strand DNA containing the lesion (de Laat et al., 1998). The activity of these endonucleases and thereby the excision of the DNA lesion is tightly orchestrated. First XPG is recruited either independently (Zotter et al., 2006) or through its interaction with TFIIH (Ito et al., 2007). Next ERCC1/XPF is recruited which can only incise the DNA in the presence of XPG. Only after the 5' incision has been completed by ERCC1/XPF, the 3' incision by XPG is triggered (Staresinic et al., 2009). After incision, the DNA is restored to its original state by DNA synthesis and ligation steps.

Within GG-NER, DNA damage recognition occurs through binding of the XPC-complex to lesion-induced helix distortions (Min and Pavletich, 2007) and is essential for assembly of the core NER factors and progression of the NER reaction (Volker et al., 2001). XPC is part of a heterotrimeric complex together with one of the two mammalian orthologs (RAD23A or RAD23B) of the *Saccharomyces cerevisiae* Rad23p (Masutani et al., 1994) and centrin2 (Araki et al., 2001). Although XPC is the main DNA damage sensor of GG-NER, it does not efficiently recognize UV-induced CPDs, which are the most abundant UV-induced DNA lesions. For efficient repair of these lesions initial binding of the UV-DDB complex, a heterodimer consisting of DDB1 and DDB2 (XPE), is required (Scrima et al., 2011; Wakasugi et al., 2002). UV-DDB is not only involved in damage detection, but together with Cullin-4A (CUL4A) and Rbx1/Roc1 (Groisman et al., 2003) this complex possesses E3 ubiquitin ligase activity that - amongst others - mediates polyubiquitylation of the DNA damage sensors DDB2 and XPC. As ubiquitin can use all seven internal lysine residues (K6, K11, K27, K29, K33, K48 and K63) and its N-terminus for chain formation, different chain linkages can be formed. These various polyubiquitin chain types have distinct structures and different consequences for the target protein (Kulathu and Komander, 2012). While ubiquitylated DDB2 is targeted for degradation (Scrima et al., 2011), ubiquitylated XPC is not, but acquires increased affinity for damaged DNA *in vitro* (Sugasawa et al., 2005). Following UV-irradiation XPC is not only modified by ubiquitin, but also by the small ubiquitin-like modifier (SUMO) (Silver et al., 2011; Wang et al., 2007; Wang et al., 2005) in a DDB2-, and XPA-dependent manner (Wang et al., 2007; Wang et al., 2005), which was shown to protect XPC from proteasomal degradation .



A

UDS 3h post UV



WT A

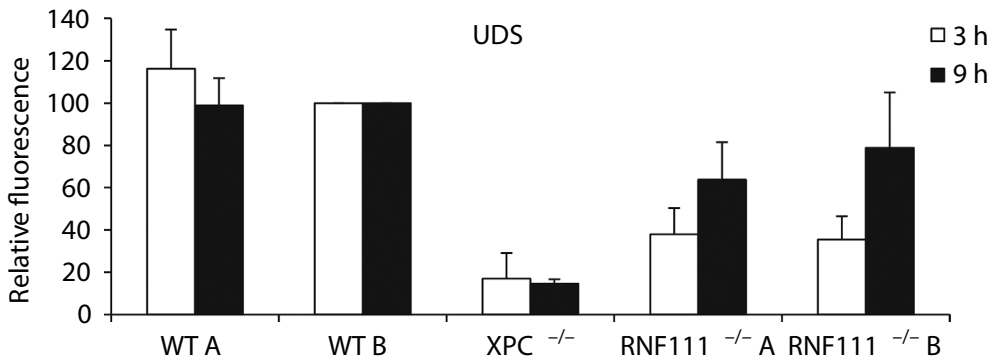
WT B

XPC ^{-/-}

RNF111 ^{-/-} A

RNF111 ^{-/-} B

B



C

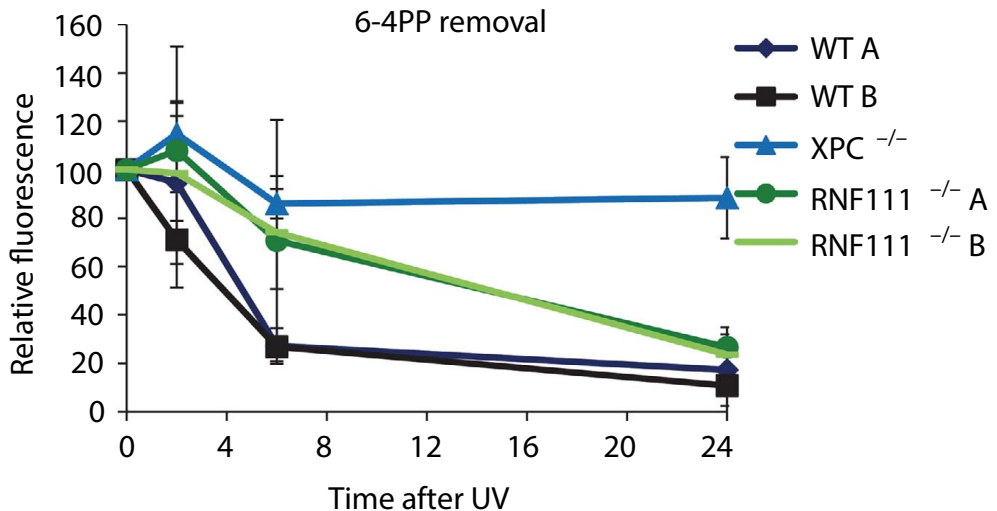


Figure 1. RNF111 is necessary for efficient GG-NER. (A) Representative pictures of Unscheduled DNA Synthesis of the indicated MEFs, determined by EdU incorporation over 3 h after UV-irradiation (16 J m⁻²). Scale bar, 25 μm. (B) Quantification of UDS levels in MEFs, as determined by EdU incorporation over a time period of 3 h or 9 h after UV-irradiation (16 J m⁻²). UDS levels in WT MEFs were set at 100% (n>100 cells per sample, in at least two independent experiment; mean ± SD). (C) 6-4PP removal assayed by immunofluorescence, using a 6-4PP specific antibody. The indicated MEFs were UV-irradiated (10 J m⁻²) and allowed to repair 6-4PPs for the indicated time points. Relative fluorescence directly after UV was set at 100%. (n>70 cells, three independent experiments; mean ± SD).

Recently, an additional ubiquitin E3 ligase; RNF111, that promotes XPC ubiquitylation was identified (Poulsen et al., 2013). RNF111, also known as Arkadia, was originally named after the arkadia mutation in mice. Homozygous Arkadia mutants are non-viable since they fail to form the regulatory primitive node, which is crucial during early gastrulation. This problem in the development of the mouse embryo is most likely caused by the loss of the ubiquitin ligase activity of RNF111 that promotes transforming growth factor β (TGF- β) signaling (Episkopou et al., 2001; Mavrikis et al., 2007). RNF111 belongs to the class of SUMO-targeted ubiquitin ligases (STUbLs), which facilitate crosstalk between SUMOylation and ubiquitylation. Accordingly, RNF111 specifically targets SUMOylated XPC and modifies it with K63-linked ubiquitin chains dependent on the E2-conjugating enzyme UBC13 (Poulsen et al., 2013). Together these observations illustrate the importance of ubiquitin and ubiquitin-like modifications in regulating the DNA damage recognition factors that initiate NER (van Cuijk et al., 2014). In this study, we investigated the molecular function of the RNF111-dependent ubiquitylation of XPC and its role in NER. We show that although RNF111 is not essential for GG-NER, it strongly enhances the repair reaction by stimulating the release of XPC from damaged DNA, thereby enabling the progress of NER by recruitment of the endonucleases XPG and XPF/ERCC1.

Results

RNF111 is required for efficient GG-NER

To study the role of RNF111 during NER we first determined the repair capacity in the absence of RNF111 by measuring the UV-induced unscheduled DNA synthesis (UDS) in the first 3 h after UV (Mavrikis et al., 2007), which is a measure of GG-NER activity. In line with a previous study (Poulsen et al., 2013), NER-deficient *Xpc*^{-/-} MEFs and *Rnf111*^{-/-} MEFs (clone A and B) displayed a strongly reduced repair capacity as compared to NER-proficient wild type (WT) MEFs (Fig. 1A and B). To test whether this reduced repair capacity in *Rnf111*^{-/-} MEFs is caused by a blocked or delayed NER reaction, 6-4PP repair kinetics were determined in WT, *Xpc*^{-/-} and *Rnf111*^{-/-} MEFs. Cells were fixed at different time points after global UV-irradiation (10 J m⁻²) and immunostained for 6-4PPs. In WT MEFs the vast majority (\approx 75%) of 6-4PPs was removed within 6 h after UV-irradiation (Fig. 1C and Supplementary Fig. 1A). As expected, 6-4PP repair was not observed in GG-NER-deficient *Xpc*^{-/-} MEFs, not even after 24 h. *Rnf111*^{-/-} MEFs displayed an intermediate phenotype; 6 h after UV-irradiation 6-4PP removal was severely inhibited, with approximately 70% of these lesions remaining (Fig. 1C and Supplementary Fig. 1A). Strikingly, 24 h after UV exposure 6-4PP repair was almost completed, suggesting that the NER reaction is not fully blocked, but rather seems to be retarded. This was further corroborated by measuring UDS levels over an increased time window of 9 h instead of 3 h. UDS levels of *Xpc*^{-/-} MEFs remained low, indicative of their full repair deficiency. However, residual UDS levels in *Rnf111*^{-/-} MEFs increased from 40% over 3 h, up to 60-80% after 9 h as compared to WT MEFs (Fig. 1B and Supplementary Fig. 1B). Together these results indicate that although RNF111 is not essential for GG-NER, it strongly enhances the repair reaction.

RNF111 is required for XPC release from sites of UV damage

RNF111 ubiquitylates XPC in response to UV (Poulsen et al., 2013). Therefore, the reduced GG-NER capacity in the absence of RNF111 suggests that RNF111-dependent ubiquitylation facilitates GG-NER by regulating XPC function. To further investigate this, we measured XPC-GFP accumulation kinetics at sites of local UV-C laser (266 nm) induced DNA damage (LUD) using quantitative live cell confocal imaging. Surprisingly, knockdown of RNF111, using two independent siRNAs (Supplementary Fig. 1C) resulted in a 2-fold increase in XPC-GFP accumulation at LUD (Fig. 2A and Supplementary Fig. 1D). These data argue for an increase in XPC binding to lesions

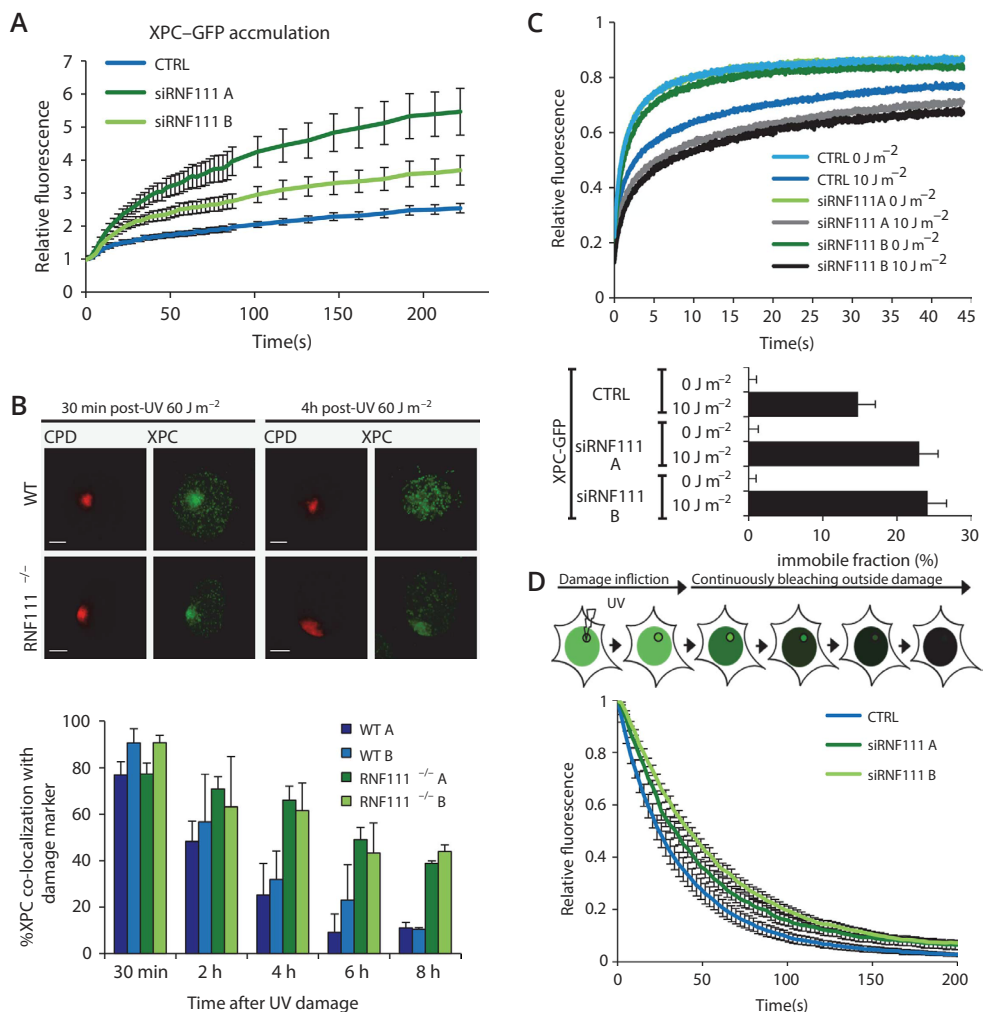


Figure 2. RNF111 is required for XPC release. (A) Relative XPC-GFP accumulation at sites of local UV-damage (LUD) in control and RNF111 depleted cells. GFP fluorescence intensity at UV-C laser induced LUD was measured over time using live cell confocal imaging and quantified to pre-damage intensity set at 1 at $t=0$ ($n>15$ cells per sample, measured in two independent experiments; mean \pm 2* SEM). (B) Top panel: Representative immunofluorescence pictures of co-localization of XPC with CPD at LUD in WT and Rnf111^{-/-}MEFs at the indicated time points after UV-irradiation (60 J m⁻²) are shown. Scale bars: 5 μ m. Lower panel: Quantification of the XPC co-localization with CPD ($n>50$ cells with LUD were analyzed per sample in three independent experiments; mean \pm SD). (C) Top panel: FRAP analysis of XPC-GFP in mock treated or global UV-irradiated (10 J m⁻²) XP4PA (XPC-deficient) cells, upon transfection with the indicated siRNA's. XPC-GFP was bleached in a small strip within the nucleus and fluorescence recovery was measured over 45 s and normalized to pre-bleach intensity ($n=40$; from two independent experiments mean \pm 2* SEM). The immobilized fraction (%) = $1 - \frac{\text{Average fluorescence intensity UV-irradiated cells - the first data point after bleaching}}{\text{Average fluorescence intensity unchallenged cells - the first data point after bleaching}}$ is plotted in the lower panel. The immobilized fraction was calculated over the last 10s. (D) Inverse FRAP (iFRAP) analysis of XPC-GFP at LUD. XP4PA cells stably expressing XPC-GFP were transfected with the indicated siRNA's. 72h after transfection, cells were locally exposed to a 266 nm UV-C laser. After the accumulation plateau was reached (5 min after exposure) the undamaged part of the nucleus was continuously bleached and fluorescence in the damaged area was monitored. Fluorescence was normalized to pre-bleach intensity ($n>15$ cells per sample, measured in two independent experiments; mean \pm SEM).

in the absence of RNF111 and suggest an improved DNA damage detection, which is seemingly at odds with the observed reduction in repair capacity in the absence of RNF111. The RNF111-dependent XPC binding properties were further investigated by determining long term binding of XPC to DNA damage by scoring XPC co-localization with a damage marker (anti-CPD) using immunofluorescence (Fig. 2B). At 30 min after local UV-irradiation, no difference in co-localization of XPC with LUD was observed. However, at later time points (4, 6 and 8 h) after UV a strikingly higher co-localization with LUD was observed in *Rnf111*^{-/-} MEFs as compared to WT MEFs (Fig. 2B). Similar results were observed in U2OS cells treated with two different siRNAs targeting RNF111 (Supplementary Fig. 2). In contrast, knockdown of RNF4, another STUbL involved in the mammalian DNA damage response (Galanty et al., 2012; Yin et al., 2012), had no effect on the UV-induced co-localization of XPC with DNA damage (Supplementary Fig. 2), showing the specificity of RNF111 for XPC regulation. This increased XPC accumulation could either be explained by a more stable binding of XPC to DNA damage or by a higher concentration of substrates, as RNF111 loss resulted in slower repair kinetics, or both. To distinguish between these possibilities and to resolve the apparent contradiction between more XPC binding and slower repair, we determined XPC using fluorescence recovery after photobleaching (FRAP) on XPC-GFP in RNF111-depleted cells. The mobility of XPC-GFP was unaffected by RNF111 depletion under unperturbed conditions (Fig. 2C, 0 J m⁻²), indicating that the probing of DNA by XPC in the absence of UV-lesions is not affected (Hoogstraten et al., 2008). Upon UV-exposure (10 J m⁻²) XPC is engaged in damage recognition, resulting in an increased XPC-GFP immobilization (Hoogstraten et al., 2008). Knockdown of RNF111 resulted in a further increase in XPC-GFP immobilization, as shown by the FRAP curves (Fig. 2C, upper panel) and by plotting of the calculated immobile fractions (Fig. 2C, lower panel). These data suggest that XPC is more strongly associated with damaged DNA in the absence of RNF111, which might be a consequence of increased association (K_{on}) and/or decreased dissociation kinetics (K_{off}). To study whether the K_{off} is affected, we applied inverse FRAP (iFRAP) to measure the dissociation of XPC from sites of DNA damage. To this end, LUD was first introduced to locally accumulate XPC-GFP until steady-state was reached. Subsequently, the entire nucleus, with exception of the damaged area, was continuously bleached and the loss of fluorescence at the site of damage was measured at regular time intervals (Fig. 2D). Depletion of RNF111 resulted in reduced dissociation kinetics (K_{off}) of XPC-GFP at LUD ($t_{1/2}$ =33-43 s) as compared to control transfected cells ($t_{1/2}$ =24 s), indicative of an increased residence time. Together our results suggest that RNF111 plays an important role in promoting the release of XPC from damaged DNA. The reduced clearance of XPC from damaged sites may thus explain the increased accumulation of XPC-GFP at LUD and may cause the delayed repair.

RNF111 is essential for efficient XPG and XPF/ERCC1 loading

Our finding that knockdown of RNF111 results in prolonged binding of XPC to DNA damage provides a good model system to study NER factor handover during the repair reaction and to determine which NER factors depend on XPC release to be incorporated into the NER complex. To this end, we tested whether a panel of NER factors (DDB2, XPB, XPG, XPF and ERCC1) co-localized to LUD 30 min after UV-irradiation (60 J m⁻²), as marked by CPD-photolyase-mCherry (Aydin et al., 2014), in RNF111 siRNA-depleted U2OS cells. Co-localization of early factors, like DDB2 (upstream of XPC) and XPB (subunit of TFIIH, directly downstream of XPC) with the DNA damage marker, was not affected by RNF111 knockdown. Interestingly, co-localization of the endonucleases XPG and XPF/ERCC1 with DNA damage was significantly lower (20-50%) in RNF111-depleted cells than in control siRNA-transfected cells (Fig. 3A). In contrast, depletion of RNF4 had no effect on UV-induced co-localization of NER factors with DNA damage (Fig. 3A). To study the

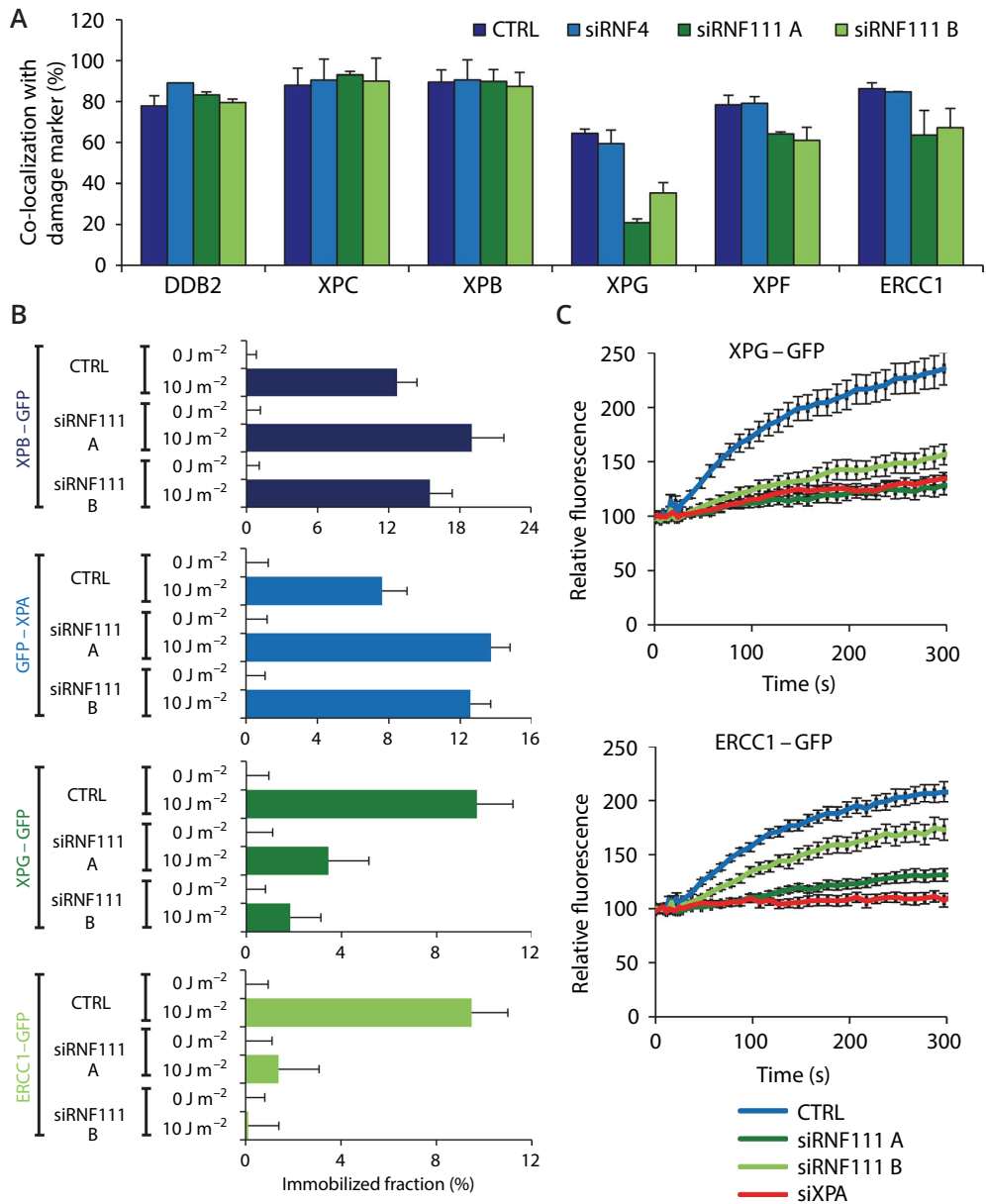


Figure 3. RNF111 is required for binding of XPG and XPF/ERCC1 to the NER complex. (A) U2OS cells expressing CPD-photolyase-mCherry were transfected with the indicated siRNA's three days before the immunofluorescence experiment. Cells were locally UV-irradiated (60 J m^{-2}) and immunostained for the indicated proteins 30 min later. The percentage of co-localization with the damage marker CPD-photolyase-mCherry at LUD is plotted in the graph ($n > 50$ cells containing a LUD were scored in at least three independent experiments; mean \pm SD). (B) The immobilized fraction of XPB-GFP, GFP-XPA, XPG-GFP and ERCC1-GFP as determined by FRAP analysis in mock or UV-treated (10 J m^{-2}) cells upon transfection with the indicated siRNA's ($n > 32$ cells from at least 2 independent experiments; mean \pm 2* SEM). (C) Cells stably expressing XPG-GFP and ERCC1-GFP transfected with the indicated siRNA's were locally irradiated using a 266 nm UV-C laser. GFP fluorescence intensity at LUD was monitored for 6 min, with 10 s intervals and normalized to pre-damage values. ($n = 24$ cells from three independent experiments; mean \pm SEM).

in vivo binding characteristics of these factors to active NER complexes in the absence of RNF111 in a quantitative manner, we determined the mobility of these proteins by FRAP analysis in RNF111 depleted cells expressing GFP-tagged versions of XPB, XPA, XPG and ERCC1 upon UV irradiation. Previous studies have shown that for each of these NER factors a clear UV-induced immobilization could be measured by FRAP (Hoogstraten et al., 2002; Houtsmuller et al., 1999; Rademakers et al., 2003; Zotter et al., 2006). Under unperturbed conditions (0 J m^{-2}), no difference in mobility was observed for the indicated NER factors between control and RNF111 depleted cells (Fig. 3B). In contrast, after UV-irradiation (10 J m^{-2}) both the XPB and XPA proteins showed a further increased immobilization upon RNF111 depletion, similar to what was observed for XPC (Fig. 2C). These results suggest that, like XPC, also XPB and XPA are more associated with DNA damage in the absence of RNF111. This increased association most likely represents longer dwell times of these factors into transiently trapped NER reaction intermediates that cannot finalize the repair reaction due to loss of RNF111. FRAP analysis of XPG-GFP and ERCC1-GFP in cells lacking RNF111 revealed a striking opposite effect shown by a dramatic decrease in UV-induced immobilization, in line with the immunofluorescence experiments. This strong reduction of UV-induced immobilization likely reflects the inability of these endonucleases to stably integrate into active NER complexes in the absence of RNF111 (Fig. 3B). This was further confirmed by the strongly reduced UV-induced accumulation of XPG-GFP and ERCC1-GFP to LUD in living cells upon RNF111 depletion, almost to the same extent as observed upon siRNA mediated XPA depletion (Fig. 3C). As ERCC1/XPF binding to DNA damage is dependent on the presence of XPG (Staresinic et al., 2009), these data suggest that when XPC remains bound to the initiating NER complex, both XPG and XPF/ERCC1 cannot be efficiently recruited to or stably incorporated in the NER complex.

XPC release and ongoing NER is SUMO and K63-chain dependent

As RNF111 is a STUbL that mediates UV-induced K63-linked ubiquitylation of XPC (Poulsen et al., 2013), we investigated whether K63-linked ubiquitylation is required for XPC release from DNA damage and subsequent recruitment of the NER endonucleases. Towards this goal, siRNA targeting UBC13, the cognate E2-enzyme promoting K63-linked ubiquitylation (David et al., 2010; Komander and Rape, 2012), was used and XPC co-localization at LUD with CPD as damage marker was scored in U2OS cells at several time points after UV-irradiation. UBC13 depletion, as confirmed by western blot (Supplementary Fig. 3A), resulted in prolonged XPC co-localization with sites of DNA damage (Fig. 4A, red bars), similar to the observations in *Rnf111*^{-/-} cells. In contrast, depletion of another E2 conjugating enzyme, UBE2Q2, which is not involved in K63-mediated ubiquitylation (David et al., 2010) had no effect on UV-induced co-localization of XPC with DNA damage (Fig. 4A, light blue bars). RNF111-mediated XPC ubiquitylation is dependent on XPC SUMOylation (Poulsen et al., 2013). Therefore, we depleted UBC9, the E2 conjugating enzyme crucial for SUMOylation (Vertegaal, 2007), which indeed also resulted in more XPC co-localization with LUD at later time points (Fig. 4A, orange bars). Moreover, FRAP analysis of XPC-GFP showed that depletion of either UBC9 or UBC13 resulted in an increased UV-induced immobilization (Fig. 4B), to a similar extent as seen for RNF111 depletion. In addition, FRAP studies on ERCC1-GFP showed a decrease in UV-induced immobilization upon depletion of UBC9 or UBC13 (Fig. 4C), indicating that XPC release from damaged DNA and the subsequent stable incorporation of the NER endonucleases into the repair complex is not only dependent on RNF111, but also on SUMOylation and K63-linked ubiquitylation. To address whether the SUMO-dependent ubiquitylation of XPC itself is sufficient to explain the observed effects on the release of XPC and recruitment of the downstream NER endonucleases, we set out to generate an XPC mutant that was refractory to SUMOylation (Poulsen et al., 2013; Wang et al., 2005). With this approach, RNF111-mediated XPC ubiquitylation would be inhibited without affecting RNF111 activity towards other putative substrates.



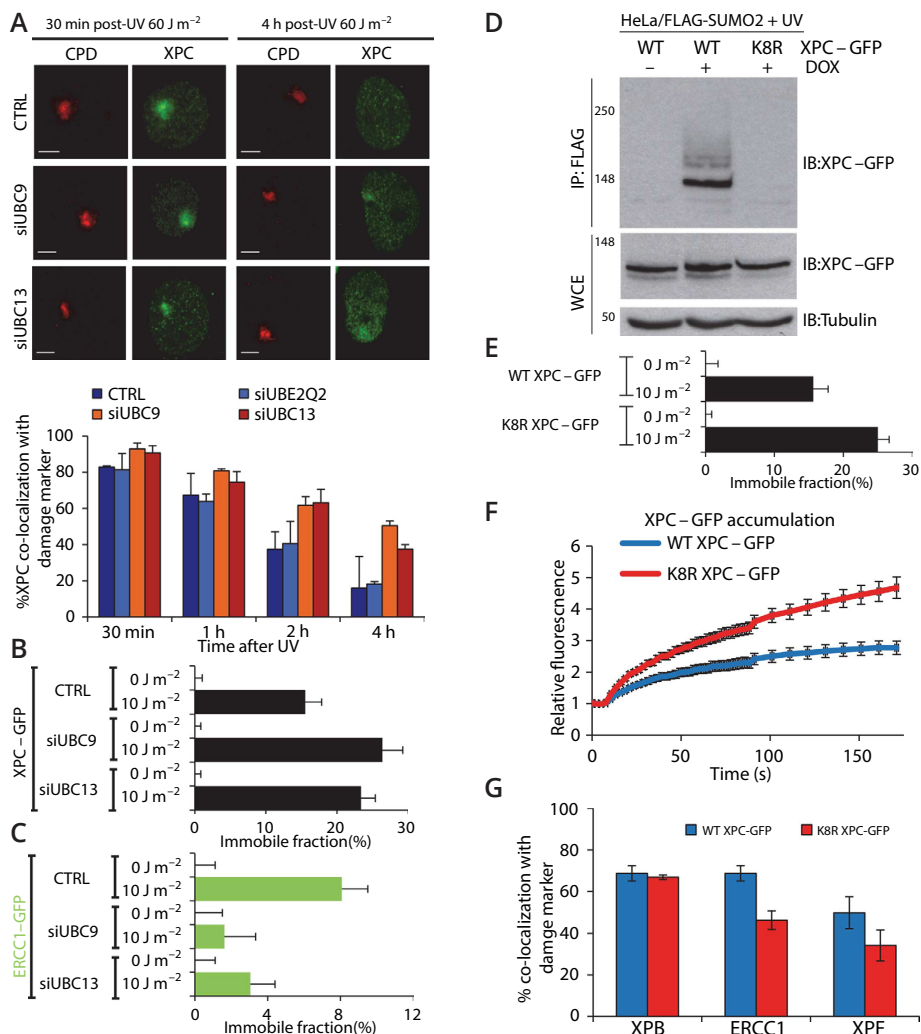


Figure 4. XPC release is SUMO and K63-ubiquitylation dependent. (A) Top panel: Representative pictures of co-localization of XPC with CPD at LUD in U2OS cells transfected with the indicated siRNA's 30 min or 4 h after local UV-irradiation (60 J m⁻²) are shown. Scale bar: 5µm. Bottom panel: Quantification of XPC co-localization with the damage marker CPD. (n≈50 cells containing a LUD were scored per sample in three independent experiments; mean ± SD). The immobilized fraction of XPC-GFP (B) or ERCC1-GFP (C) as determined by FRAP analysis in mock or UV-treated (10 J m⁻²) cells depleted by siRNA of UBC9 or UBC13 (n=40 from 2 experiments; mean ± 2* SEM). (D) HeLa/FLAG-SUMO2 cells were transfected with plasmids expressing WT or K8R XPC-GFP, then left untreated or incubated with doxycycline (DOX) to induce FLAG-SUMO2 expression. One hour after UV exposure (16 J m⁻²), cells were lysed under denaturing conditions, and XPC SUMOylation was analyzed by immunoblotting of FLAG IPs with GFP antibody. (E) The immobilized fraction of WT XPC-GFP or K8R XPC-GFP as determined by FRAP analysis in mock or UV-treated (10 J m⁻²) cells (n>40 from 3 experiments; mean ± 2* SEM). (F) Cells stably expressing WT XPC-GFP or K8R XPC-GFP were locally irradiated using a 266 nm UV-C laser. GFP fluorescence intensity at UV-C laser induced LUD was measured over time using live cell confocal imaging and quantified to pre-damage intensity set at 1 at t=0 (n>25 cells per sample, measured in two independent experiments; mean ± SEM). (G) XP4PA cells stably expressing WT XPC-GFP or K8R XPC-GFP were locally UV-irradiated (60 J m⁻²) and immunostained for endogenous XPB, ERCC1 and XPF proteins 30 min later. The percentage of co-localization with GFP-XPC at LUD is plotted in the graph (n>100 cells containing a LUD were scored in at two independent experiments; mean ± SD).

Using the GPS-SUMO algorithm (Zhao et al., 2014) we identified 8 putative SUMOylation sites in XPC (Supplementary Fig. 3B). By mutating each of the 8 lysine residues present in these SUMO consensus sites to arginines, we obtained an XPC mutant (K8R XPC-GFP) that could no longer be SUMOylated (Fig. 4D). The K8R XPC-GFP mutant was stably expressed in XP-C cells and its mobility and DNA damage kinetics were analyzed using live cell imaging. No difference in mobility was detected under unperturbed conditions (0 J m^{-2}) as determined by FRAP. However, upon UV-induced DNA damage (10 J m^{-2}) the K8R XPC-GFP was more immobilized than WT XPC-GFP, to a similar magnitude as was observed after depletion of RNF111 or UBC9 (Fig. 4E). In line with this, the K8R XPC mutant showed an approximately 2-fold increase in accumulation at LUD compared to WT XPC. Finally, similar to RNF111 depletion, we observed a clear reduction in ERCC1 and XPF accumulation at LUD in K8R XPC-GFP compared to WT XPC-GFP expressing cells (Fig. 4G), while no difference in the localization of XPB was found. Together these experiments demonstrate that the XPC release and subsequent binding of the NER endonucleases is dependent on the SUMOylation of XPC.

Discussion

The recent identification of RNF111 as a SUMO-targeted ubiquitin ligase (STUbL) involved in UV-induced ubiquitylation of XPC (Poulsen et al., 2013) has added another level of complexity to the ubiquitin-dependent regulation of this DNA damage sensor, as previously also CRL4^{DDB2} was identified as an E3-ligase complex acting on XPC (Sugasawa et al., 2005). Interestingly, while both ubiquitin ligase activities are required for efficient GG-NER, they may have opposing effects on XPC. Whereas CRL4^{DDB2}-induced ubiquitylation has been suggested to increase XPC DNA binding affinity *in vitro* (Sugasawa et al., 2005), we provide evidence that RNF111 and its cognate E2 - UBC13 - are required for efficient release of XPC from UV-lesions, which permits the progress of the NER reaction. How can XPC ubiquitylation by two different E3 ligases have such a diverse functional outcome? One obvious explanation is that these E3 ligases modify XPC with different types of ubiquitin chains. While RNF111 in cooperation with UBC13 generates K63-linked ubiquitin chains on XPC, the exact type of ubiquitin chains formed by CRL4^{DDB2} is currently unknown. However, in line with the finding that CRL4^{DDB2} auto-ubiquitylates DDB2 resulting in its subsequent degradation (Chen et al., 2001; Nag et al., 2001; Puumalainen et al., 2014; Ropic-Otrin et al., 2002), most CRL4-type ubiquitin ligases promote proteasomal degradation of their substrates (Hannah and Zhou, 2009; Higa and Zhang, 2007), which suggests that CRL4^{DDB2} might form K48-linked ubiquitin chains on XPC. If indeed XPC is ubiquitylated by K48 chains in response to UV to increase its DNA binding affinity, other factors may shield or protect it from proteolytic attack. One such candidate is the XPC complex partner RAD23B, which is known to protect XPC from proteasomal degradation, already in non UV-challenged cells (Ng et al., 2003). Other proteins involved in the stabilization of XPC might be the deubiquitylating enzymes (DUBs) OTUD4 and USP7, which were shown to deubiquitylate XPC upon UV-induced DNA damage (He et al., 2014; Lubin et al., 2014). It will be interesting to study whether these DUBs are only involved in the protection of XPC from proteolytic degradation or if they are also important for ubiquitin chain editing on XPC. In this latter scenario, XPC would first be ubiquitylated by CRL4^{DDB2} after which the K48-linked ubiquitin chains might be trimmed down to permit K63-linked ubiquitylation by RNF111 on the same lysines modified by CRL4^{DDB2}, resulting in the subsequent release of XPC from sites of DNA damage.



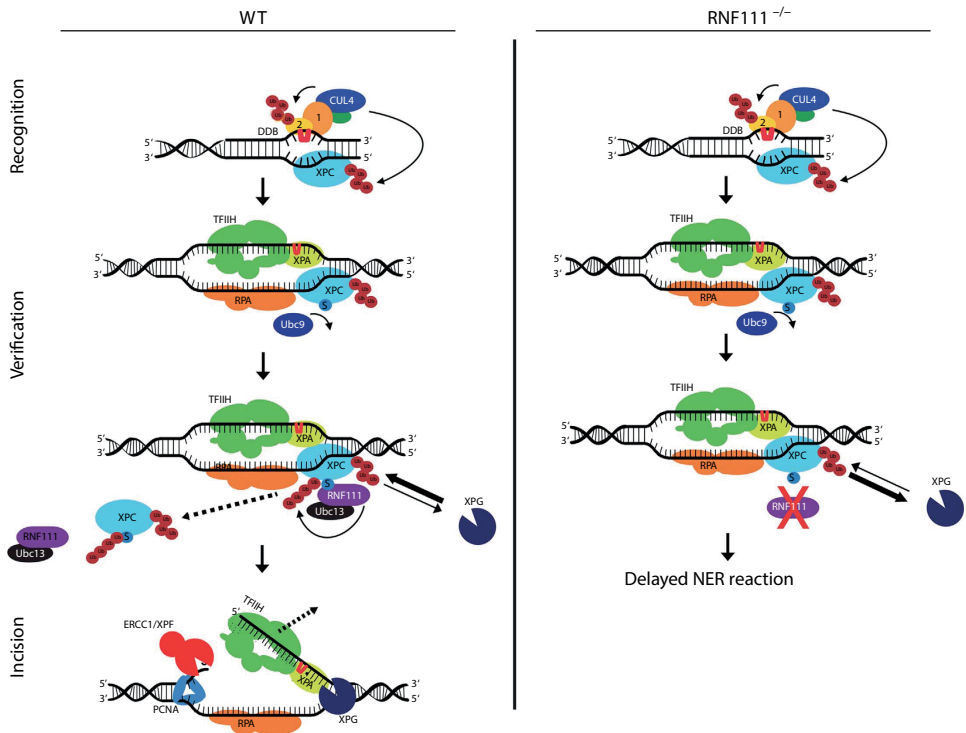


Figure 5. Proposed model for RNF111-dependent XPC ubiquitylation in controlling NER. In WT cells SUMOylated XPC is ubiquitylated by RNF111, promoting its release from damaged DNA. This RNF111-mediated XPC release facilitates XPG and ERCC1/XPF recruitment, thereby enabling an efficient NER reaction. In RNF111^{-/-} cells, where XPC is not modified by RNF111-dependent K63 ubiquitin chains, XPC remains more stably associated with the pre-incision NER complex. This interferes with proper loading of XPG, thereby inhibiting the NER reaction. Branched 'Ub' represents K48-linked Ub chains, linear 'Ub' represents K63-linked Ub chains; 'S' represents SUMOylation; '1' and '2' represent DDB1 and DDB2, respectively.

Intriguingly, the RNF111-mediated ubiquitylation occurs on one of the NER-initiating enzymes, but it affects one of the last NER steps; the loading of the endonucleases XPG and ERCC1/XPF. While we cannot exclude that RNF111 might also target other NER factors downstream of XPC that may contribute to the reduced NER-incision complex assembly, the reduced accumulation of ERCC1 and XPF at sites of UV damage in cells expressing an XPC mutant that cannot be SUMOylated (Fig.4D-G) strongly suggests that this is caused by the action of RNF111 on XPC. In addition, no UV-damage induced SUMO modification of other NER factors have been described thus far. We therefore propose a model in which chromatin-bound, SUMOylated XPC is ubiquitylated by RNF111 upon DNA damage (Poulsen et al., 2013), thereby stimulating its release from the NER pre-incision complex that contains TFIIH and XPA (Fig. 3B). This key step most likely generates better access of XPG or increased stable binding of XPG to the NER pre-incision complex. In addition, more efficient binding of XPG will promote the 5' incision by ERCC1/XPF and progression of the NER reaction (Fig. 5, left panel). In contrast, in the absence of RNF111, damage-bound SUMOylated XPC is not ubiquitylated and remains stably bound to the NER complex, interfering with XPG loading and the subsequent recruitment of ERCC1/XPF, which are required for the excision of the damaged DNA strand by these endonucleases (Fig. 1B and Fig. 5, right panel). The need for XPC release for proper XPG incorporation into the NER complex is in line with *in vitro* experiments showing

that upon the arrival of RPA and XPG, XPC is released from the NER complex (Riedl et al., 2003). It should also be noted that the position where XPC is bound, the junction between ds-DNA and ss-DNA at the strand opposite of the lesion, 3' with respect to the lesion-containing strand (Min and Pavletich, 2007), is also the site where the XPG endonuclease acts. For this reason of potential steric hindrance, it is logical to assume that XPC must be released prior to XPG loading.

Further research should uncover whether the ubiquitin-binding UBM domain present in XPG (Fagbemi et al., 2011) might play a role in this process. UBM domains have been shown to interact with mono-ubiquitin and K63-linked, but not K48-linked, chains (Burschowsky et al., 2011). This suggests that XPG might be able to interact with the K63-linked ubiquitylated form of XPC, generated by RNF111. In addition to the presence of TFIIH, this interaction could be required for efficient recruitment of XPG and for the subsequent or simultaneous extraction of XPC from the NER pre-incision complex (Zotter et al., 2006). Furthermore, it has been shown that XPG constitutively interacts with TFIIH (Ito et al., 2007), which may suggest that TFIIH brings XPG into the NER complex. Interestingly however, and in line with earlier observations (Zotter et al., 2006), our data suggest that XPG is recruited to sites of DNA damage independent of TFIIH as it shows different RNF111-dependent binding kinetics than TFIIH: upon RNF111 knockdown XPC is more stably immobilized on sites of DNA damage, whereas XPG immobilization could hardly be detected. However, another possibility is that XPG arrives as part of the TFIIH complex at sites of DNA damage, but will dissociate as long as XPC remains bound to the pre-incision NER complex.

The dynamic DNA association of XPC (Hoogstraten et al., 2008) could give XPG the possibility to compete with XPC for binding to the NER pre-incision complexes even if XPC release is slowed down in the absence of RNF111-mediated ubiquitylation. This will eventually result in a functional NER reaction, however at a much slower rate, which could explain the proficient, but strongly delayed, NER phenotype upon RNF111 knockdown (Fig. 1B and C).

Based on current knowledge it is expected that the different ubiquitylation events on XPC are regulated in a tightly coordinated manner to ensure that XPC binds and dissociates at the right time and place. Within NER, different – partially overlapping - stages can be recognized, e.g. damage recognition and verification, establishment of the pre-incision complex and final dual incision. All steps prior to the actual incision are considered to be reversible, but once the incision by ERCC1/XPF is made the process reaches a “point of no return” (Marteijn et al., 2014). We speculate that in response to UV, XPC is first modified by CRL4^{DDB2}, resulting in more stable binding to sites of DNA damage. Subsequently, XPC is SUMOylated and recognized by RNF111, which mediates K63-linked ubiquitylation of XPC to promote its release from the NER complex. This XPC SUMOylation is dependent on the presence of DDB2 and XPA (Wang et al., 2005). As XPA plays an important role during the damage verification step, it is expected that this XPC SUMOylation and its subsequent release occurs only upon damage verification by the NER pre-incision complex (Fig. 5). We propose that RNF111-mediated ubiquitylation of XPC, required for stable integration of XPG, marks a decisive stage in the progression of NER reaction to reach the “point of no return”.

In summary, we have uncovered a new layer of ubiquitin regulation of the DNA damage recognition step of NER. We propose a first-in/first-out model: the ubiquitylation-driven release of the NER-initiating factor XPC is required to make room for the incorporation of the downstream NER endonucleases. This UBC13 and RNF111-dependent process is required to pass the NER reaction through the successive steps thereby facilitating efficient damage removal. In addition to



the regulation by RNF111 and UBC13 as XPC ubiquitylation factors, this process is dependent on SUMOylation mediated by UBC9. This indicates the importance of crosstalk between SUMOylation and ubiquitylation in the regulation of damage recognition. Our findings not only show the importance of precise regulation of damage recognition, but also the regulation of the progression of the NER reaction. Taken together, we conclude that RNF111-mediated ubiquitylation of XPC is a key regulator of NER efficiency. The sequential SUMOylation and differential ubiquitylation of XPC to control the NER reaction might serve as a paradigm for the spatiotemporal regulation of other processes involving different types of sequential post-translational protein modifications.

Methods

Cell culture and treatments

U2OS cells also including those expressing CPD-photolyase-mCherry (Aydin et al., 2014) and the SV40-immortalized human fibroblasts: XP4PA (expressing XPC-GFP) (Hoogstraten et al., 2008), XPCS2BA (expressing XPB-GFP) (Hoogstraten et al., 2002), XP2OS (expressing GFP-XPA) (Rademakers et al., 2003) and XPCS1RO (expressing XPG-GFP) (Zotter et al., 2006) were cultured under standard conditions in DMEM/F10 supplemented with 10% fetal calf serum (FCS) and 1% penicillin-streptomycin (PS) at 37°C and 5% CO₂. Wild type (clone A littermate of *Xpc*^{-/-} and clone B littermate of *Rnf111*^{-/-}), *Xpc*^{-/-} (Sands et al., 1995) and two independent clones of *Rnf111*^{-/-} knockout MEFs, indicated as A and B (Mavrakis et al., 2007) were grown in DMEM/F10 containing 10% FCS, 1% PS and 1% non-essential amino acids. HeLa cells stable expressing FLAG-SUMO2 in a doxycycline-inducible manner were generated by co-transfection of HeLa/FRT/TRex cells (Invitrogen) with pcDNA5/FRT/TO-3×FLAG-SUMO2 and pOG44 followed by selection with 200 µg/ml hygromycin B (Danielsen et al., 2012; Poulsen et al., 2013).

For global and local UV irradiation cells were treated with a UV-C germicidal lamp (254 nm, Philips) at the indicated dose (Marteiijn et al., 2009). Local UV irradiation was applied through an isopore membrane filter (Millipore), containing 5µm pores.

siRNA transfections were performed using hiperfect (Qiagen) or RNAiMax (Invitrogen) 2-3 days before the described experiments according to manufacturer's protocol. siRNA target sequence used were: CTRL (Thermo Scientific Dharmacon, D10-001210-05), RNF111(A) (5'-GGAUUAAUUGCAGAGGAA-3'), RNF111(B) (Invitrogen, HSS182646), RNF4 (5'-GAAUGGACGUCUCAUCGUU-3'), UBC9 (5'-GGGAUUGGUUUGGCAAGAA-3'), UBC13 (5'-GAGCAUGGACUAGGCUAUA-3'), UBE2Q2 (Thermo Scientific Dharmacon, L-008326-01) and XPA (5'-CUGAUGAUAAACACAAGCUUAUU-3').

Construction and expression of ERCC1-GFP and K8R XPC-GFP

ERCC1-GFP was PCR amplified from the plasmid pBL-ERCC1-GFP-hisha using the following primers: Fw 5'-CCACATGGACCCTGGGAAGGACAAAG-3' Rv 5'-CTACTTGTACAGCTCGTCCATGCCGA-3', cloned into pENTR-D-TOPO (Invitrogen) and recombined into the pLenti PGK Blast Destination vector (Addgene, plasmid 19065) using the Gateway LR Clonase II Enzyme Mix (Invitrogen). Third-generation lentivirus was produced in HEK293T cells and used to generate U2OS stably expressing ERCC1-GFP by Blasticidin selection. K8R XPC-GFP construct was generated by fusion PCR performed by Baseclear (Leiden, The Netherlands) and was sequence verified.

Unscheduled DNA Synthesis (UDS)

Fluorescent-based UDS was performed as described (Nakazawa et al., 2010). In short, MEFs were

seeded on 24mm coverslips three days before the UDS assay and cultured in serum free medium to reduce the number of S-phase cells. Cells were UV irradiated with 16 J m^{-2} and incubated for 3 or 9h in medium containing 5-ethynyl-2'-deoxyuridine (EdU; Invitrogen). Subsequently, cells were washed with PBS and fixed with 3.7% formaldehyde. Cells were permeabilized with 0.5% triton in PBS and EdU incorporation was visualized using Click-it Alexa Fluor 594 according to manufacturer's instructions (Invitrogen). Images were obtained using a LSM700 microscope equipped with a 63x oil Plan-apochromat 1.4 NA oil immersion lens (Carl Zeiss Micro imaging Inc.). Repair capacity, quantified in at least 100 cells by determining the overall nuclear fluorescence using ImageJ software, was normalized to fluorescence in wild type cells which was set at 100%.

Live cell confocal laser-scanning microscopy

For local UV-C irradiation in living cells, a 2 mW pulsed (7.8 kHz) diode pumped solid state laser emitting at 266 nm (Rapp Opto Electronic, Hamburg GmbH) was connected to a Leica SP5 laser-scanning confocal microscope as described (Dinant et al., 2007; Schwertman et al., 2012). Cells were grown on quartz coverslips and imaged and irradiated at the indicated dose using an Ultrafluor quartz 100x, 1.35 NA glycerol immersion lens (Carl Zeiss) at 37°C and 5% CO_2 . Imaging medium was the same as culture medium. Images were acquired using the LAS AF software (Leica). Accumulation kinetics were quantified using Fiji image analysis software. Resulting curves were normalized to the relative fluorescence before irradiation and corrected for background values. To determine the dissociation kinetics of XPC from damaged DNA, the undamaged part of the nucleus was continuously bleached and the fluorescence decrease in the local damage was measured.

For FRAP analysis (Houtsmuller and Vermeulen, 2001), a narrow strip spanning the nucleus (512-16 pixels at zoom 8) was bleached for 100 ms using 100% of the power of a 488nm laser. Recovery of fluorescence in the strip was monitored every 22ms at 2% power of a 488 nm laser until fluorescence reached a steady-state level. All Frap data was acquired on a Leica SP5 laser-scanning confocal microscope equipped with a 63x/1.4NA HCX PL APO CS oil-immersion objective and normalized to the average pre-bleach fluorescence after subtraction of the background signal. At least two independent experiments of >12 cells were performed for each condition. To determine the immobile fraction (F_{imm}) from the FRAP measurements, we renormalized the data, using the fluorescence intensity recorded immediately after bleaching (I_0) and the average fluorescence between 35 and 45s after the start of the FRAP experiment (once recovery is complete) from the unchallenged cells ($I_{\text{final,unc}}$) and UV-irradiated cells ($I_{\text{final,uv}}$) and using the formula:

$$F_{\text{imm}} = 1 - (I_{\text{final,uv}} - I_{0,\text{uv}}) / (I_{\text{final,unc}} - I_{0,\text{uv}}).$$


Western blot

Cells were collected by scraping in 200ul 2x sample buffer and boiled at 98°C for 3min. Lysates were separated by SDS PAGE and transferred to a PVDF membrane (0.45 um). Membranes were blocked with 5% milk in PBS for 1h at RT and incubated with primary antibodies against RNF111 (H00054778-M05, Abnova), UBC9 (sc-5231, Santa Cruz Biotechnology), UBC13 (ab38795, abcam) and Tubulin (T5286, Sigma Aldrich). Membranes were washed 5 times for 5 min with PBS containing 0.05% Tween and incubated with secondary antibodies from LI-COR to visualize antibody complexes with the Odyssey CLx Infrared Imaging System (LI-COR Biosciences). Uncropped scan of the western blots depicted in figure 4D can be found in Supplementary Fig. 3C.

Immunofluorescence

Cells were grown on 24 mm coverslips and fixed using 2% paraformaldehyde supplemented with





triton X-100. For XPG stainings, cells were fixed with 2% paraformaldehyde. Subsequently cells were permeabilized with PBS containing 0.1% triton X-100 and washed with PBS containing 0.15% glycine and 0.5% BSA. To visualize CPD or 6-4pp, nuclear DNA was denatured by incubation with 0.07M NaOH for 5 min at room temperature. Coverslips were washed with PBS containing 0.15% glycine and 0.5% BSA and incubated with primary antibodies for 1-2 h at room temperature. Cells were washed three times and two times for 10min with 0.1% triton X-100 and once with PBS containing 0.15% glycine and 0.5% BSA. To visualize primary antibodies coverslips were incubated for 1 hour with secondary antibodies labeled with ALEXA fluorochromes 488 or 555 (Invitrogen). Again cells were washed with 0.1% Triton X-100 and PBS⁺. Subsequently coverslips were embedded in Dapi Vectashield mounting medium (Vector Laboratories). Images were obtained using a LSM700 microscope equipped with a 63x oil Plan-apochromat1.4. NA oil immersion lens (Carl Zeiss Microimaging Inc.). The following primary antibodies were used : anti-CPD(1:1000; TDM-2; MBL International), anti-DDB2 (1:400; MybioSource), anti-XPC (1:200; fraction 5), anti-TFIIH p89 (1:1000; S19; Santa Cruz), anti-XPG (1:400; 8H7; Thermo Scientific), anti-XPF (1:100; 3F2, Santa Cruz) and anti-ERCC1 (1:200; D10; Santa Cruz).

Quantification of 6-4PP removal by immunofluorescence

MEFs were cultured to 80% confluence on 24 mm coverslips and exposed to global UV-irradiation (10J m^{-2}). Cells were fixed after various time points and immunostained with anti-6-4pp (1:1000; 64M-2; Cosmo Bio), as described above. Images were obtained using a Zeiss LSM 510 META confocal microscope equipped with a 63x oil Plan-apochromat 1.4 NA oil immersion lens. 6-4PP levels were quantified in at least 70 cells per sample by measuring the overall nuclear fluorescence using ImageJ software, which was set at 100% for 0h after UV-irradiation.

Acknowledgements

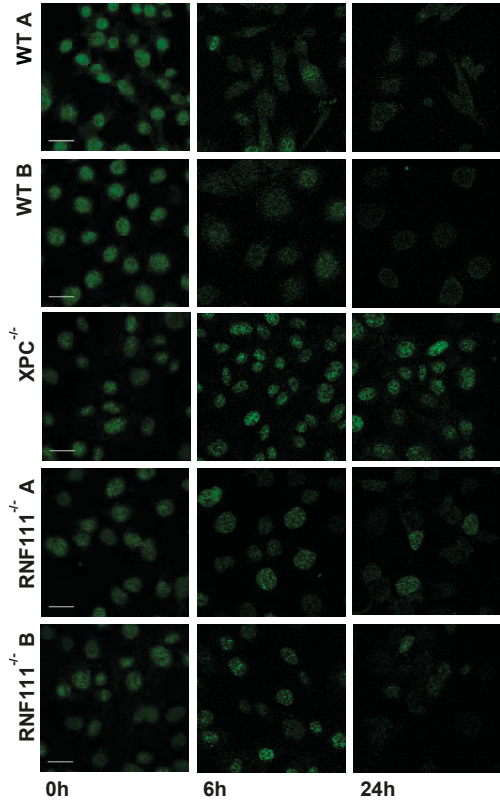
We thank Dr. V. Episkopou for providing RNF111^{-/-} primary mouse fibroblasts. This work was supported by the Dutch Organization for Scientific Research ZonMW TOP Grants (912.08.031 and 912.12.132), Dutch Organization for Scientific Research ALW VIDI grant (846.13.004), Horizon Zenith (935.11.042), Dutch Science Organization (NWO), Chemical Sciences (CW), ECHO.12.B1.043, European Research Council Advanced Grant (340988-ERC-ID), FP7 Marie Curie International Training Network aDDress and Erasmus MC fellowship.

Author contribution

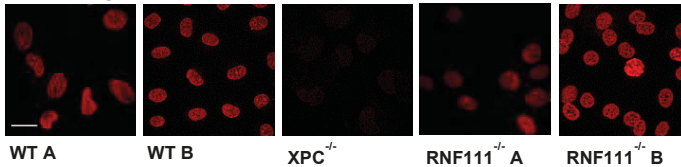
Lv.C and G.J.v.B performed the majority of experiments, Y.T. and R.C.J. performed experiments on the K8R XPC mutant. S.P. performed SUMOylation assays, A.F.T. performed FACS sorting experiments. M.S. and H.L. performed cloning of mCherry Photolyase and ERCC1-GFP. N.M., A.B.H., W.V. and J.A.M. designed the experiments, analyzed the data and authored the manuscript. All authors reviewed the manuscript. The authors declare no competing financial interests.

Supplemental figures

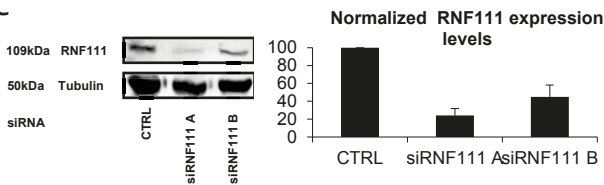
A 6-4pp removal



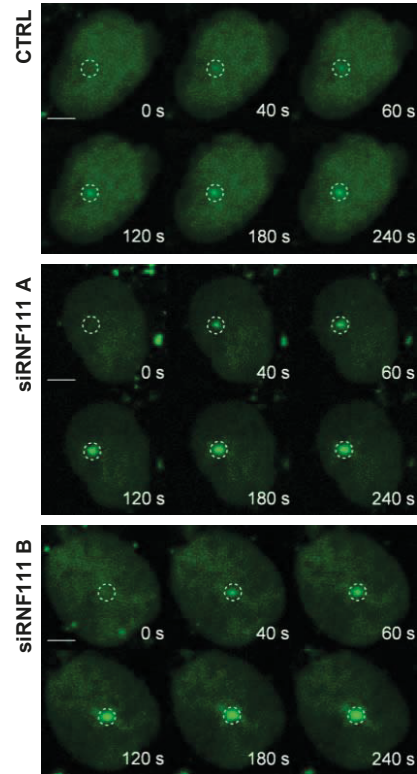
B UDS 9h post UV



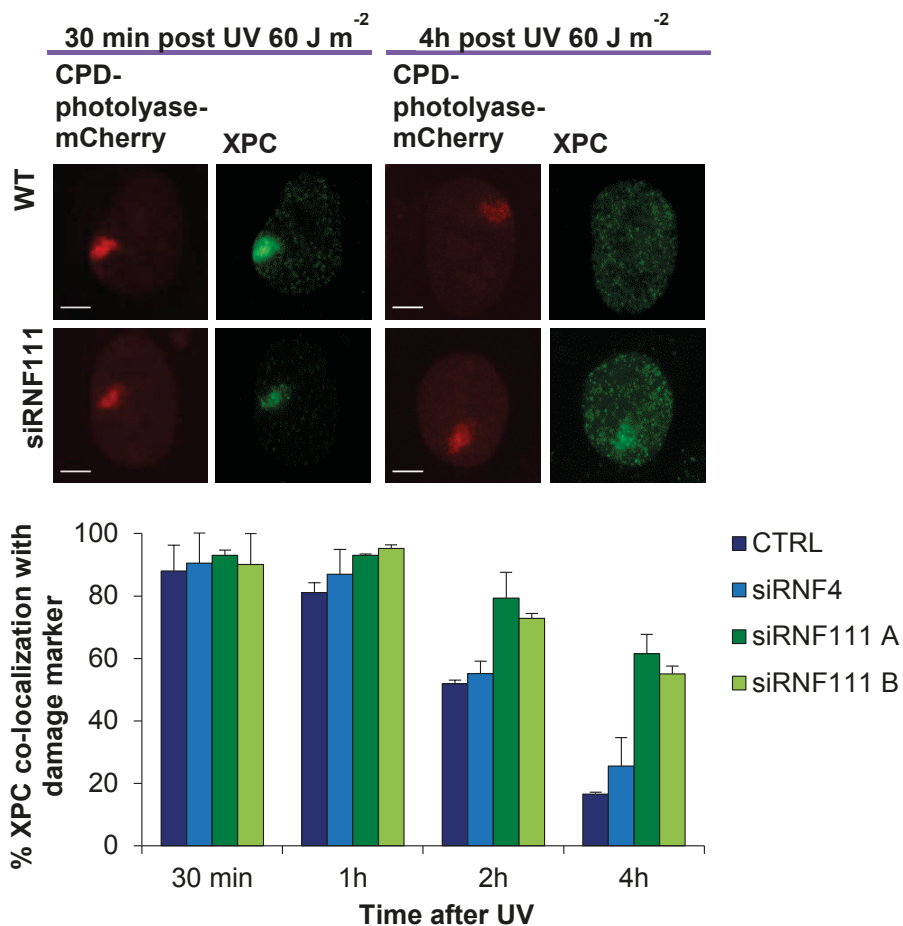
C



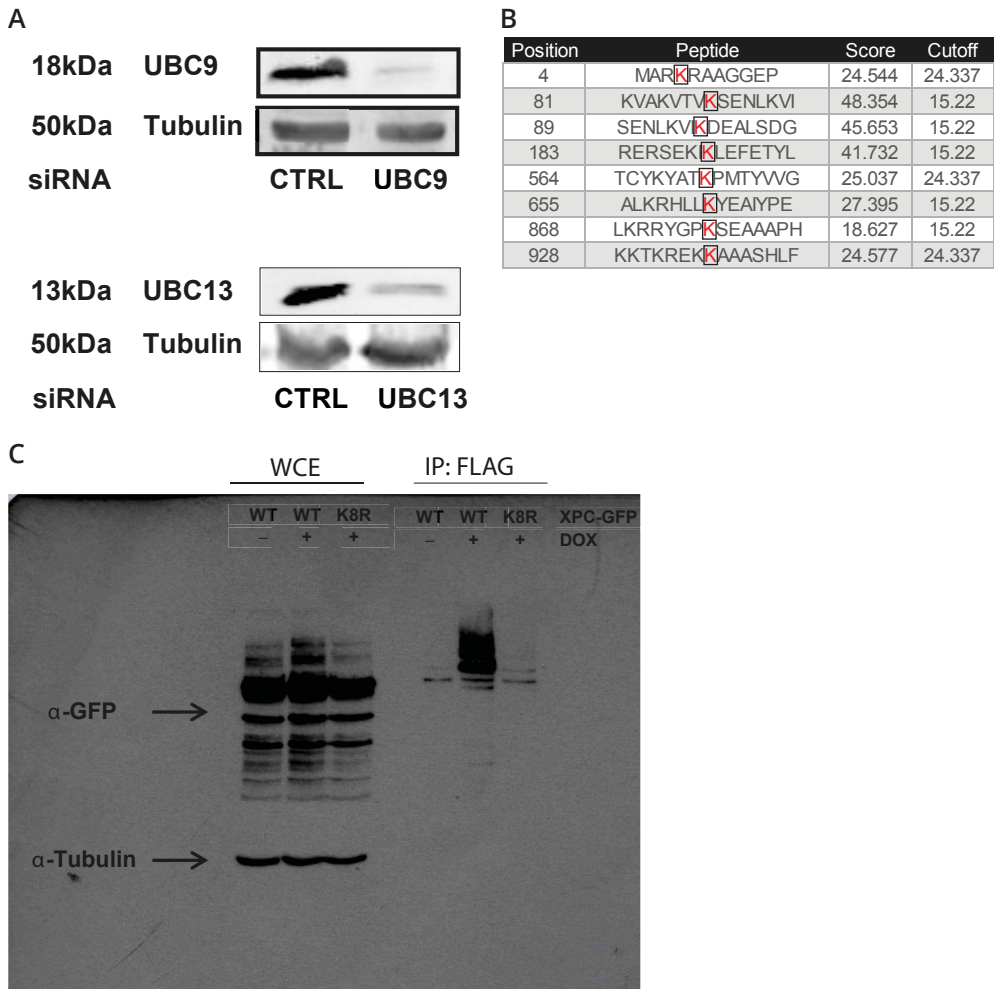
D XPC-GFP accumulation



Supplementary Figure 1. (A) Representative pictures of the presence of 6-4pp in the indicated MEFs at the indicated times after UV-irradiation, measured by immunofluorescence. Scale bars: 25 μ m. **(B)** Representative pictures of UDS of the indicated MEFs, determined by EdU incorporation over 9 h after UV-irradiation (16 J/m²). Scale bar: 25 μ m. **(C)** Left panel: RNF111 protein levels, as determined by western blotting, in U2OS cell were determined 72 h after siRNA transfection with non-targeting (CTRL) or RNF111 siRNA A or B. Anti-Tubulin staining was used as loading control. Right panel: quantification of the western blots of the left panel. **(D)** Representative pictures (stills) of live-cell imaging analysis of XPC-GFP after LUD infliction in XP4PA cells transfected with CTRL and RNF111 siRNA A or B. Dotted circle indicates the site of damage inflection.



Supplementary Figure 2. Top panel: Representative pictures of localization of XPC and CPD-photolyase-mCherry at LUD in U2OS cells transfected with the indicated siRNA's 30 min or 4 h after local UV-irradiation (60 J/m²) are shown. Scale bar: 5µm. Lower panel: Quantification of XPC co-localization with the damage marker CPD-photolyase-mCherry. (n=50 cells containing a LUD were scored per sample in two independent experiments; mean ± SD).



Supplementary Figure 3. (A) U2OS cells transfected with non-targeting (CTRL) siRNA or siRNA targeting UBC9 or UBC13 were collected 48 h after siRNA transfection. The amount of protein was analyzed by immunoblotting using the indicated antibodies. Anti-Tubulin was used as loading control. **(B)** Table showing the putative SUMOylation sites of XPC, as identified by the GPS-SUMO algorithm. **(C)** Uncropped scan of Figure 4D.

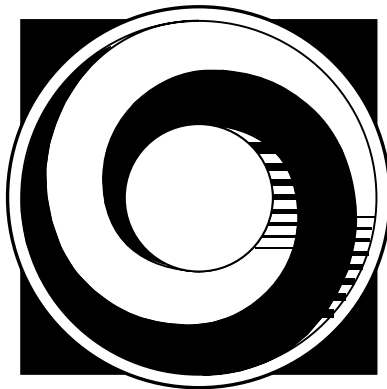
References

- Araki, M., C. Masutani, M. Takemura, A. Uchida, K. Sugawara, J. Kondoh, Y. Ohkuma, and F. Hanaoka. 2001. Centrosome protein centrin 2/caltractin 1 is part of the xeroderma pigmentosum group C complex that initiates global genome nucleotide excision repair. *J Biol Chem.* 276:18665-18672.
- Aydin, O.Z., J.A. Martejijn, C. Ribeiro-Silva, A. Rodriguez Lopez, N. Wijgers, G. Smeenk, H. van Attikum, R.A. Poot, W. Vermeulen, and H. Lans. 2014. Human ISWI complexes are targeted by SMARCA5 ATPase and SLIDE domains to help resolve lesion-stalled transcription. *Nucleic Acids Res.*
- Burschowsky, D., F. Rudolf, G. Rabut, T. Herrmann, M. Peter, and G. Wider. 2011. Structural analysis of the conserved ubiquitin-binding motifs (UBMs) of the translesion polymerase iota in complex with ubiquitin. *J Biol Chem.* 286:1364-1373.
- Camenisch, U., R. Dip, S.B. Schumacher, B. Schuler, and H. Naegeli. 2006. Recognition of helical kinks by xeroderma pigmentosum group A protein triggers DNA excision repair. *Nature structural & molecular biology.* 13:278-284.
- Chen, X., Y. Zhang, L. Douglas, and P. Zhou. 2001. UV-damaged DNA-binding proteins are targets of CUL4A-mediated ubiquitination and degradation. *J Biol Chem.* 276:48175-48182.
- Danielsen, J.R., L.K. Povlsen, B.H. Villumsen, W. Streicher, J. Nilsson, M. Wikstrom, S. Bekker-Jensen, and N. Mailand. 2012. DNA damage-inducible SUMOylation of HERC2 promotes RNF8 binding via a novel SUMO-binding Zinc finger. *J Cell Biol.* 197:179-187.
- David, Y., T. Ziv, A. Admon, and A. Navon. 2010. The E2 ubiquitin-conjugating enzymes direct polyubiquitination to preferred lysines. *J Biol Chem.* 285:8595-8604.
- de Laat, W.L., E. Appeldoorn, K. Sugawara, E. Weterings, N.G. Jaspers, and J.H. Hoeijmakers. 1998. DNA-binding polarity of human replication protein A positions nucleases in nucleotide excision repair. *Genes & development.* 12:2598-2609.
- Dinant, C., M. de Jager, J. Essers, W.A. van Cappellen, R. Kanaar, A.B. Houtsmuller, and W. Vermeulen. 2007. Activation of multiple DNA repair pathways by sub-nuclear damage induction methods. *J Cell Sci.* 120:2731-2740.
- Episkopou, V., R. Arkell, P.M. Timmons, J.J. Walsh, R.L. Andrew, and D. Swan. 2001. Induction of the mammalian node requires Arkadia function in the extraembryonic lineages. *Nature.* 410:825-830.
- Fagbemi, A.F., B. Orelli, and O.D. Scharer. 2011. Regulation of endonuclease activity in human nucleotide excision repair. *DNA Repair (Amst).* 10:722-729.
- Galanty, Y., R. Belotserkovskaya, J. Coates, and S.P. Jackson. 2012. RNF4, a SUMO-targeted ubiquitin E3 ligase, promotes DNA double-strand break repair. *Genes & development.* 26:1179-1195.
- Groisman, R., J. Polanowska, I. Kuraoka, J. Sawada, M. Saijo, R. Drapkin, A.F. Kisselev, K. Tanaka, and Y. Nakatani. 2003. The ubiquitin ligase activity in the DDB2 and CSA complexes is differentially regulated by the COP9 signalosome in response to DNA damage. *Cell.* 113:357-367.
- Hannah, J., and P. Zhou. 2009. Regulation of DNA damage response pathways by the cullin-RING ubiquitin ligases. *DNA Repair (Amst).* 8:536-543.
- He, J., Q. Zhu, G. Wani, N. Sharma, C. Han, J. Qian, K. Pentz, Q.E. Wang, and A.A. Wani. 2014. Ubiquitin-specific protease 7 regulates nucleotide excision repair through deubiquitinating XPC protein and preventing XPC protein from undergoing ultraviolet light-induced and VCP/p97 protein-regulated proteolysis. *J Biol Chem.* 289:27278-27289.
- Higa, L.A., and H. Zhang. 2007. Stealing the spotlight: CUL4-DDB1 ubiquitin ligase docks WD40-repeat proteins to destroy. *Cell Div.* 2:5.
- Hoogstraten, D., S. Bergink, J.M. Ng, V.H. Verbiest, M.S. Luijsterburg, B. Geverts, A. Raams, C. Dinant, J.H. Hoeijmakers, W. Vermeulen, and A.B. Houtsmuller. 2008. Versatile DNA damage detection by the global genome nucleotide excision repair protein XPC. *J Cell Sci.* 121:2850-2859.
- Hoogstraten, D., A.L. Nigg, H. Heath, L.H. Mullenders, R. van Driel, J.H. Hoeijmakers, W. Vermeulen, and A.B. Houtsmuller. 2002. Rapid switching of TFIIH between RNA polymerase I and II transcription and DNA repair *in vivo*. *Mol Cell.* 10:1163-1174.
- Houtsmuller, A.B., S. Rademakers, A.L. Nigg, D. Hoogstraten, J.H. Hoeijmakers, and W. Vermeulen. 1999. Action of DNA repair endonuclease ERCC1/XPF in living cells. *Science.* 284:958-961.
- Houtsmuller, A.B., and W. Vermeulen. 2001. Macromolecular dynamics in living cell nuclei revealed by fluorescence redistribution after photobleaching. *Histochem Cell Biol.* 115:13-21.
- Ito, S., I. Kuraoka, P. Chymkowitz, E. Compe, A. Takedachi, C. Ishigami, F. Coin, J.M. Egly, and K. Tanaka. 2007. XPG stabilizes TFIIH, allowing transactivation of nuclear receptors: implications for Cockayne syndrome in XP-G/CS patients. *Mol Cell.* 26:231-243.
- Komander, D., and M. Rape. 2012. The ubiquitin code. *Annual review of biochemistry.* 81:203-229.
- Kulathu, Y., and D. Komander. 2012. Atypical ubiquitylation - the unexplored world of polyubiquitin beyond Lys48 and Lys63 linkages. *Nature reviews. Molecular cell biology.* 13:508-523.
- Lubin, A., L. Zhang, H. Chen, V.M. White, and F. Gong. 2014. A human XPC protein interactome--a resource. *Int J Mol Sci.* 15:141-158.
- Martejijn, J.A., S. Bekker-Jensen, N. Mailand, H. Lans, P. Schwertman, A.M. Gourdin, N.P. Dantuma, J. Lukas, and W. Vermeulen. 2009. Nucleotide excision repair-induced H2A ubiquitination is dependent on MDC1 and RNF8 and reveals a universal DNA damage response. *J Cell Biol.* 186:835-847.
- Martejijn, J.A., H. Lans, W. Vermeulen, and J.H. Hoeijmakers. 2014. Understanding nucleotide excision repair and its roles in cancer and ageing. *Nature reviews. Molecular cell biology.* 15:465-481.
- Masutani, C., K. Sugawara, J. Yanagisawa, T. Sonoyama, M. Ui, T. Enomoto, K. Takio, K. Tanaka, P.J. van der Spek, D. Bootsma, and et al. 1994. Purification and cloning of a nucleotide excision repair complex involving the xeroderma pigmentosum group C protein and a human homologue of yeast RAD23. *EMBO J.* 13:1831-1843.
- Mavrakis, K.J., R.L. Andrew, K.L. Lee, C. Petropoulou, J.E. Dixon, N. Navaratnam, D.P. Norris, and V. Episkopou. 2007. Arkadia enhances Nodal/TGF-beta signaling by coupling phospho-Smad2/3 activity and turnover. *PLoS Biol.* 5:e67.

- Min, J.H., and N.P. Pavletich. 2007. Recognition of DNA damage by the Rad4 nucleotide excision repair protein. *Nature*. 449:570-575.
- Nag, A., T. Bondar, S. Shiv, and P. Raychaudhuri. 2001. The xeroderma pigmentosum group E gene product DDB2 is a specific target of cullin 4A in mammalian cells. *Mol Cell Biol*. 21:6738-6747.
- Nakazawa, Y., S. Yamashita, A.R. Lehmann, and T. Ogi. 2010. A semi-automated non-radioactive system for measuring recovery of RNA synthesis and unscheduled DNA synthesis using ethynyluracil derivatives. *DNA Repair (Amst)*. 9:506-516.
- Ng, J.M., W. Vermeulen, G.T. van der Horst, S. Bergink, K. Sugawara, H. Vrieling, and J.H. Hoeijmakers. 2003. A novel regulation mechanism of DNA repair by damage-induced and RAD23-dependent stabilization of xeroderma pigmentosum group C protein. *Genes & development*. 17:1630-1645.
- Poulsen, S.L., R.K. Hansen, S.A. Wagner, L. van Cuijk, G.J. van Belle, W. Streicher, M. Wikstrom, C. Choudhary, A.B. Houtsmuller, J.A. Marteijn, S. Bekker-Jensen, and N. Mailand. 2013. RNF111/Arkadia is a SUMO-targeted ubiquitin ligase that facilitates the DNA damage response. *J Cell Biol*. 201:797-807.
- Puimalainen, M.R., D. Lessel, P. Ruthemann, N. Kaczmarek, K. Bachmann, K. Ramadan, and H. Naegeli. 2014. Chromatin retention of DNA damage sensors DDB2 and XPC through loss of p97 segregase causes genotoxicity. *Nature communications*. 5:3695.
- Rademakers, S., M. Volker, D. Hoogstraten, A.L. Nigg, M.J. Mone, A.A. Van Zeeland, J.H. Hoeijmakers, A.B. Houtsmuller, and W. Vermeulen. 2003. Xeroderma pigmentosum group A protein loads as a separate factor onto DNA lesions. *Mol Cell Biol*. 23:5755-5767.
- Rapic-Otrin, V., M.P. McLenigan, D.C. Bisi, M. Gonzalez, and A.S. Levine. 2002. Sequential binding of UV DNA damage binding factor and degradation of the p48 subunit as early events after UV irradiation. *Nucleic Acids Res*. 30:2588-2598.
- Riedl, T., F. Hanaoka, and J.M. Egly. 2003. The comings and goings of nucleotide excision repair factors on damaged DNA. *EMBO J*. 22:5293-5303.
- Sands, A.T., A. Abuin, A. Sanchez, C.J. Conti, and A. Bradley. 1995. High susceptibility to ultraviolet-induced carcinogenesis in mice lacking XPC. *Nature*. 377:162-165.
- Schwertman, P., A. Lagarou, D.H. Dekkers, A. Raams, A.C. van der Hoek, C. Laffeber, J.H. Hoeijmakers, J.A. Demmers, M. Fouteri, W. Vermeulen, and J.A. Marteijn. 2012. UV-sensitive syndrome protein UVSSA recruits USP7 to regulate transcription-coupled repair. *Nat Genet*. 44:598-602.
- Scrima, A., E.S. Fischer, G.M. Lingaraju, K. Bohm, S. Cavadini, and N.H. Thoma. 2011. Detecting UV-lesions in the genome: The modular CRL4 ubiquitin ligase does it best! *FEBS letters*. 585:2818-2825.
- Silver, H.R., J.A. Nissley, S.H. Reed, Y.M. Hou, and E.S. Johnson. 2011. A role for SUMO in nucleotide excision repair. *DNA Repair (Amst)*. 10:1243-1251.
- Staresincic, L., A.F. Fagbemi, J.H. Enzlin, A.M. Gourdin, N. Wijgers, I. Dunand-Sauthier, G. Giglia-Mari, S.G. Clarkson, W. Vermeulen, and O.D. Scharer. 2009. Coordination of dual incision and repair synthesis in human nucleotide excision repair. *EMBO J*. 28:1111-1120.
- Sugawara, K., J. Akagi, R. Nishi, S. Iwai, and F. Hanaoka. 2009. Two-step recognition of DNA damage for mammalian nucleotide excision repair: Directional binding of the XPC complex and DNA strand scanning. *Mol Cell*. 36:642-653.
- Sugawara, K., Y. Okuda, M. Saijo, R. Nishi, N. Matsuda, G. Chu, T. Mori, S. Iwai, K. Tanaka, and F. Hanaoka. 2005. UV-induced ubiquitylation of XPC protein mediated by UV-DDB-ubiquitin ligase complex. *Cell*. 121:387-400.
- van Cuijk, L., W. Vermeulen, and J.A. Marteijn. 2014. Ubiquitin at work: The ubiquitous regulation of the damage recognition step of NER. *Exp Cell Res*.
- Vertegaal, A.C. 2007. Small ubiquitin-related modifiers in chains. *Biochem Soc Trans*. 35:1422-1423.
- Volker, M., M.J. Mone, P. Karmakar, A. van Hoffen, W. Schul, W. Vermeulen, J.H. Hoeijmakers, R. van Driel, A.A. van Zeeland, and L.H. Mullenders. 2001. Sequential assembly of the nucleotide excision repair factors *in vivo*. *Mol Cell*. 8:213-224.
- Wakasugi, M., A. Kawashima, H. Morioka, S. Linn, A. Sancar, T. Mori, O. Nikaïdo, and T. Matsunaga. 2002. DDB accumulates at DNA damage sites immediately after UV irradiation and directly stimulates nucleotide excision repair. *J Biol Chem*. 277:1637-1640.
- Wang, Q.E., M. Praetorius-Ibba, Q. Zhu, M.A. El-Mahdy, G. Wani, Q. Zhao, S. Qin, S. Patnaik, and A.A. Wani. 2007. Ubiquitylation-independent degradation of Xeroderma pigmentosum group C protein is required for efficient nucleotide excision repair. *Nucleic Acids Res*. 35:5338-5350.
- Wang, Q.E., Q. Zhu, G. Wani, M.A. El-Mahdy, J. Li, and A.A. Wani. 2005. DNA repair factor XPC is modified by SUMO-1 and ubiquitin following UV irradiation. *Nucleic Acids Res*. 33:4023-4034.
- Yin, Y., A. Seifert, J.S. Chua, J.F. Maure, F. Golebiowski, and R.T. Hay. 2012. SUMO-targeted ubiquitin E3 ligase RNF4 is required for the response of human cells to DNA damage. *Genes & development*. 26:1196-1208.
- Yokoi, M., C. Masutani, T. Maekawa, K. Sugawara, Y. Ohkuma, and F. Hanaoka. 2000. The xeroderma pigmentosum group C protein complex XPC-HR23B plays an important role in the recruitment of transcription factor IIH to damaged DNA. *J Biol Chem*. 275:9870-9875.
- Zhao, Q., Y. Xie, Y. Zheng, S. Jiang, W. Liu, W. Mu, Z. Liu, Y. Zhao, Y. Xue, and J. Ren. 2014. GPS-SUMO: a tool for the prediction of sumoylation sites and SUMO-interaction motifs. *Nucleic Acids Res*. 42:W325-330.
- Zotter, A., M.S. Luijsterburg, D.O. Warmerdam, S. Ibrahim, A. Nigg, W.A. van Cappellen, J.H. Hoeijmakers, R. van Driel, W. Vermeulen, and A.B. Houtsmuller. 2006. Recruitment of the nucleotide excision repair endonuclease XPG to sites of UV-induced dna damage depends on functional TFIIH. *Mol Cell Biol*. 26:8868-8879.

Chapter IV

A bimodal switch regulates priority for repair of active genes under mild genotoxic stress



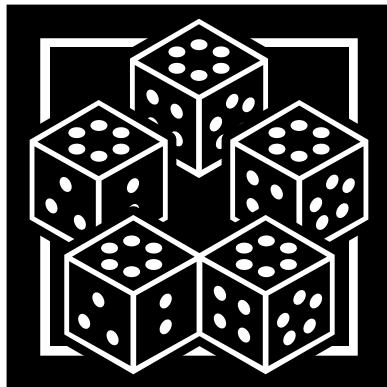
Gijsbert J. van Belle¹, Loes van Cuijk², Ilona M. Vuist³, Bart Geverts¹, Martin E. van Royen¹, Pernette J. Verschure³, Jurgen A. Martelijn², Wim Vermeulen^{2*}, Adriaan B. Houtsmuller^{1*}

¹Department of Pathology, Josephine Nefkens Institute, Erasmus MC, Dr. Molewaterplein 50, 3015 GE Rotterdam, The Netherlands. ²Department of Genetics, Cancer Genomics Netherlands, Erasmus MC, Wytemaweg 80, 3015 CN Rotterdam, The Netherlands. ³Swammerdam Institute for Life Science (SILS), University of Amsterdam, Science Park 904, P.O. Box 94215, 1098 GE Amsterdam, The Netherlands.

Manuscript in preparation

Chapter V

A minimal model for regulation of DNA damage recognition by XPC



Gijsbert J. van Belle, Bart Geverts, Adriaan B. Houtsmuller

Department of Pathology, Josephine Nefkens Institute, Erasmus MC, Dr. Molewaterplein 50, 3015 GE Rotterdam,
The Netherlands.

Manuscript in preparation

Appendix



Summary
Samenvatting
Curriculum Vitae
List of publications
PhD portfolio
Dankwoord

Summary

All life on earth can only exist because of the high stability and integrity of its genome. This integrity and stability is continuously challenged by internal and external DNA damaging agents that induce DNA lesions. If not properly repaired, these lesions may disrupt important cellular processes like replication and transcription. Eventually they can lead to accelerated ageing and malignant transformation of cells. Maintenance and protection of the DNA is therefore of crucial importance. To ensure this a complex network of dedicated DNA repair- and associated signalling pathways is in place. Collectively, these pathways are known as the DNA Damage Response (DDR).

Chapter I gives a general background for this thesis, introducing the DDR pathways and describes the current knowledge of which lesions they recognize and how they repair them. The Nucleotide excision repair (NER) pathway is examined in higher detail. This pathway recognizes and removes a wide variety of DNA lesions, including those induced by UV irradiation. Recognition of these lesions can occur via one of two different mechanisms: transcription-coupled repair (TC-NER) and global genome repair (GG-NER). In the TC-NER pathway, lesions are detected by the stalling of a RNA polymerase II (RNAP2) when it is actively transcribing a gene. Lesions in other parts of the genome, including the non-transcribed strands of active genes, are detected by GG-NER. The DNA binding protein Xeroderma pigmentosum group C (XPC) is the main damage sensor in GG-NER. After lesion recognition has taken place the core NER machinery is recruited and the damage is repaired. The chapter further introduces principles of regulation and signalling via post translational modifications (PTMs), with special interest for the process of (de)ubiquitylation. These PTMs are the basis for intricate signalling pathways, using positive and negative feedback loops, which are active in numerous biological systems. Furthermore, this chapter introduces confocal microscopy techniques, most importantly fluorescence recovery after photobleaching (FRAP), which are used in all the chapters of this thesis.

Chapter II describes the identification of a new SUMO-targeted ubiquitin ligase (STUbL), RNF111/Arkadia. Immunoprecipitation (IP) experiments show RNF111 uses three adjacent Sumo Interacting Motives (SIMs) for specific recognition of poly-SUMO2/3 chains. To gain insight into the functional significance of RNF111 SUMO binding, quantitative mass spectrometry (MS)-based analysis of cellular RNF111-interacting proteins was performed. This approach identified the E2 ligase UBC13-MMS2 as a cognate E2 enzyme to promote non-proteolytic, K63-linked ubiquitylation of SUMOylated target proteins. Damage sensor XPC is known to be SUMOylated upon UV irradiation and using knock down and IP experiments we show that RNF111 indeed ubiquitylates SUMOylated XPC. Using the Unscheduled DNA Synthesis (UDS) assay we show that when this SUMO mediated ubiquitylation of XPC is abrogated, the result is an impaired NER reaction. Using local UV-C laser irradiation microscopy techniques we show that more XPC accumulates at the site of damage. This leads to the hypothesis that the ubiquitylation by RNF111 of XPC is needed for its dissociation and normal progression of the NER reaction.

Chapter III takes this hypothesis and investigates the molecular function of the RNF111-dependent ubiquitylation of XPC and its role in NER. Using a UDS assay setup to measure over a longer period of time we although the NER reaction is impaired, it is not abolished, only severely slowed. Immunofluorescence experiments show a longer residence of XPC on lesions with a knock down of RNF111. FRAP experiments performed on XPC after UV irradiation with a knock down of RNF111 show that the immobile fraction increase 1.6 fold. To check if this is due to a higher K_{on} or a lower K_{off} iFRAP experiments on local damages were performed. These show a lower K_{off} when RNF111 is knocked down and point the need of RNF111 mediated ubiquitylation of XPC for efficient release of XPC from the damage. By performing more FRAP experiments, but

then using other factors of the NER pathway, we could determine where the NER reaction stalls. The factors XPA and XPB show similar results as XPC and are more and longer associated with the damage, where XPG and ERCC1 do not immobilize on the damage any more. As ERCC1/XPF binding to DNA damage is dependent on the presence of XPG, these data suggest that when XPC remains bound to the initiating NER complex, both XPG and ERCC1/XPF cannot be efficiently recruited to or stably incorporated in the NER complex. Similar results were found when either the cognate ubiquitin E2-enzyme UBC13 or the SUMO E2-enzyme UBC9 were knocked down. Taken together, we conclude that RNF111 mediated ubiquitylation of XPC is a key regulator of NER. The sequential SUMOylation and differential ubiquitylation of XPC to control the NER reaction might serve as a paradigm for the spatiotemporal regulation of other processes involving different types of sequential post-translational protein modifications.

Chapter IV focusses on the binding behaviour of the damage sensor XPC at different doses of UV-C irradiation. Since there is not much known about the functioning of the NER pathway at low UV dose we designed FRAP experiments looking at just that. Contrary to an expected linear dose response induced by UV-C irradiation, we observed a switching behaviour in the binding properties of XPC. We find that below a threshold level of UV irradiation XPC does not immobilize and that core NER factors are not recruited, while this does occur above the threshold. Furthermore, we show that this bi-stable response is regulated by Cullin4A (Cul4a) dependent ubiquitylation of XPC. When Cul4a is knocked down, FRAP experiments show a linear dose response of XPC binding after increasing doses of UV-C irradiation. Using quantitative ms-based techniques we identified lysine residue 174 as being highly ubiquitylated after UV. When we subjected the XPC mutant K174R to similar FRAP experiments we again found abolishment of the switching behavior. To further investigate the accumulation of core NER factors below and above the threshold dose of UV irradiation, we used a U2OS cell line containing a stably integrated Tet-inducible transcription array. Using this system we could visually discriminate between the two damage recognition systems in NER. Indeed below the threshold core NER factors accumulated on the array where transcription was taking place. Above the threshold this accumulation was lost in the background accumulation. Together these findings suggest a prioritizing mechanism which allows cells under mild genotoxic stress to prioritize repair of lesions detected by RNA polymerase II in transcribed strands of active genes, which may constitute a more acute threat to cellular homeostasis than damage in non-transcribed DNA.

Chapter V utilizes the bi-stable switch described in Chapter IV as model for bi-stability. Using in house Monte Carlo simulation software we dissect the switch of XPC using *in silico* experiments. The simulations gave us the chance to test the possible models we hypothesised in a fast and flexible manner. By starting with a model which reacts in a linear dose dependant manner and enhancing that model with an in detail studied self-enhancing feedback loop system, we managed to create a bi-stably responding system. The readout of this system also recreated the *in vivo* obtained data very closely. We also saw a difference in systems with and without a damage marking ability. If this system was present the system would switch later compared to a non-damage marking system. After showing that repair of transcribed genes is hampered by competition for downstream factors we hypothesized that the observed bimodal switch ensures priority for repair of transcribed genes. Only when the damage load is so high that the structural integrity of the DNA is threatened is it acceptable for coding genes to wait on repair. Build-up of damages outside of active genes would continue in such a system, until the threshold value is reached and the system switches.

Samenvatting

Al het leven op aarde kan alleen maar bestaan vanwege de hoge stabiliteit en integriteit van het genoom. Deze integriteit en stabiliteit worden continue verstoord door interne en externe DNA beschadigende invloeden, welke DNA schades kunnen veroorzaken. Wanneer deze schades niet worden gerepareerd, kunnen belangrijke cellulaire processen, zoals replicatie of transcriptie, worden verstoord. Dit kan uiteindelijk leiden tot versnelde veroudering of de kwaadaardige transformatie van cellen. Onderhoud en bescherming van het DNA is daarom van cruciaal belang. Dit wordt bewerkstelligd door een complex netwerk van gespecialiseerde DNA herstel- en daaraan gelieerde signaaltransductiewegen. Samen staan deze mechanismen bekend als de DNA schade respons (DDR).

Hoofdstuk I schetst de algemene achtergrond voor dit proefschrift. Verder worden de verschillende DDR routes geïntroduceerd, welke schades ze herkennen en hoe deze worden gerepareerd. De Nucleotide Excisie Herstel (NER) route wordt in meer detail besproken. Deze herstelroute herkent en repareert een grote variëteit aan DNA schades, waaronder schades veroorzaakt door UV straling. Herkenning van deze schades geschiedt over het algemeen via een van de twee beschikbare mechanismen: transcriptie gekoppeld herstel (TC-NER) en globaal genoom herstel (GG-NER). Bij TC-NER worden schades herkend door het eiwit RNA polymerase II (RNAP2) tijdens het transcriberen van actieve genen. Schades in andere stukken van het genoom, inclusief de niet getranscribeerde streng van de actieve genen, worden gedetecteerd via GG-NER. Het DNA bindend eiwit Xeroderma pigmentosum group C (XPC) is de belangrijkste schade sensor in GG-NER. Wanneer de schadeherkenning heeft plaats gevonden wordt de rest van de NER herstel eiwitten gerekruteerd en de schade hersteld. Verder worden in dit hoofdstuk de principes van regulatie en signaaltransductie via post-translationele modificaties (PTMs) geïntroduceerd, met speciale aandacht voor het proces van (de)ubiquitinatie. Deze PTMs vormen de basis voor complexe signaaltransductiewegen, die gebruik maken van positieve en negatieve terugkoppelingen, welke veel voorkomen in biologische systemen. Ook worden in dit hoofdstuk verschillende confocale microscopie technieken geïntroduceerd. De meest belangrijke van deze genoemde technieken is fluorescence recovery after photobleaching (FRAP), die in alle hoofdstukken van dit proefschrift gebruikt wordt.

Hoofdstuk II beschrijft de identificatie van een nieuwe SUMO-targeted ubiquitin ligase (STUbL) eiwit, RNF111/Arkadia. Immunoprecipitatie (IP) experimenten laten zien dat RNF111 drie naast elkaar gelegen SUMO Interactie Motieven (SIMs) gebruikt voor specifieke herkenning van poly-SUMO2/3 ketens. Om meer inzicht te krijgen in de functionele significantie van de binding van RNF111 aan SUMO zijn er op kwantitatieve massa spectrometrie (MS) gebaseerde analyses van cellulair RNF111 interacterende eiwitten uitgevoerd. Uit deze analyses blijkt dat de E2 ligase UBC13-MMS2 het verwante E2 enzym is. Dit enzym bevordert de non-proteolytische, K63 gelinkte ubiquitinering van geSUMOyleerde eiwitten. Het is bekend dat de schade sensor XPC wordt geSUMOyleerd na bloot gesteld te zijn aan UV licht. Verdere experimenten laten inderdaad zien dat RNF111 geSUMOyleerd XPC ubiquitineert. Het Unscheduled DNA Synthesis (UDS) assay laat zien dat wanneer deze SUMO gemedieerde ubiquitinering verstoord wordt de NER reactie niet meer efficiënt verloopt. Door gebruik te maken van lokale bestraling met behulp van UV-C laser bestralingstechnieken is de ophoping van XPC op de gecreëerde schade gevolgd. Wanneer er geen RNF111 aanwezig is in deze cellen is er meer ophoping van XPC te zien. Dit leidt tot de hypothese dat de ubiquitinering van XPC door RNF111 nodig is voor de dissociatie van de schadesensor en voor normale progressie van de NER reactie.

Hoofdstuk III gaat verder met deze hypothese en bekijkt het verdere moleculaire func-

tioneren van RNF111-afhankelijke ubiquitineren van XPC en de rol die deze heeft in NER. Door gebruik te maken van een UDS assay, die meet over een langere periode, laten we zien dat hoewel de NER reactie wel vertraagd wordt, maar niet compleet verstoord. Immunofluorescentie experimenten tonen aan dat wanneer de hoeveelheid RNF111 verminderd is, XPC langer aanwezig is op schades. Ook uit FRAP experimenten op dergelijk behandelde cellen blijkt dat de mobiele fractie van XPC in de cel 1,6 keer hoger is dan onder controle omstandigheden. Om te kijken of deze langere retentie van XPC veroorzaakt wordt door een hogere K_{on} of een lagere K_{off} dan onder normale omstandigheden zijn iFRAP experimenten op lokale schades uitgevoerd. In cellen waar de hoeveelheid RNF111 is verminderd blijkt XPC een lagere K_{off} te hebben. Deze data lijken inderdaad te bevestigen dat RNF111-afhankelijke ubiquitineren van XPC nodig is voor het efficiënt loslaten van de gedetecteerde schade. Door FRAP experimenten uit te voeren op andere factoren welke een rol spelen in NER konden we nagaan waar de reactie vast loopt als er geen RNF111 aanwezig is. FRAP experimenten met factoren als XPA en XPB lieten vergelijkbare resultaten zien als XPC; meer van het eiwit zat langer vast op schades. Factoren die pas later tijdens de NER reactie een rol spelen, zoals XPG en ERCC1, immobiliseerden niet meer op de schades. Gezien de binding van ERCC1/XPF aan een schade afhankelijk is van de aanwezigheid van XPG op de schade, suggereren deze metingen dat wanneer XPC gebonden blijft op het NER initiërend complex, zowel XPG als ERCC1/XPF niet meer efficiënt gerekruteerd en stabiel geïncorporeerd kunnen worden. Ook wanneer de hoeveelheden van het E2 enzym UBC13 of het SUMO E2 enzym UBC9 verminderd zijn, laten de FRAP experimenten eenzelfde resultaten zien. Uit al deze data samen is te concluderen dat de RNF111 gemedieerde ubiquitineren van XPC een sleutelrol speelt in NER. Deze wijze van controle over het NER proces, de sequentiële SUMOylatie en differentiële ubiquitineren van XPC, kan een nieuw paradigma zijn voor de spatio-temporele regulatie van andere processen waarbij verschillende soorten sequentiële post-translationale eiwit modificaties plaatsvinden.

Hoofdstuk IV focust zich op het bindingsgedrag van de schade sensor XPC bij verschillende hoeveelheden UV-C straling. Gezien er nog niet veel bekend is over het functioneren van NER bij lage UV dosissen zijn er FRAP experimenten gedaan die juist daar naar kijken. Anders dan de verwachte lineaire dosis response na UV-C bestraling, namen we een omschakelend gedrag waar in de bindingseigenschappen van XPC. Bij een UV-C dosis lager dan de drempelwaarde zien we geen immobilisatie van XPC en geen rekrutering van de kern NER factoren, terwijl dit wel gebeurt boven de drempelwaarde. Verder laten we zien dat deze bi-stabiele response gereguleerd wordt door de ubiquitineren van XPC door Cullin4A (Cul4a). In cellen waar de hoeveelheid Cul4a is vermindert laten FRAP experimenten een lineaire dosis response van XPC binding zien na bestraling met een steeds oplopende dosis UV-C straling. Door gebruik te maken van kwantitatieve massaspectrometrie technieken is lysine 174 van het XPC eiwit geïdentificeerd als residu welke na UV-C bestraling het meest wordt gebuquitineerd. Een gemuteerde versie van het XPC eiwit, waarbij de lysine op plek 174 is vervangen door een arginine, blijkt bij eenzelfde FRAP experiment geen omschakelend gedrag meer te vertonen. Om de ophoping van kern NER factoren boven en onder de drempelwaarde verder te onderzoeken is er gebruik gemaakt van een U2OS cellijn welke een stabiel geïntegreerde Tet-induceerbare transcriptie array in zich draagt. Door gebruik te maken van dit systeem kan er visueel onderscheid gemaakt worden tussen de twee schadeherkenningsmechanismen van NER. Bij blootstelling aan UV onder de drempelwaarde accumuleerde de kern NER factoren op de transcriptie array. Wanneer het experiment wordt herhaald met een dosis boven de drempelwaarde is deze accumulatie niet meer te zien door dat het weg valt in het achtergrond signaal. Deze bevindingen suggereren een mechanisme wat bij cellen die blootgesteld zijn aan milde genotoxische stress de prioriteit legt bij schades die herkend zijn door RNA polymerase II in de getranscribeerde streng van actieve genen. Deze schades zijn waarschijnlijk een

meer acuut gevaar voor de homeostase in de cel dan schades in niet actief getranscribeerd DNA.

Hoofdstuk V gebruikt de bi-stabiele schakeling die beschreven is in hoofdstuk IV om een minimaal model voor bi-stabiliteit te ontwerpen. We ontlede deze omschakeling in het bindingsgedrag van XPC door gebruik te maken van eigen Monte Carlo simulatie software en het uitvoeren van *in silico* experimenten. Deze simulaties stelden ons in staat om snel en flexibel de door ons gehypothetiseerde modellen te testen. We zijn begonnen bij een model wat reageert op een lineaire dosis afhankelijke manier. Deze is vervolgens uitgebreid met een systeem van zelfversterkende terugkoppelingen en hiermee is een bi-stabiel reagerend systeem gecreëerd. Niet alleen de overall reactie van het systeem, ook de gegenereerde FRAP curves zijn vergelijkbaar met de *in vivo* data. Tijdens het bestuderen van de verschillende modellen werd er ook een verschil gezien in modellen waar de schades wel of niet gemarkeerd worden na herkenning. Wanneer een systeem functioneert door middel van schademarkering blijkt het omslagpunt van het evenwicht bij een hogere schade dosis te liggen dan wanneer schades niet gemarkeerd worden. Verder laten we zien dat het herstel van schades in getranscribeerde genen wordt gehinderd door competitie voor late kern NER factoren. Dit versterkt ons vertrouwen in de hypothese dat de gevonden bimodale schakeling van XPC zorg draagt voor het prioriteren van reparatie van getranscribeerde genen. Pas wanneer het aantal schades zo groot wordt dat de structurele integriteit van het DNA bedreigt wordt is het acceptabel om coderende genen te laten wachten op reparatie. In een dergelijk systeem zal het aantal schades buiten de actieve genen op blijven lopen, tot uiteindelijk een drempelwaarde bereikt wordt en het systeem omschakelt.

Curriculum Vitae

Name: Gijsbert Jacob Christiaan van Belle
Date of birth: 11 October 1982
Place of birth: Zoetermeer, The Netherlands

Education

2010–2014: **PhD-candidate**, Department of Pathology, Erasmus Medical Center, Rotterdam, The Netherlands
Thesis subject: *Differential Pathway Control in Nucleotide Excision Repair*
Promotor: Prof Dr Adriaan Houtsmuller

2001–2009: **BSc & MSc, Life Science & Technology**, Leiden University/Technical University Delft, The Netherlands
Master track: Functional Genomics
Additional Master track: Science-based Business

Master thesis: *MicroRNA regulation of the c-MYC oncogene*
Supervisors: Prof Dr Reuven Agami and Dr Carlos le Sage
Division of Tumour Biology, The Netherlands Cancer Institute, Amsterdam, The Netherlands

Bachelor thesis: *Chicken Anemia Virus: Methods of Translation investigated*
Supervisors: Prof Dr Kees Pleij and Dr René Olsthoorn
Department of Molecular Genetics, Leiden University, Leiden, The Netherlands

1995–2001 VWO (pre-university secondary education) Oranje Nassau College Zoetermeer, The Netherlands

List of publications

Poulsen SL, Hansen RK, Wagner SA, van Cuijk L, **van Belle GJ**, Streicher W, Wikström M, Choudhary C, Houtsmuller AB, Marteijn JA, Bekker-Jensen S, Mailand N. **RNF111/Arkadia is a SUMO-targeted ubiquitin ligase that facilitates the DNA damage response.** *J Cell Biol.* 2013 Jun 10;201(6):797–807.

Reuter M*, Zelensky* A, Smal I, Meijering E, van Cappellen WA, de Gruiter HM, **van Belle GJ**, Houtsmuller AB, Essers J, Kanaar R, Wyman C. **BRCA2 diffuses as oligomeric clusters with RAD51 and changes mobility after DNA damage in live cells.** *J Cell Biol.* 2014 Dec 8;207(5):599–613. **Authors contributed equally*

van Cuijk L,* **van Belle GJ,*** Turkyilmaz Y, Poulsen SL, Janssens RC, Theil AF, Sabatella M, Lans W, Mailand N, Houtsmuller AB, Vermeulen W, Marteijn JA. **SUMO and ubiquitin-dependent XPC exchange drives nucleotide excision.** *Nat. Comms.* 2015 Jul 7; 6 **Authors contributed equally to the work*

van Belle GJ, van Cuijk L, Vuist I, Geverts B, Van Royen ME, Verschure PJ, Marteijn JA, Vermeulen W, Houtsmuller AB. **A bimodal switch regulates priority for repair of active genes under mild genotoxic stress** (Manuscript in preparation)

van Belle GJ, Geverts B, Houtsmuller AB **A minimal model for regulation of DNA damage recognition by XPC** (Manuscript in preparation)

Piebes DG*, Kempe H*, Vuist I, Bruggeman FJ, **van Belle GJ**, Houtsmuller AB, Verschure PJ. **Single cell transcription repression dynamics** (Manuscript in preparation) **Authors contributed equally*

PhD Portfolio

Courses

In vivo imaging: from molecule to organism OIC course 2010
Photoshop and Illustrator CS6 2013

Seminars and workshops

Josephine Nefkens Institute Annual Symposium, 2010–2014
Rotterdam, The Netherlands. Attended.

The Netherlands Society for Microscopy Annual Meeting 2010
Amsterdam, The Netherlands. Poster presentation.

Annual Molecular Medicine Day 2011–2014
Rotterdam, The Netherlands. Poster presentation

The Netherlands Society for Microscopy Annual Meeting 2012
Veldhoven, The Netherlands. Poster presentation.

Joint Dutch Chromatin Meeting & NVBMB Fall Symposium 2013
Rotterdam, The Netherlands. Poster presentation.

TRR81 Methods Club 2013
Marburg, Germany. Invited speaker.

Medical Genetics Centre Symposium 2013
Rotterdam, The Netherlands. Selected talk.

International conferences

Advanced Light Microscopy Symposium 2010
Advanced imaging strategies for illuminating biological and molecular dynamics
Gent, Belgium. Attended.

Winter School of the Collaborative Research Centre TRR81 2011-2013
“Chromatin Changes in Differentiation and Malignancies”
Kleinwalsertal, Austria. Oral presentation.

Responses to DNA Damage: from molecular mechanism to human disease 2011
Egmond aan Zee, the Netherlands. Poster selected for flash presentation.

12th European Light Microscopy Initiative ELMI Meeting 2012
Leuven, Belgium. Poster presentation.

Spatial 2013: From spatial signalling to sensing spatiality, EMBO Conference 2013
Dead Sea, Israel. Poster presentation.

2nd International Symposium *“Chromatin Changes in Differentiation and Malignancies”* 2013
Egmond aan Zee, The Netherlands. Poster presentation.

Teaching

Bachelor student

2011-2012

In vivo imaging: from molecule to organism OIC course

2010-2013

Dankwoord

En dan zijn we eindelijk daar aangeland waar je zo lang naar uitkijkt. Alle hoofdstukken zijn geschreven, de lay-out is gedaan en zelfs dat ene hele moeilijk stukje is gedaan (NL samenvatting). Tijd om 'even' terug te kijken en alle mensen te bedanken die op de een of andere manier mee hebben geholpen aan het tot stand komen van dit proefschrift. En dat blijken er in mijn geval heel veel te zijn, wat maar weer aangeeft dat een promotietraject alleen doen gewoonweg niet kan.

Adriaan, heel erg bedankt voor de kans om in je groep te werken. Niet alleen op het gebied van microscopie heb ik heel veel van je geleerd, ook hoe kansen de wereld beïnvloeden en bij elkaar houden staat me nu scherp voor ogen. Verder bedankt voor de vele nevingesprekken tijdens de werkbesprekingen over alles wat de wereld bezig houdt. Alhoewel we soms van denkbeelden verschillen is er erg veel overlap en konden we daar uren over praten. Dank voor je openheid, het opendeur beleid wat je voert, het serieus nemen van ons als OIO's en het aanmoedigen van regelmatige 'werkbesprekingen' op het terras. Dit alles is zo belangrijk voor de groep als geheel en ik hoop dat het zich in de toekomst voortzet. Het is een eer dat ik de eerste promovendus ben die jou als promotor heeft. Ik hoop dat er nog vele na mij zullen volgen.

Wim, bedankt dat ik ook in jouw groep mocht werken. De zeer intensieve samenwerking was heel belangrijk voor mijn promotie en dit alles was niet mogelijk geweest als je niet zo'n enorm goede groep bij elkaar had gezocht. Je dossierkennis en je inzicht in het biologische aspect van mijn proeven waren onmisbaar. Ik voelde me zeer welkom in de groep, mede door het deelnemen aan de labuitjes, de BBQ's in je achtertuin en natuurlijk de aanwezige taart in de groep. Ook voor de open deur en de open mindset met betrekking tot mijn proeven en resultaten voor/tijdens/na onze gezamenlijke werkbesprekingen ben ik je erg dankbaar.

Hartelijk dank aan de leescommissie en de overige leden van de commissie voor het kritisch lezen van mijn proefschrift. Pernette, dank voor de (helaas korte) samenwerking en de enorme bijdrage net aan het einde van mijn traject. Leon, dank voor de kritische feedback tijdens onze ZONMW meetings, maar ook voor de gezellige gesprekken daar omheen. Jan, dank voor je kritische bijdragen tijdens de werkbesprekingen en ik blijf onder de indruk van hoe je zo snel nieuwe inzichten kunt doorgronden en ook daar direct mee aan de slag kunt. Sjaak en Joost, dank voor de feedback en goede gespreken tijdens de winterschool. Erik, dank voor de input en het meedenken tijdens de gezamenlijke werkbesprekingen en de single molecule meetings.

Hoofdstuk 2 en 3 hadden er niet geweest zonder Jurgen. De samenwerking tijdens het RNF111 project was geweldig. Alle technieken liepen en door je gestroomlijnde benadering hebben we in korte tijd een heel leuk verhaal neer weten te zetten. Dank dat je deze nederige koelkastenverkoper (IK VERKOCHT BRUINGOED!!!) in pak de kans hebt gegeven zijn vreemde microscopietechnieken los te laten op de vraagstukken. Ook voor je bijdrage aan het XPC verhaal, de werkbesprekingen en de steun via foute grappen en serieuze gespreken ben ik je heel dankbaar. Ik kom graag nog eens taart eten.

Hetzelfde geldt voor Loes. Waar het in het begin leek dat onze onderzoeken verschillende kanten op gingen, kwamen we tegen het einde van onze promoties weer bij elkaar. Samen hebben we een verhaal neergezet waar we beiden trots op kunnen zijn. Ik was erg blij met onze gesprekken, of het nu ging over werk of privé, in de kweek of achter de microscoop.

Aparte vermelding verdienen ook mijn paranimfen. Maarten, ook jij werkt aan DNA schade, jammer genoeg alleen aan de verkeerde soort ;). Nee het was erg prettig om iemand in de Houtsmuller groep te hebben die net van de andere kant keek zodat we veel kennis konden delen en discussiëren over artikelen en proeven. Ook je bijdrages aan de laatste Rad23B FRAPs stel ik erg op prijs. Tijdens het schrijven was het erg prettig om een directe lijn naar de groep te hebben zodat ik ook op de hoogte bleef. Ik hoop snel jouw promotie bij te mogen wonen! Imke, ik was heel blij dat ondanks dat Loes je net had weg gekaapt je toch ook bereid was om mijn paranimf te zijn. Naast onze gedeelde smart over de nukken van de SP5 microscopen was het gelukkig ook altijd erg gezellig. Het lachen om alle foute ideeën voor de promoties van anderen zal ik ook nooit vergeten. Op naar de foute grappen voor die van jou!

De Houtsmullergroep fungeerde als uitvalsbasis de afgelopen jaren en was een bron van gezelligheid en steun. Bart, dank voor het altijd tijd willen maken voor mijn vragen over de simulaties en de gesprekken tijdens borrels en koffiepauzes (eigenlijk ook altijd wel even tussendoor). Tsion, ongeveer tegelijk begonnen in de groep en er samen 'groot geworden'. Dank voor alle hulp in het lab ,achter de microscoop en de daarbij behorende gezelligheid . Martijn, van student naar OIC medewerker, en wat hebben wij heerlijk kunnen discussiëren. Of het nu over maatschappelijke problemen was of een software probleem; praten, argumenteren en uiteindelijk naar een gezamenlijke visie komen. Dank voor de steun en voor het nodige tegengas! In de groep kon ik mijn enthousiasme over bepaalde soorten boeken gelukkig kwijt bij Karin, dank daarvoor. Altijd prettig om tussen het kweken door even over het laatst gelezen hoofdstuk te praten. Thomas, het positivisme wat je uitstraalt werkt enorm aanstekelijk, je vrolijkte mijn lange kweeksessies altijd erg op als je even binnen viel (letterlijk, ik schrok me vaak in eerste instantie wild :P). Jeroen, de beste student die ik bij het Erasmus heb mogen begeleiden! ;) Dank voor alle koffie en natuurlijk ook het gedane werk. Wanneer is die taart er nu precies? Ilona, ik voeg jou hier ook maar aan toe, je bent in mijn ogen ook onderdeel van de groep. Heel erg bedankt voor je bijdrages aan dit proefschrift, voornamelijk hoofdstuk 4. Mochten we ooit eens samen in Zoetermeer zijn moeten we zeker de 'Big Five' eens aflopen ;P. En natuurlijk heel veel dank aan Martin. Bijna dagelijks in de metro naar huis nog even praten over die of die resultaten, een paper of gewoon over dagelijkse dingen. Zonder jou steun en koppen koffie was ik er een stuk meer gehavend doorheen gekomen. Hedy, wellicht nooit officieel werkzaam in de Houtsmuller groep, je war er toch zeker er wel een onderdeel van. Dank je voor je al je steun, wetenschappelijke en net 'iets' minder wetenschappelijke gesprekken, en het zijn van zo'n ongelofelijk goede vriendin!

Alle microscopie in dit proefschrift was niet mogelijk zonder de enorm goede faciliteit die we in het Erasmus MC hebben. Dank daarom aan de mensen van het OIC voor het draaiende houden van alle microscopen. Gert en Gert-Jan, dank voor het geduld als ik weer kwam met vage klachten over net weer een andere SP5. Alex dank voor alle hulp met de LSM700 en de koffiepauzegesprekken over muziek, films en natuurlijk Game of Thrones. Johan, dank voor stimulerende discussies over alle data en voor het aanzetten tot het kijken van Twin Peaks!

Thanks to all the people of the Vermeulen group who tolerated my work discussions about all those FRAP experiments and strange simulations, and even provided me with much useful feedback on the topics. Maikel, thanks for the introduction to Rotterdam, I really love this city now... ow and for all the comic relief of course. It was a blast! Kasper, thanks for all the Mac knowhow, the GoT discussions and my daily dose of Dumpert. Thank you Özge, for the Turkish sweets and food, for the great stories about being a sales representative and for your trust in me. A lot of thanks goes

to Petra. Thanks for defending me just when I came out of my first job interview by saying 'he is quite nice', despite of my suit. But of course also for all the scientific input, the long talks behind the microscope, the boardgame nights and being a fertile ground for my 'getting people addicted to certain book series' plots <insert evil laugh here>. Franzi, thanks for the extra German lessons and the chances to teach you some funny and strange Dutch expressions. Mariangela, thanks for the help with the ERCC1 lines and I'm still very impressed with your great advances in speaking Dutch. Yasemin, thanks for the help with the last pieces of the RNF111 paper. I'm glad there is a strong Turkish presence back in the lab. Thanks Serena, for the short time I had someone else also working on XPC a bit, making talking about it with someone a bit easier ;) Christina, I hope you will mail if you have any other FRAP questions! Thanks for having someone to practice a secret handshake with, there should always be someone in a lab with whom you have that! Roel, short overlap, but thanks for the work on the RNF111 paper and the extra bad jokes during cake eating sessions. Karen, thanks for always having some time to stand around and talk, even if it meant turning of your gels for a bit or staying way longer than you were planning. Your support in the end was invaluable! Jana, I hope the Dutch weather didn't (yet) ruin the positivity with which you started in The Netherlands. Good luck with your postdoc! Thank you Maria, for all the help with ATM and ATR inhibitors and allowing me to help with all your FRAP questions, in the end it really paid off. Even though you are now part of the PostDoc crew Arjan, I still want to thank you for all the bad jokes, movie and book talk, and serious conversations. Your opinion was always clear, but that was always the best way to start a discussion. Hannes, thanks for all the input on various topics of my thesis. Next to all the friendly banter about Futurama, science, and science fiction I highly appreciated our more personal conversations. Please keep doing that with all who might need it in the and outside the lab.

Of course my interactions with people in the Erasmus MC weren't confined to these two groups. Far more people made my residing there the great experience it was. The collaborations, work discussions, the cake, and pub-quizzes with the people from the sixth floor were great. Thanks Anja, Nicole, Kishan, Inger, Paula, Klaas, Marcel, and Claire.

A lot of great people I met during the Kleinwalsertal Winterschools. Thank all of you for all the great time there, the scientific discussions and the great games of Werewolves. Especially I would like to thank Fabrizia. Although I will never completely trust you again since that one game ;), sharing our experiences during the last stages of the promotion helped me a lot!

Also in the JNI a lot of people were very supportive and a great help. Without going into details I would like to thank all of you for the input, help, and support during my period there.

Maar de hulp en steun kwam niet alleen van binnen uit het Erasmus MC en de werkomgeving, ook vrienden en familie hebben daar enorm in bijgedragen. Jirka, ook al zat je de laatste jaren wat verder weg, je interesse, steun, enthousiasme, en vertrouwen waren en zijn nog steeds van onschatbare waarde. Dank voor het blijven luisteren, kritische vragen stellen en alle uitstapjes die de zon weer liet schijnen, ook al was het maar een beetje. Erik, de reis naar China met jou tijdens mijn PhD traject zal ik nooit vergeten. Het was een geweldige manier om afstand te nemen van alles. Ook zonder onze regelmatige (bordspel)avonden of LAN weekenden met de daarbij behorende diepe gesprekken was ik al lang afgehaakt. Bart, de avonden ToS/L4D/RL co-op waren soms hard nodig om wat te ontspannen en te ontladen. Dank voor het blijven luisteren, accepteren en aan het einde van een gesprek er toch weer om kunnen lachen (Black Humor FTW!).

De vriendengroep uit Zoetermeer: Saskia, Almar, Wouter, Sanne, Lennart, Ineke, Mark, Irene, Astrid, Christian. Dank voor de steun en het blijvende begrip voor mijn drukke OIO bestaan. Ik heb veel te vaak 'sorry ik kan niet want...' moeten zeggen door experimenten en schrijfwerk. Almar en Sanne, succes met jullie PhD's!

De rest van mijn vrienden ook bedankt. Bas, Chris, Kevin.... Ook tegen jullie sorry dat ik het zo druk had de laatste jaren. Jullie waren allemaal geïnteresseerd en bleven mij steunen ondanks mijn (virtuele) afwezigheid. Ik hoop snel jullie zowel virtueel als IRL weer meer te zien!

Einen großen Dank auch an die Familie Hessenkemper (inklusive der „kalten Seite“ ;)) für die Unterstützung während der letzten Phase meiner Doktorarbeit und den Momenten der Erholung zur richtigen Zeit. Es war sehr schön so herzlich aufgenommen zu werden und mit so viel Interesse für meine Forschung.

Vanaf het begin heeft mijn familie me door dik en dun gesteund. Valentijn, Madelief, Rozemarijn, Inger, Annick, Tom, Inez en Chris: Dank jullie voor de steun en het geïnteresseerd blijven in al die (ingewikkelde) dingen waar ik het altijd over had. Nicolaas-Jurgen, grote broer, zonder jouw grote voorbeeld en het mij altijd maar enthousiasmeren voor de wetenschap, was ik nooit zover gekomen. Dank voor al die feitjes, het maar blijven uitleggen hoe dingen werken en de interesse in mijn onderzoek. Lonneke, grote zus, zonder jou jarenlange coaching op het sociale vlak was dit boekje er nooit geweest. Dank voor de open deur, het altijd willen praten en het blijven doorvragen. Mam en Pap, dank jullie voor het altijd maar stimuleren van mijn nieuwsgierigheid (ook al moesten jullie daar voor stad en land aflopen), voor de onvoorwaardelijke zorgen en steun, voor het begrip voor alle stress en voor zo veel meer.

Liebe Wiebke, du bist die wichtigste "Entdeckung", die ich während meiner Zeit am Erasmus MC gemacht habe. Vielen Dank für deine Liebe, dein Verständnis und deine Unterstützung. Jetzt, wo diese anstrengende Zeit für uns beide vorbei ist, freue ich mich darauf, mit dir gemeinsam unser "Adventure Book" zu füllen. Ich liebe dich!



